

Combination treatments and dose optimization to enhance peptide receptor radionuclide therapy

Sander Michiel Bison

Combination treatments and dose optimization to enhance peptide receptor radionuclide therapy

Sander Michiel Bison

Combination treatments and dose optimization to enhance peptide receptor radionuclide therapy

PhD Thesis, Erasmus Universiteit Rotterdam, The Netherlands

© Sander M. Bison, 2018
ISBN 978-94-6332-387-1
cover Stuart J. Koelewijn
layout Loes Kema
printed by GVO drukkers & vormgevers, Ede, NL

All rights reserved. No part of this publication may be reproduced, stored in a retrieval system, or transmitted in any form or by any means, without prior written permission of the author or, when appropriate, of the publishers of the respective journals.

Combination treatments and dose optimization to enhance peptide receptor radionuclide therapy

Combinatietherapie en doseroptimalisatie om peptide-receptor-
radionuclide-therapie te verbeteren

Proefschrift

ter verkrijging van de graad van doctor aan de
Erasmus Universiteit Rotterdam
op gezag van de
rector magnificus

Prof.dr. H.A.P. Pols

en volgens besluit van het College voor Promoties.
De openbare verdediging zal plaatsvinden op

4 september 2018 om 15:30 uur

Sander Michiel Bison
geboren te Amsterdam

Promotiecommissie:

Promotor(en): Prof. dr. M. de Jong

Overige leden: Prof. dr. F.W.B. van Leeuwen
Prof. dr. C.W.G. Lowik
Dr. D.C. van Gent

Copromotor(en): Dr. M.R. Bernsen
Dr. M.K. Konijnenberg

CONTENT

CHAPTER 1	General Introduction	5
CHAPTER 2	Peptide receptor radionuclide therapy using radiolabeled somatostatin analogs: focus on future developments. <i>Clin Transl Imaging. 2014;2:55-66. Epub 2014 Mar 5. Review.</i>	19
CHAPTER 3	mTOR inhibitor RAD001 promotes metastasis in a rat model of pancreatic neuroendocrine cancer. <i>Cancer Res. 2013 Jan 1;73(1):12-8.</i>	43
CHAPTER 4	Peptide receptor radionuclide therapy (PRRT) with (¹⁷⁷ Lu-DOTA ⁰ ,Tyr ³) octreotate in combination with RAD001 treatment: further investigations on tumor metastasis and response in the rat pancreatic CA20948 tumor model. <i>EJNMMI Res. 2014 May 30.</i>	57
CHAPTER 5	Optimization of combined temozolomide and peptide receptor radionuclide therapy (PRRT) in mice after multimodality molecular imaging studies. <i>EJNMMI Res. 2015 Dec;5.</i>	75
CHAPTER 6	Treatment planning options for ¹⁷⁷ Lu-DOTA, Tyr ³ -octreotate; therapeutic responses in an animal model. Submitted.	95
CHAPTER 7	Summary and Future Perspectives	115
CHAPTER 8	Nederlandse Samenvatting	127
	Curriculum Vitae	131
	PhD portfolio	133
	List of publications	135
	Dankwoord	137

CHAPTER 1

General Introduction

INTRODUCTION

Therapeutic, radiolabeled ligands that target tumour receptors are attractive for treatment of several types of malignancies. An excessive receptor expression on tumour cells versus like that on normal organ cells might enable delivery of a significant radiation dose to the tumour without severe toxicity in normal organs. An appealing receptor is the somatostatin receptor subtype 2, overexpressed on neuroendocrine tumours (NETs) (1). Somatostatin is a peptide hormone that binds to somatostatin receptors, inhibiting the secretion of multiple other hormones. Native somatostatins, SS14 and SS28, have a poor biological stability due to relatively quick enzymatic degradation (2). To overcome this drawback, somatostatin analogues like octreotide and octreotate (Figure 1) containing eight amino acids, have been created. Because of several modifications these analogues are much more resistant to enzymatic degradation. The somatostatin (STT) receptors (R), of which 5 different subtypes have been described, are G-protein coupled receptors expressed on the cell membrane. Most NETs abundantly express these receptors, of which the subtype 2 is the most commonly expressed (3, 4).

Neuroendocrine tumours

With an incidence of 2-5 per 100,000 inhabitants, NETs form a rare disease (5-7). Considering the age distribution, the highest incidence of NETs is between 60 to 70 years (7, 8). The rise in the incidence of NETs, which has been reported for the past decades (6, 7, 9), is likely not only a result of increased awareness of NETs by clinicians, but also of improved diagnostic procedures because of an increased use of imaging and improved imaging techniques.

Prognosis

Due to large tumour heterogeneity, there is variability considering the prognosis of NET patients. Besides extensiveness of disease at diagnosis, prognosis for NET patients also depends on the primary organ of tumour origination. Colonic, gastric and hepatic NETs have shown worse overall survival in the metastatic setting compared to e.g. pancreatic NETs (7). Also NETs originating from the same primary site can differ in prognosis however; for patients with Grade 1 midgut NETs median survival is 16.6 years, compared to 1.1 years for Grade 3 NETs (10).

Imaging

When a patient is suspected from a NET, nuclear imaging can be performed to confirm this diagnosis. Performing a positron emission tomography (PET) scan, using e.g. 6-¹⁸F-fluoro-L-DOPA (11) or ¹¹C-5-hydroxytryptophan, brings several imaging advantages, including a higher resolution compared to SPECT imaging. Performing a SPECT scan with ¹¹¹Indium-DTPA-octreotide (OctreoScan) (12) comes with the advantage of giving information on STTR expression of the NET, but offers a lower

resolution compared with PET scanning (13, 14). The introduction of ⁶⁸Ga-labelled DOTA, Tyr³-octreotate for PET scanning offers the advantage of a high resolution as well as information on receptor expression. The use of ¹⁷⁷Lu-labelled DOTA, Tyr³-octreotate (¹⁷⁷Lu-TATE) for a SPECT scan after PRRT enables tumour imaging as well as treatment of the tumour at the same time. The emission of gamma radiation as well as tumour destructive beta radiation makes ¹⁷⁷Lu-TATE a valuable so-called "theranostic" tracer (15). Performing a SPECT scan after administration of ¹⁷⁷Lu-TATE during treatment cycles enables visualization of response to earlier administrations.

TREATMENT OPTIONS FOR NETS

There are multiple treatment options for NET patients. In various institutes different kinds of treatment are being applied, based on e.g. experience of the institute. Depending on disease stage and location below described are general applied treatment options:

Surgery is the treatment that can cure patients. About fifty percent of patients however present with metastasized disease (7), leaving little chance for curative surgery. Neoadjuvant treatment with e.g. peptide receptor radionuclide therapy (PRRT, see below) might increase the number of patients that could benefit from curative surgery (16, 17).

Somatostatin receptor targeting treatment with unlabelled somatostatin analogues such as lanreotide and octreotide can reduce hormonal overproduction and has been shown to result in symptomatic relieve in most patients with liver metastases (18-20). Besides this symptomatic relieve treatment, octreotide LAR, a long acting somatostatin analogue, has also been shown to significantly increase time to progression of functionally active as well as inactive metastatic midgut NETs (21). More specifically, administration of octreotide or placebo in patients suffering from a midgut NET resulted in a median progression free survival of 14.3 months in the octreotide group and of 6 months in the placebo group (21).

Chemotherapy: as most chemotherapeutics target highly replicating cells, for the relatively slowly growing NETs the role of chemotherapeutics is limited. In patients with pancreatic NETs chemotherapeutics like capecitabine or temozolomide have nevertheless successfully been applied (22). In a study in which 30 NET patients were treated with a combination of capecitabine and temozolomide 70% of the patients showed a partial response (> 30% decrease from baseline) and 8 had stable disease. Progression free survival was 18 months (23). In another study for the combination of capecitabine and oxaliplatin a partial response of 30% and stable disease for 22% of the patients was found (24).

Molecular Targeted therapies like the tyrosine kinase inhibitor sunitinib (25) or the mTOR inhibitor everolimus (26) have been shown to increase progression-free survival of NET patients. In a trial in which 429 NET patients were included, median PFS with everolimus and octreotide was 16.4 months versus 11.3 months for placebo and octreotide (27).

Radiotherapy: as for most other malignancies external beam radiotherapy can be used in a palliative setting to irradiate symptomatic brain metastases or bone metastases which are painful or give myelium compression. As a primary treatment however, radiotherapy has a limited role for NET patients, although it has been shown to be of value in localized bronchial NETs (28).

Radiolabeled somatostatin analogues: Targeting the somatostatin receptors overexpressed on a vast majority of NET cells with radiolabeled peptides is another treatment option for NETs. Application of this so-called **peptide receptor radionuclide therapy (PRRT)** has been shown to result in improvement of survival as well as quality of life (29, 30). Various radionuclides have been used for this treatment. Treatment with ^{111}In labelled DTPA-octreotide has been shown to give relieve of symptoms in patients with metastasized NETs, objective responses were rare however (31, 32). After treatment with beta emitting ^{90}Y -labelled DOTA, Tyr³-octreotide or ^{177}Lu -TATE (Figure 1), complete and partial responses have been obtained (29, 33). When comparing these radionuclides, ^{177}Lu has the advantage of emitting beta as well as gamma radiation, enabling treatment as well as imaging. Further information on comparison of different radionuclides as well as developments in treatment options is reviewed in Chapter 2.

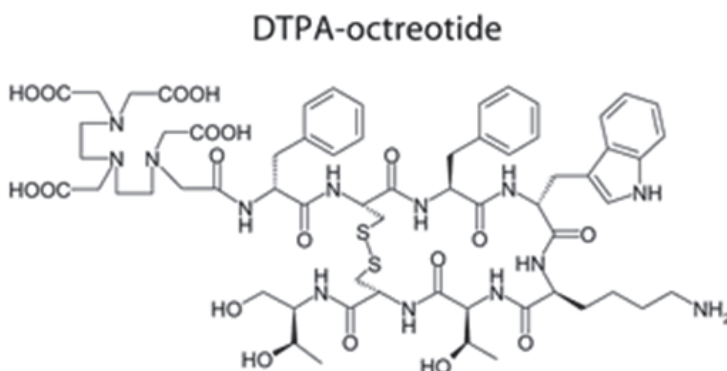
To label a radiometal to an STT analogue a chelator is needed. For clinical use several chelators are being used. The chelators used for the experiments in this thesis include DTPA for labelling of ^{111}In and DOTA for labelling of ^{177}Lu (Figure 1). Radionuclides applied were:

^{177}Lu : - γ -radiation + β -radiation

^{111}In - γ -radiation

Somatostatin targeting peptides applied were:

- DTPA-octreotide:



- DOTA, Tyr³-octreotate:

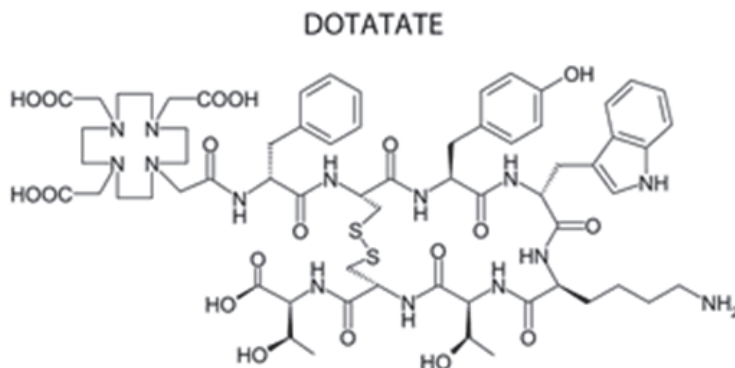


Figure 1: Radionuclides and somatostatin analogues used for tumour treatment and diagnosis in this thesis

CURRENT RESULTS ACHIEVED AFTER TREATMENT OF PATIENTS WITH PRRT

In recent studies in which patients have been treated with ¹⁷⁷Lu-TATE, a response rate of 18 to 44% has been found (34, 35). The phase III NETTER-1 trial showed a tumour response rate of 18% and an estimated rate of progression-free survival at month 20 of 65.2% in the PRRT group compared with a response rate of 3% and an estimated rate of progression-free survival at month 20 of 10,8% in the control group. This study evaluated the efficacy and safety of ¹⁷⁷Lu-TATE (compared with high-dose octreotide LAR) in patients with advanced STTR2-positive intestinal NETs (35). The results show that although at least stable disease has been reported in the majority of patients, the number of patients showing a decline in tumour volume after treatment is still a minority. Options for therapeutic improvement, like combining PRRT with other treatments have been studied in patients as well. Till now there are however no clear results on anti-tumour response and progression-free survival (36) from these studies. The preclinical studies on improvement of PRRT as described in this thesis are therefore of much value to point out which options for improvement might be promising and which treatment schemes could be expected to be most beneficial.

AIMS OF THIS THESIS

For this thesis we have performed preclinical studies in laboratory animals with the ultimate aim to improve PRRT. The aims of the studies presented in this thesis were to:

- 1 Evaluate tumour responses after a combination of PRRT with the mTOR inhibitor everolimus (RAD001)

2 Evaluate tumour responses after a combination of PRRT and the chemotherapeutic temozolomide and optimize the treatment scheme

3 Evaluate the effects of different treatment schemes and different molar activities on tumour responses and dosimetry of tumour and organs.

1

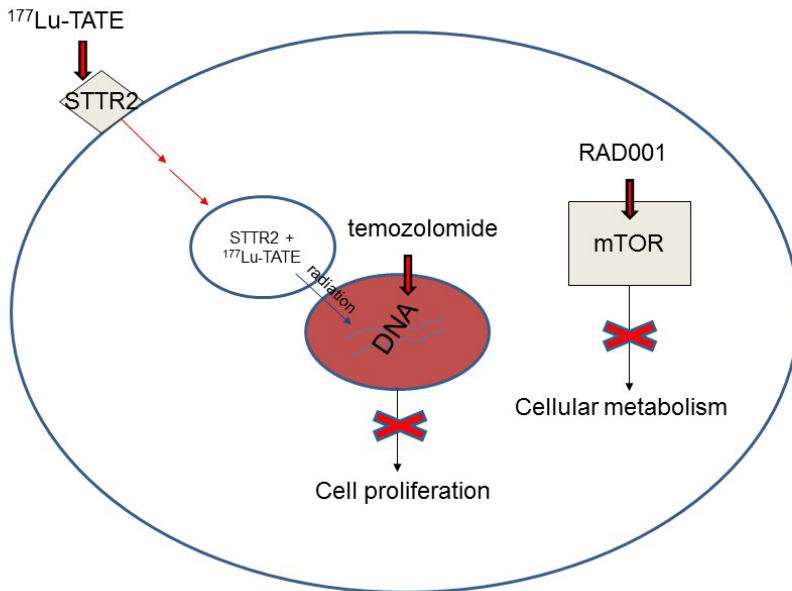


Figure 2: Mechanism of action of $^{177}\text{Lu-DOTA,Tyr3-octreotate}$ ($^{177}\text{Lu-TATE}$), temozolomide (TMZ) and RAD001, the treatments that were used for combination therapy studies in this thesis. $^{177}\text{Lu-TATE}$ emitting β -radiation causing double stranded DNA-breaks in tumour cells after $^{177}\text{Lu-TATE}$ has bound to the somatostatin receptor subtype2 (SSTR2). TMZ, methylating the DNA in tumour cells, disables further cell proliferation. RAD001 targets mTOR, which regulates metabolism, growth and proliferation of the tumour cells.

ANIMALS AND TUMOUR MODEL USED FOR THE PRECLINICAL EXPERIMENTS

The experiments described in this thesis have been performed using the H69 human small cell lung cancer xenograft in nude mice and the CA29048 rat pancreatic tumour model in rats and nude mice.

The H69 cell line is a human derived small cell lung cancer model, overexpressing SSTR2. The tumour cells were inoculated subcutaneously in immune deficient nude mice. This human tumour model has been shown to be of great value in earlier preclinical experiments studying PRRT (37-39).

CA20948 cells were derived from a rat SSTR2-positive pancreatic tumour of acinar origin that was originally induced by azaserine and that is transplantable in syngeneic Lewis rats. In our experiments the cells were inoculated subcutaneously in Lewis rats. This syngeneic tumour has been shown to be very useful as a model for preclinical peptide receptor radionuclide scintigraphy and therapy experiments (40, 41).

IMAGING

Preclinical imaging methods used in this thesis consisted of SPECT/ CT scans to determine uptake of Octreoscan or ^{177}Lu -TATE and MRI scans to determine tumour perfusion.

In the combination therapy studies SPECT scans were performed to study effects of other types of treatment, like temozolomide or everolimus, on uptake of radiolabelled peptide. In the last study in which the effect of treatment scheme and molar activity was studied, SPECT quantifications were used to measure the concentration of radioactivity in the tumour. This concentration of radioactivity was used to calculate the absorbed tumour dose and to relate this absorbed dose to the therapeutic effects being measured.

In this thesis imaging of ^{177}Lu -TATE has been applied when re-treating rats suspected of metastases. Using SPECT after ^{177}Lu -TATE administration to a rat suspected of having metastases enabled us to clearly visualize metastasis, while during follow-up the retreatment effects could be determined as well.

MRI

To determine perfusion of tumour lesions, dynamic contrast enhanced (DCE)-MRI data were acquired. DCE-MRI is a method to non-invasively measure permeability of vessels and determine tumour perfusion using small molecular contrast agents. Following intravenous injection, the contrast agents circulate through the blood vessels in extravascular-space. The kinetics of the accumulation of contrast agents can be imaged and quantified. By following a bolus intravenous injection of the contrast agent Gadobutrol we determined tumour perfusion during treatment with ^{177}Lu -TATE or chemotherapeutics.

Multi-modality imaging

By combining SPECT and DCI-MRI, relations between tumour characteristics like e.g. perfusion and uptake of radiolabelled peptide can be observed. By performing DCE-MRI scans during PRRT or treatment with chemotherapeutics the effect of these treatments on tumour perfusion can be analysed. By performing SPECT scans using Octreoscan after DCE-MRI, the effect of tumour perfusion on uptake of radiolabelled peptide can be determined. The results from the multi-modality imaging studies were used to optimize treatment schemes in which PRRT is combined with chemotherapeutics.

OUTLINE OF THE THESIS

Chapter 2 gives an overview of the current literature on PRRT with somatostatin analogues. Options to improve PRRT described in this chapter might include combination of PRRT with molecular therapy or chemotherapeutics and application of personalised dosimetry, as described in this thesis. In **Chapters 3 and 4** combination studies of ^{177}Lu -TATE with the mTOR inhibitor everolimus are described. In these chapters the therapeutic effects of the combinations are evaluated, moreover the unexpected development of metastases of the CA20948 rat pancreatic tumour after treatment with everolimus has been studied. In **Chapter 5** the successful treatment combination of ^{177}Lu -TATE with the chemotherapeutic temozolomide is described as well as the importance of multimodality imaging to achieve an optimal treatment scheme. In **Chapter 6** we focussed on dosimetry and optimal individualized treatment. We compared the effects of different treatment schemes and molar activities of ^{177}Lu -TATE on dosimetry of tumour and several healthy organs. Finally, **Chapter 7** provides a summary of the data presented in this thesis, together with a short general discussion and overview of future perspectives.

REFERENCES

1. Reubi, J.C., et al., *Detection of somatostatin receptors in surgical and percutaneous needle biopsy samples of carcinoids and islet cell carcinomas*. *Cancer research*, 1990. **50**(18): p. 5969-77.
2. Peters, G.E., McMartin, C., *The breakdown of somatostatin in rat intestinal juice*. 1983. **Suppl., 18 (83), 215–217**.
3. Patel, Y.C., *Somatostatin and its receptor family*. *Front Neuroendocrinol*, 1999. **20**(3): p. 157-98.
4. Reubi, J.C., et al., *Somatostatin receptor sst1-sst5 expression in normal and neoplastic human tissues using receptor autoradiography with subtype-selective ligands*. *Eur J Nucl Med*, 2001. **28**(7): p. 836-46.
5. Hemminki, K. and X. Li, *Incidence trends and risk factors of carcinoid tumors: a nationwide epidemiologic study from Sweden*. *Cancer*, 2001. **92**(8): p. 2204-10.
6. Modlin, I.M., K.D. Lye, and M. Kidd, *A 5-decade analysis of 13,715 carcinoid tumors*. *Cancer*, 2003. **97**(4): p. 934-59.
7. Yao, J.C., et al., *One hundred years after "carcinoid": epidemiology of and prognostic factors for neuroendocrine tumors in 35,825 cases in the United States*. *J Clin Oncol*, 2008. **26**(18): p. 3063-72.
8. Quaedvlieg, P.F., et al., *Epidemiology and survival in patients with carcinoid disease in The Netherlands. An epidemiological study with 2391 patients*. *Ann Oncol*, 2001. **12**(9): p. 1295-300.
9. Kuiper, P., et al., *Pathological incidence of duodenopancreatic neuroendocrine tumors in the Netherlands: a Pathologisch Anatomisch Landelijk Geautomatiseerd Archief study*. *Pancreas*, 2010. **39**(8): p. 1134-9.
10. Ahmed, A., et al., *Midgut neuroendocrine tumours with liver metastases: results of the UKINETs study*. *Endocr Relat Cancer*, 2009. **16**(3): p. 885-94.
11. Binderup, T., et al., *Functional imaging of neuroendocrine tumors: a head-to-head comparison of somatostatin receptor scintigraphy, 123I-MIBG scintigraphy, and 18F-FDG PET*. *J Nucl Med*, 2010. **51**(5): p. 704-12.
12. Toumpanakis, C., et al., *Combination of cross-sectional and molecular imaging studies in the localization of gastroenteropancreatic neuroendocrine tumors*. *Neuroendocrinology*, 2014. **99**(2): p. 63-74.
13. Antunes, P., et al., *Are radiogallium-labelled DOTA-conjugated somatostatin analogues superior to those labelled with other radiometals?* *Eur J Nucl Med Mol Imaging*, 2007. **34**(7): p. 982-93.
14. Poeppel, T.D., et al., *68Ga-DOTATOC versus 68Ga-DOTATATE PET/CT in functional imaging of neuroendocrine tumors*. *J Nucl Med*, 2011. **52**(12): p. 1864-70.
15. Das, T. and S. Banerjee, *Theranostic Applications of Lutetium-177 in Radionuclide Therapy*. *Curr Radiopharm*, 2016. **9**(1): p. 94-101.
16. Kaemmerer, D., et al., *Neoadjuvant peptide receptor radionuclide therapy for an inoperable neuroendocrine pancreatic tumor*. *World J Gastroenterol*, 2009. **15**(46): p. 5867-70.

17. Stoeltzing, O., et al., *Staged surgery with neoadjuvant 90Y-DOTATOC therapy for down-sizing synchronous bilobular hepatic metastases from a neuroendocrine pancreatic tumor*. *Langenbecks Arch Surg*, 2010. **395**(2): p. 185-92.
18. Arnold, R., et al., *Gastroenteropancreatic endocrine tumours: effect of Sandostatin on tumour growth*. *The German Sandostatin Study Group*. *Digestion*, 1993. **54 Suppl 1**: p. 72-5.
19. Janson, E.T. and K. Oberg, *Long-term management of the carcinoid syndrome. Treatment with octreotide alone and in combination with alpha-interferon*. *Acta Oncol*, 1993. **32**(2): p. 225-9.
20. Ducreux, M., et al., *The antitumoral effect of the long-acting somatostatin analog lanreotide in neuroendocrine tumors*. *Am J Gastroenterol*, 2000. **95**(11): p. 3276-81.
21. Rinke, A., et al., *Placebo-controlled, double-blind, prospective, randomized study on the effect of octreotide LAR in the control of tumor growth in patients with metastatic neuroendocrine midgut tumors: a report from the PROMID Study Group*. *J Clin Oncol*, 2009. **27**(28): p. 4656-63.
22. Strosberg, J.R., et al., *First-line chemotherapy with capecitabine and temozolomide in patients with metastatic pancreatic endocrine carcinomas*. *Cancer*, 2011. **117**(2): p. 268-75.
23. Strosberg, J., et al., *Effective treatment of locally advanced endocrine tumors of the pancreas with chemoradiotherapy*. *Neuroendocrinology*, 2007. **85**(4): p. 216-20.
24. Bajetta, E., et al., *Capecitabine plus oxaliplatin and irinotecan regimen every other week: a phase I/II study in first-line treatment of metastatic colorectal cancer*. *Ann Oncol*, 2007. **18**(11): p. 1810-6.
25. Raymond, E., et al., *Sunitinib malate for the treatment of pancreatic neuroendocrine tumors*. *N Engl J Med*, 2011. **364**(6): p. 501-13.
26. Yao, J.C., et al., *Everolimus for advanced pancreatic neuroendocrine tumors*. *The New England journal of medicine*, 2011. **364**(6): p. 514-23.
27. Pavel, M., Hainsworth JD, Baudin E et al., *A randomized, double-blind, placebo-controlled, multi-center phase III trial of everolimus / octreotide LAR vs placebo/ octreotide LAR in patients with advanced neuroendocrine tumors (NET) (RADIANT 2)*. *Ann Oncol*, 2010. **21 Suppl 8**. : p. LBA8.
28. Oberg, K., et al., *Neuroendocrine bronchial and thymic tumours: ESMO Clinical Practice Guidelines for diagnosis, treatment and follow-up*. *Ann Oncol*, 2010. **21 Suppl 5**: p. v220-2.
29. Kwekkeboom, D.J., et al., *Treatment with the radiolabeled somatostatin analog (177 Lu-DOTA 0,Tyr3)octreotate: toxicity, efficacy, and survival*. *J Clin Oncol*, 2008. **26**(13): p. 2124-30.
30. Teunissen, J.J., D.J. Kwekkeboom, and E.P. Krenning, *Quality of life in patients with gastroenteropancreatic tumors treated with (177Lu-DOTA0,Tyr3)octreotate*. *J Clin Oncol*, 2004. **22**(13): p. 2724-9.
31. Valkema, R., et al., *Phase I study of peptide receptor radionuclide therapy with (In-DTPA)octreotide: the Rotterdam experience*. *Semin Nucl Med*, 2002. **32**(2): p. 110-22.

32. Anthony, L.B., et al., *Indium-111-pentetreotide prolongs survival in gastroenteropancreatic malignancies*. Semin Nucl Med, 2002. **32**(2): p. 123-32.
33. Valkema, R., et al., *Survival and response after peptide receptor radionuclide therapy with (90Y-DOTA0,Tyr3)octreotide in patients with advanced gastroenteropancreatic neuroendocrine tumors*. Semin Nucl Med, 2006. **36**(2): p. 147-56.
34. Cives, M. and J. Strosberg, *Radionuclide Therapy for Neuroendocrine Tumors*. Curr Oncol Rep, 2017. **19**(2): p. 9.
35. Strosberg, J., et al., *Phase 3 Trial of 177Lu-Dotatate for Midgut Neuroendocrine Tumors*. N Engl J Med, 2017. **376**(2): p. 125-135.
36. Kwekkeboom, D.J. and E.P. Krenning, *Peptide Receptor Radionuclide Therapy in the Treatment of Neuroendocrine Tumors*. Hematol Oncol Clin North Am, 2016. **30**(1): p. 179-91.
37. Schmitt, A., et al., *Biodistribution and dosimetry of 177Lu-labeled (DOTA0,Tyr3) octreotate in male nude mice with human small cell lung cancer*. Cancer biotherapy & radiopharmaceuticals, 2003. **18**(4): p. 593-9.
38. Erlandsson, A., et al., *Binding of TS1, an anti-keratin 8 antibody, in small-cell lung cancer after 177Lu-DOTA-Tyr3-octreotate treatment: a histological study in xenografted mice*. EJNMMI Res, 2011. **1**(1): p. 19.
39. Bison, S.M., et al., *Optimization of combined temozolomide and peptide receptor radionuclide therapy (PRRT) in mice after multimodality molecular imaging studies*. EJNMMI Res, 2015. **5**(1): p. 62.
40. Lewis, J.S., et al., *Radiotherapy and dosimetry of 64Cu-TETA-Tyr3-octreotate in a somatostatin receptor-positive, tumor-bearing rat model*. Clin Cancer Res, 1999. **5**(11): p. 3608-16.
41. Melis, M., et al., *Up-regulation of somatostatin receptor density on rat CA20948 tumors escaped from low dose (177Lu-DOTA0,Tyr3)octreotate therapy*. Q J Nucl Med Mol Imaging, 2007. **51**(4): p. 324-33.

CHAPTER 2

Peptide receptor radionuclide therapy using radiolabeled somatostatin analogs: focus on future developments.

Bison SM, Konijnenberg MW, Melis M, Pool SE, Bernsen MR, Teunissen JJ, Kwekkeboom DJ, de Jong M.

Published in Clin Transl Imaging. 2014;2:55-66. Epub 2014 Mar 5. Review.

ABSTRACT

Peptide receptor radionuclide therapy (PRRT) has shown to be an effective treatment of neuroendocrine tumors (NETs) if curative surgery is not an option. A majority of NETs abundantly express somatostatin receptors (SSTRs) therefore after administration of somatostatin (SST) analogs labeled with gamma emitting radionuclides tumors can be imaged for diagnosis, staging or follow-up of NET patients. When labeled with β -emitting radionuclides, such radiolabelled peptides ("radiopeptides") are being used for treatment of NET patients. Despite the fact that excellent results have been achieved with PRRT complete responses are still rare, so there is a need for improvement.

In this review we highlight some of the directions currently investigated in pilot clinical studies or in preclinical development to achieve this goal. Although randomized clinical trials are lacking until now, the first studies have shown that application of other radionuclides such as α -emitters, or radionuclide combinations as well as adjustment of the administration routes of radiopeptides might improve tumor response. Individualized dosimetry and better insight into tumor and normal organ radiation doses may lead to adjustment of the amount of administered activity per cycle or the number of treatment cycles, resulting in more personalized treatment schedules. Other options include the application of novel (radiolabeled) SST analogs with improved tumor uptake and radionuclide retention time, or a combination of PRRT with other systemic therapies, such as chemotherapy or treatment with radio sensitizers. Directions for improvement are promising and available at this moment, but additional research, including randomized clinical trials are warranted to obtain further improvement of PRRT.

INTRODUCTION

Neuroendocrine tumors (NETs) comprise well-differentiated tumors derived from diffuse neuroendocrine cells in the lung, gut or pancreas, with a rare incidence of 2-5 per 100,000 inhabitants (1-3), the prevalence being much higher though because of the relatively slow progression rate of the disease (3). In general, NETs are diagnosed at a relatively late stage, with metastatic spread present at time of diagnosis in the majority of patients (3). Therefore, curative surgery is often not an option anymore. Since chemotherapy and external beam therapy is incapable of treating distant metastases, in most cases these therapeutic options are of limited value(4). Peptide receptor radionuclide therapy (PRRT) using radiolabeled somatostatin (SST) analogs, enabling a targeted delivery of therapeutic radionuclides to tumor cells, has proven to be an effective therapeutic option for NET patients with metastasized disease (5, 6). Despite the fact that high tumor response rates have been reported after treatment with ^{177}Lu -DOTA,Tyr³-octreotate (DOTA=1,4,7,10-tetraazacyclododecane-1,4,7,10-tetra-acidic acid) (^{177}Lu -DOTATATE) (7) and ^{90}Y -DOTA,Tyr³-octreotide (^{90}Y -DOTATOC) (8), complete responses are still rare, indicating room for improvement of this radiopeptide therapy. The aim of this review is to describe directions that may lead to improvement of imaging and especially treatment of NETs with radiolabeled SST analogs.

SST is a biologically active neuro-peptide secreted by the hypothalamus. It acts by binding to G-protein coupled somatostatin receptors (SSTRs) expressed in different organs in the body, such as the gastro intestinal tract and the pancreas (9). SST inhibits the secretion of a wide range of hormones. Besides the normal organ expression, SSTRs are (over)expressed on certain malignant tissues, in particular most NETs (10). SSTRs consist of five G-protein coupled receptors, subtypes SSTR1-SSTR5 (11), of which especially SSTR2 is (over)expressed on NETs (12). The abundant expression of SSTRs by the majority of NETs enables their visualization in patients using nuclear imaging techniques, by receptor targeting with radiolabeled SST peptide analogs such as octreotide (D-Phe-c(Cys-Phe-D-Trp-Lys-Thr-Cys)-Thr(ol)) or Tyr³-octreotate (D-Phe-c(Cys-Tyr-D-Trp-Lys-Thr-Cys)-Thr) (13, 14). These stabilized 8-amino acid compounds are derived from native SSTs which consist of 14 or 28 amino acids (15). Unlabeled SST analogs like octeotide LAR are currently applied as initial treatment for patients with metastatic midgut NETs (16). Octreotide LAR has shown to have positive influence on clinical symptoms as well as some tumor stabilizing effects with lengthening of time to progression compared to placebo (16).

Functional imaging using SPECT or PET imaging with the radiolabeled SST analogs ^{111}In -DTPA-octreotide (^{111}In -octreotide or Octreoscan; Mallinckrodt, Petten, the Netherlands) (13) (DTPA= diethylenetriamidopentaacetic acid), ^{68}Ga -DOTA-Tyr³-octreotide (^{68}Ga -DOTATOC), ^{68}Ga -DOTA, 1-Nal³-octreotide (^{68}Ga -DOTANOC) ^{68}Ga -DOTA-Tyr³-octreotate (^{68}Ga -DOTATATE)(17), $^{99\text{m}}\text{Tc}$ -EDDA/HYNIC-octreotate (18), or $^{99\text{m}}\text{Tc}$ -EDDA/HYNIC-octreotide (19) is widely being applied in clinical practice for diagnosis, staging and monitoring of NETS.

Until now ^{111}In -octreotide is the only registered imaging tracer (20). During the last few years however, SST analogues radiolabelled with the positron emitter ^{68}Ga have been used increasingly for PET imaging. Compared to SPECT using ^{111}In -analogs, PET using ^{68}Ga -analogs resulted in a higher spatial resolution, better tissue contrast, and a higher sensitivity for detection of metastases. Several studies have shown PET with ^{68}Ga -labelled SST analogs to be superior to SPECT using ^{111}In -labeled STT analogs (21, 22). In addition, as ^{68}Ga is generator-produced (23), it allows for in-house labeling and applications of ^{68}Ga in nuclear medicine departments without a cyclotron in the vicinity.

Based on the successful applications of ^{111}In -octreotide for imaging of NETs, the next logical step was to apply this radionuclide, not only emitting γ -radiation but also therapeutic Auger- and conversion electrons, at high activities for PRRT of metastasized disease as well (24, 25). Although treatment with ^{111}In -octreotide often resulted in symptoms relief in patients with metastasized NETs, objective tumor responses were rare, especially in patients with advanced disease and in patients with large tumors (8, 24, 25). Application of ^{177}Lu -DOTATATE and ^{90}Y -DOTATOC on the other hand resulted in impressive therapeutic effects (8, 26-29). Since ^{177}Lu also emits γ rays, ^{177}Lu -labelled peptides can be used for treatment as well as for dosimetry, and monitoring of tumor response. Currently the first clinical phase-3 study is running in several countries to evaluate safety and tolerability of ^{177}Lu -DOTATATE and compare therapeutic responses after ^{177}Lu -DOTATATE with those after treatment with high dose of the unlabeled SST analogue octreotide LAR (<http://clinicaltrials.gov/ct2/show/NCT01578239?term=NCT01578239&rank=1>).

As mentioned above, PRRT has shown to be a promising treatment option for NET patients. Several excellent reviews have recently described the current status of PRRT in great detail (30, 31). Within the space constraints of this article we cannot cover every aspect of this exciting field, but we aimed at conferring an appreciation of options available to increase tumor response after PRRT and point out some of the latest developments. Based on published research, below we will discuss 5 ways to increase therapeutic effects of PRRT:

Recently developed STT analogs acting as receptor antagonists instead of the now clinically applied receptor agonists are most promising, as several newly developed SSTR-antagonists showed an increased tumor uptake compared to STTR-agonists (32-34), leading to higher tumor radiation doses. Below we report on recently achieved results in different tumor models, the possible mechanism behind these results and translation of preclinical studies into the clinic.

1. Combinations of selected radionuclides labeled to SST-analogs might improve tumor responses. As dose rate, emitted energies and linear energy transfer (LET) are characteristic for every radionuclide, the radionuclides with most appropriate characteristics could be combined for optimal effects. Since the size of metastases within most patients varies from small to large tumor masses we

report on the published advantages of combined applications of ^{177}Lu and ^{90}Y for treatment of small and large metastases, respectively. Furthermore we highlight the use of several most promising α -emitters, which are being applied for PRRT in experimental studies currently.

2. Increased uptakes of radionuclides in liver metastases has been achieved after intra-arterial (i.a.) administration into the hepatic artery, compared to those after intravenous injection. Below, we describe preclinical and clinical results achieved after i.a. injection and focus on points of interest concerning this new therapeutic approach.
3. Dosimetry during PRRT is of great interest and application of patient-specific dosimetry might enable safe administration of additional treatment cycles to possibly increase tumor response to PRRT.
4. Finally, the combination of PRRT with other therapies might increase the effectiveness of treatment for NET patients. Considering this combination of treatments, a new application of PRRT includes treatment in a neo-adjuvant or adjuvant setting, enabling curative surgery after tumor mass reduction by PRRT or preventing development of metastases after spread of tumor cells during surgery. We also focus on increased therapeutic responses after the combination of PRRT and chemotherapy. Promising combinations of PRRT and chemotherapeutics are under preclinical as well as clinical evaluation.

1 RECENTLY DEVELOPED SOMATOSTATIN ANALOGS

Currently the most widely clinically used SST analogs include ^{111}In - octreotide (Octreoscan®) and ^{68}Ga -DOTATOC/DOTATATE/DOTANOC for imaging, as well as ^{177}Lu -DOTATATE and ^{90}Y -DOTATOC for therapy. Several novel, radiolabeled SST analogs are currently under preclinical and clinical evaluation, as recently reviewed by Fani et al. (30). Of particular interest are the pansomatostatin analogs, targeting multiple SSTR subtypes (35), and SSTR-antagonists. As pansomatostatin analogues like DOTA-lanreotide target more SSTR subtypes compared to e.g. DOTATOC, the use of DOTALAN can be considered in patients lacking pathologic uptake of DOTATOC (36).

Most promising results have been reported on the application of SSTR-antagonists. Until recently it was generally assumed that receptor targeting ligands should act as receptor agonists because of efficient receptor-mediated internalization into the tumor cells, leading to accumulation and long retention of radionuclides within the tumor (37). The internalization step was considered to be essential in this process. However, recent studies have shown significantly increased tumor targeting using SSTR-antagonists, despite minimal or no internalization of the receptor antagonist complex into tumor cells (32). Receptor antagonists (e.g. ^{111}In -DOTA-SST-ANT) with comparable receptor affinity as SSTR-agonists, readily bind SSTR-expressing tumors,

to a higher extent than the agonists and with a long tumor retention time, as described in a HEK-SSTR2 tumor-bearing mouse study (38). Factors that caused this phenomenon include the fact that receptor antagonists occupy more binding sites and show a lower dissociation rate than agonists (32). Cescato et al. (33) evaluated the in vitro binding of the receptor antagonist ^{177}Lu -DOTA-BASS in comparison with that of ^{177}Lu -DOTATATE in a study on tissue sections of surgically-resected SSTR2-expressing tumor samples. In all cases the tumor tissues were more intensely labeled using the SSTR antagonist, demonstrating more binding sites were detected by the antagonistic radioligand for a large variety of different tumor types, including NETs. On average a 4.2 times higher binding was found using ^{177}Lu -DOTA-BASS. This improved binding may increase the sensitivity of imaging with such receptor antagonist tracers. The first clinical data published thus far comprise a feasibility study in 5 patients, in whom it was confirmed that ^{111}In DOTA-BASS provided a higher tumor uptake and better visualization of metastatic neuroendocrine tumors than ^{111}In -DTPA-octreotide (34). Moreover, the kidney retention of the antagonistic compound was lower, resulting in a 5.2 times higher tumor to kidney ratio in favor of the receptor antagonist. Also the liver radiation dose appeared to be lower using the receptor antagonists. The lower renal and liver doses, as seen in preclinical and clinical studies (32, 34, 39) can be explained by a charge differences between the 2 compounds.

High tumor uptake, long tumor retention time and less physiologic retention of radioactivity in healthy organs indicate that SSTR antagonists are very promising not only for diagnostic, but also for therapeutic purposes. A disadvantage of these antagonists is the fact that tumor uptake and retention of these compounds is highly influenced by the choice of the chelator and radionuclide being used (40). Therefore, it can be difficult to predict tumor dosimetry for PRRT using a diagnostic SSTR antagonist labeled with another radionuclide.

Since SST is a hormone with a repressive effect on tumor growth, SSTR antagonists may theoretically exert a tumor-proliferating effect. As yet, there has been no clinical or preclinical report of increased tumor proliferation after treatment with SSTR antagonists though. More clinical trials confirming the applications of these peptide analogs to be safe and effective need to be performed now.

2 APPLICATION OF NEW AND COMBINATION OF RADIONUCLIDES

Currently ^{90}Y and ^{177}Lu are the most widely applied radionuclides for treatment with radiolabeled SST analogs. The high energy electrons (11 mm maximum tissue penetration) emitted by ^{90}Y indicate that this radionuclide will be more effective in larger tumor masses (optimal diameter of 34 mm (41)) as smaller tumors will not absorb all energy released. The low energy electrons emitted by ^{177}Lu (1.8 mm maximum tissue penetration) concordantly make this radionuclide more suitable for treatment of smaller tumor masses (optimal diameter of 2 mm) (41). These characteristics suggest that an optimal anti-tumor response in larger tumor masses as well as in smaller metastases could be achieved using a combination of both ^{90}Y -DOTATOC and ^{177}Lu -

DOTATATE. This was confirmed in a preclinical study in rats bearing both smaller and larger tumors, mimicking the varying size of metastases that can be found within one patient. The combination of ^{90}Y -DOTATOC and ^{177}Lu -DOTATATE gave superior results compared to a single dose of either ^{90}Y -DOTATOC or ^{177}Lu -DOTATATE (42). The first clinical applications of the combinations of both ^{90}Y -DOTATOC and ^{177}Lu -DOTATATE were published recently. Kunikowska et al. (43) performed a study in patients treated with ^{90}Y -DOTATATE-only or ^{177}Lu -DOTATATE plus ^{90}Y -DOTATATE (1:1 radioactivity ratio concurrent therapy). This treatment resulted in longer overall survival times than ^{90}Y -DOTATATE single therapies, whereas the safety of both methods was comparable. Villard et al. (44) in retrospect compared treatment with alternating sequential ^{177}Lu -DOTATOC and ^{90}Y -DOTATOC (DUO-PRRT) in 237 patients versus ^{90}Y -DOTATOC-only in 249 patients and concluded that their results suggested a longer survival after DUO-PRRT. A prospective clinical study, with a randomized control group and applying patient-specific dosimetry calculations is still lacking however. As discussed by Savolainen et al. (45), an optimal clinical combination of the two radiopharmaceuticals should be determined on a patient-specific basis. As will be discussed later, the kidneys belong to the dose limiting organs and considering the substantially lower dose rate of ^{177}Lu compared to ^{90}Y to the kidneys, the biologically effective dose (BED) to the kidneys should be calculated for the specific tandem combination being applied.

A most promising recent development has been the application of α -particle emitting radionuclides such as ^{213}Bi or its mother radionuclide ^{225}Ac (Figure 1) in PRRT. These radionuclides emit particles with a high energy (8.32 MeV for $^{213}\text{Bi}/^{213}\text{Po}$ and 27.5 MeV for ^{225}Ac) combined with small particle ranges of only 50-80 μm . The LET is much higher for α -particles than for β -particles, which might further enhance the therapeutic efficacy of PRRT, especially in small tumor lesions including micro-metastases. Moreover, the cytotoxic effect of α -radiation is independent of the cell cycle phase and oxygen concentration (46, 47), being beneficial especially for treatment of less oxygenated, hypoxic tumor regions. Moreover, the use of α -emitters minimizes the effect of cell cycle heterogeneity on tumor response to PRRT, whereas for β -emitters tumor responses do depend on cell cycle phase (48).

When α -emitters are stably complexed to targeting peptides and receptor density in normal tissue is relatively low, radiotoxicity in non-targeted normal tissues can be expected to be minimal, based on the short path length of α -radiation. This was confirmed in a rat study in which ^{213}Bi -DOTATOC showed a dose-related tumor anti-proliferative effect without side effects in normal organs (10). In a pilot study in three patients no short-term adverse side effects on kidney or bone marrow were found after ^{213}Bi -DOTATOC, whereas there was a marked reduction in tumor vascularity and no progression of metastases during follow up for 9 months in patients with NET refractory to ^{90}Y -DOTATOC or ^{177}Lu -DOTATOC (49).

One of the safety concerns of ^{225}Ac is the formation of four consecutive daughter radionuclides during decay. Safe application will be challenging, because the recoil kinetic energy delivered to the daughter nuclides during ^{225}Ac -decay is high, which

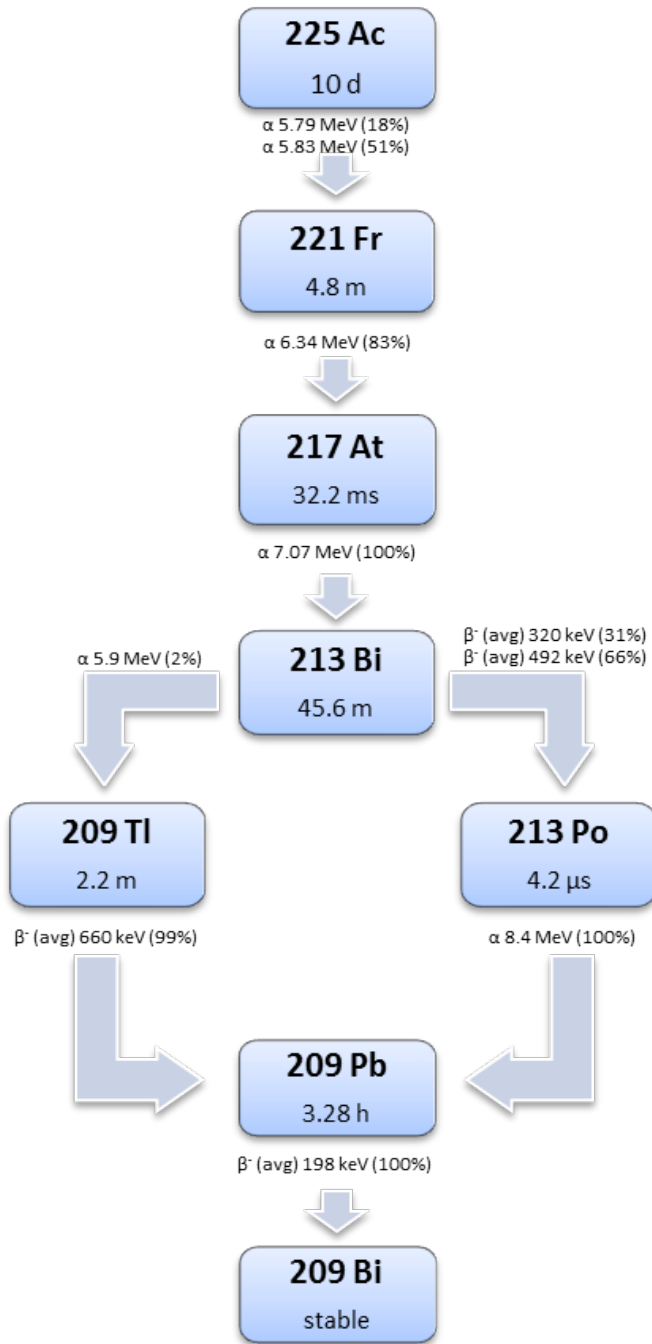


Figure 1. Decay of ^{225}Ac ; four consecutive α -particle-emitting daughter are formed during decay.

might result in α -emitting daughters free from the targeting chelator-peptide complex. An accumulation of free α -emitters like for instance ^{213}Bi in the renal cortex may cause late nephrotoxicity as was shown at the highest doses used in mice studies with ^{225}Ac -DOTATOC (47, 50). A disadvantage of the use of ^{213}Bi is its half-life of only 46 min and the fact that it is produced from a ^{225}Ac generator that generates ^{213}Bi for only 10-15 days. Nevertheless, if in phase I and II clinical trials the use of α -emitters has proven to be safe, application of these radionuclides or a combination of α - and β -emitters might be a revolutionary way to target and eradicate tumors in NET patients.

3 INTRA-ARTERIAL ADMINISTRATIONS

Unlimited growth of hepatic metastases resulting in liver failure is one of the most common causes of death in patients with gastroenteropancreatic (GEP)-NETs. Therefore liver-directed therapies are developed such as hepatic embolization of the liver metastases and debulking hepatectomy, if possible. In line with these local therapies, several research groups have examined if local intra-arterial (i.a.) administration could increase uptake of radionuclides in hepatic metastases compared to the uptake after systemic intravenous (i.v.) administration (51, 52). As hepatic metastases mainly depend on the hepatic artery for achieving their oxygen and nutrients, the higher arterial radiopeptide uptake during the first pass through the liver after i.a. administration was expected to lead to superior tumor uptake and better options for treatment of patients with a high metastatic liver load (52). In a preclinical rat liver metastasis model, Pool et al. (53) demonstrated ^{111}In -DTPA-octreotide tumor uptake to be twice as high after loco-regional administration via the hepatic artery than after i.v. administration. Also in a patient study increased uptake of radionuclides in liver metastases has been reported after i.a. administration (54). Kratochwil et al. (54) compared standard uptake values (SUV) after i.a. administration of ^{68}Ga -DOTATOC versus i.v. administration in 15 NET patients; SUVs were 3.75-fold higher after i.a. administration (54). The same group (52) performed a pilot study in which ^{90}Y - or ^{177}Lu -DOTATOC was infused via the hepatic artery in 15 patients with liver metastases arising from GEP-NETs. This resulted in a higher rate of objective radiologic responses than typically reported for the intravenous regime, i.e. 60% vs. 30% respectively. However, the promising observations of locally administered and β -particle-based PRRT need to be confirmed in a higher number of patients and compared with a proper control group treated intravenously.

Beside the favorable higher uptake of radiolabeled somatostatin analogs after i.a. administration, a locally higher serum concentration of the radiopeptide increases the risk of (partial) receptor saturation. Kratochwil et al. (52) assessed the pharmacokinetics using dynamic imaging after i.a. and i.v. infusion of ^{111}In -DOTATOC (250 MBq/150 μg) within the same patients (n=4). I.a. administration resulted in 3.5-fold increase of uptake in the initial phase, which decreased after 10 min and according to the authors this was due to saturation effects. This indicated that indeed maximum achievable tumor uptake might be limited by receptor saturation. Therefore, a higher specific activity, which means an increased amount of radioactivity labeled to the same

amount of SST analog, might be pivotal for this kind of therapy. Increased specific activity, either by optimization of the radiolabelling procedure or by application of non-carrier-added ^{177}Lu labeled to the peptide, might therefore enable enhanced levels of radionuclides within liver metastases after i.a. administration.

Even though i.a. administration is far more complex than i.v. administration, it has nevertheless been reported to be a safe procedure (54). Therefore, considering the results achieved in pilot experiments, a randomized clinical trial comparing responses to PRRT after i.a. administration versus responses after i.v. administration in NET patients with a high hepatic tumor load would be of very high interest, enabling a clear evaluation of the potential treatment benefits achieved after i.a. administration.

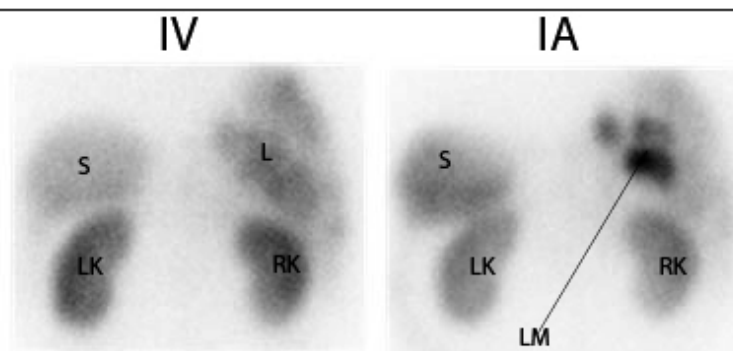


Figure 2. Planar posterior image of the liver 24h after i.v. and 24h after i.a. administration of ^{111}In -octreotide. LK: left kidney, RK: right kidney, S: spleen, L: liver and LM: points to three liver metastases visible after i.a. injection. After i.a. administration there was increased tumour uptake of ^{111}In -octreotide.

4 DOSIMETRY OF THE TUMOR AND ORGANS AT RISK

4.1 Organs at risk

Severe permanent renal toxicity (grade 4) has been observed to occur late (1 to 10 years) after the start of PRRT treatment with ^{90}Y -DOTA-octreotide in 102 out of 1109 (9%) patients after a fixed activity of 3.7 GBq/m² body surface area (55). Severe haematological toxicity (grade 3 to 4) occurred in 13% of the patients, mostly transient, but a few (3 out of 1109) developing into myelodysplastic syndrome (MDS) or leukaemia (44). Haematological toxicity of equivalent severity (grade 3 or 4) was also reported in 10% of 504 patients treated with ^{177}Lu -DOTA-octreotate according to a fixed dosing scheme of 4 x 7.4 GBq with again some (3 out of 504) developing into MDS 2 to 3 years after the last treatment (29). The same level of haematological toxicity was reported by Sabet: 23/203 (11%) developed grade 3 and 4 hematological toxicity and 3 patients (1.4%) developed MDS (56). Radiation induced renal insufficiency has

not been reported in any study of therapy with ^{177}Lu -DOTA-octreotate as single therapy.

4.2 Kidney dosimetry

Physiological uptake of peptides in the kidneys is concentrated at the proximal tubuli distributed over the cortex where reabsorption takes place of proteins from the primary urine back into the blood stream. This uptake can be partially blocked by giving the patients a co-infusion of amino-acids, which results in 35% reduction of renal uptake in the clinical practice of PRRT (57). Retrospective analysis of the cases of late-occurring renal toxicity with ^{90}Y -DOTA-octreotide showed that the absorbed dose is a predictor for renal toxicity (58). Accurate dosimetry is needed, which accounts for both the individual kidney kinetics and the actual kidney volume irradiated. The absorbed dose to the kidneys per therapy cycle was also an important risk factor; a higher dose rate and dose per fraction leads to more renal damage, as expressed by the Biologically Effective Dose according to the Linear Quadratic model:

With T_m the repair half life of repairable damage, T_{eff} the effective half life of the kidney dose build-up, a/b the radiation sensitivity parameter, d the absorbed dose per therapy cycle and D the total absorbed dose. The dose threshold for renal damage after external beam radiation given in 2 Gy fractions is 20-23 Gy, whereas after ^{90}Y -DOTA-octreotide a 5-8 Gy higher threshold was observed, which could be well explained by the LQ model-based BED (59).

Renal toxicity by radiation exposure develops slowly after the initial tubular radiation damage. Besides BED additional risk factors are older age, diabetes, hypertension and usage of nephrotoxic drugs prior to PRRT (60, 61). From these findings, two absorbed dose thresholds are now being postulated: a BED of 40 Gy for patients without risk factors and a BED of 28 Gy for patients with multiple risk factors for renal problems (61). Patients with risk factors also tend to show a higher dose to the kidneys per administered activity compared to patients without risk factors, although more patients than the 28 patients (of which 11 with risk factors) studied are needed for significance (62).

Tailoring personalized PRRT to the absorbed dose limit requires high accuracy in the dosimetric methods. The inter-patient variability in kidney dosimetry is too large to justify the use of a group-averaged absorbed dose, like customary for diagnostic radiopharmaceuticals. The BED-based limits derived for ^{90}Y -DOTA-octreotide therapy are assumed to be also valid for ^{177}Lu -DOTA-octreotate, although no renal toxicity has been observed for this therapy. Dosimetry in the phase 1 trial with ^{90}Y -DOTA-octreotide, a pure β -emitter, was based on pretherapeutic imaging with the PET analogue ^{86}Y -DOTA-octreotide (63). This method resulted in proof of a correlation between BED and renal toxicity (58). Kidney dosimetry for α -emitters is traditionally based on planar imaging with activity quantization by the conjugate view method. In a comparison between conjugate view and quantitative SPECT imaging of the kidney

uptake of ^{177}Lu -DOTA-octreotate the planar method resulted in an overestimation of the absorbed dose together with a high variance in background, both due to overlapping radioactivity (64). Post-therapeutic planar imaging after PRRT with the use of the co-administration of ^{111}In -DOTA-octreotide did, however, yield supporting evidence for the toxicity threshold with ^{90}Y -DOTA-octreotide PRRT (59, 61).

In a dosimetry study with 200 patients treated with ^{177}Lu -DOTA-octreotide the range in absorbed dose was between 2 and 10 Gy (median 4.5 Gy) per therapy cycle, corresponding to a BED range of 2-16 Gy (median: 4.9 Gy) (65).

The difference in renal toxicity incidence after ^{90}Y -DOTA-octreotide or after ^{177}Lu -DOTA-octreotate at almost equivalent kidney doses seems to be evident. The radiation exposure by ^{90}Y will be more homogeneous than by ^{177}Lu , because of the longer tissue penetration range of the particles emitted by ^{90}Y in comparison to the shorter range of those emitted by ^{177}Lu . The activity distribution of the peptide uptake in the kidney is not homogeneous as was shown in ex-vivo autoradiographs of excised kidney sections from patients injected with ^{111}In -DTPA-octreotide prior to nephrectomy (66). The radioactivity was mostly confined to the cortex with a streaky pattern gradient from high concentration in the outer part to low concentration in the medulla. (67). Yttrium-90 resulted in a much more homogeneous dose distribution than ^{177}Lu (78). The absorbed dose distribution in the kidneys has been also calculated based on SPECT/CT with ^{111}In -DTPA-octreotide (68). Uptake in the cortex and fall-off of the absorbed dose at the boundaries already introduces inhomogeneities in the dose distribution, although not as extreme as for the ex-vivo autoradiography based ^{177}Lu dose distribution. The exact dose limit for ^{177}Lu -DOTA-octreotate is still unclear without clear dose-related renal toxicity and also the sparing effect of the inhomogeneous dose distribution is speculative.

4.3 Bone marrow dosimetry

The absorbed dose to the bone marrow is not always routinely determined, as it involves regular blood sampling and determination of the whole body distribution. The blood-based method is used for β -particle bone marrow dosimetry, as for peptides the bone marrow radioactivity concentration is equivalent to the concentration in blood (69, 70). The γ -radiation from ^{177}Lu gives an additional cross-dose from the total body and from organs and tumors with radioactivity uptake, which can form more than 60% of the total bone marrow dose, but it also shows high variability (69). The cumulative limit in absorbed bone marrow dose is considered to be 2 Gy, in analogy with the limits used for ^{131}I thyroid cancer therapy (71) to prevent direct unrecoverable hematological toxicity. The probability for inducing leukemia and MDS, however, shows a linear relation with absorbed dose and it is unclear if a dose limit would help to keep this risk within reasonable risk bounds.

With standardized dosimetry methods no clear relationship has been reported for the relation between hematological toxicity and absorbed bone marrow dose (69, 72). An

almost linear relation is obtained between dose and reduction of platelet counts at nadir after ^{90}Y -DOTA-octreotide therapy (69, 72). The bone marrow dose needs to be corrected by a weight function aggravating the effects in patients with low baseline platelet counts without prior chemotherapy and normal recovery.

4.4 Tumor dosimetry

The target for PRRT is metastasized disease including smaller and microscopic lesions, but it is difficult to determine the absorbed dose in lesions smaller than 1 cm in size. The absorbed dose needed for local control of pancreatic neuroendocrine tumors with adjuvant external beam radiotherapy is in the order of 50 Gy (73). With PRRT the median absorbed dose to obtain a volume reduction of neuroendocrine tumors by ^{90}Y -DOTA-octreotide is 232 Gy (74). The difference in doses can be partly explained by the difference in target size (tumor bed with minimal disease vs. tumors ranging between 2 and 500 g) and the difference in dose rate and uniformity.

The absorbed dose to the tumor shows a huge inter-patient variance. Liver metastases were reported to get a dose of 167 ± 139 Gy for the 1st treatment cycle of 7.4 GBq (75). Responders showed a >20% decrease of absorbed dose in the following treatment cycles. Variance in the tumor dose and its reduction with each next therapy cycle was also reported by Garkavij (64); the median absorbed dose to the tumor in their study with ^{177}Lu -DOTA-octreotate treated patient was reported to be 207 Gy (range 17-387 Gy).

4.5 Treatment planning for PRRT

Hardly any centers follow a dosimetry-guided administration scheme for PRRT. Most PRRT therapies are given on a fixed activity administration scheme. With ^{90}Y -DOTA-octreotide the administered activity is scaled by the patient's body surface area at doses of 3.7 GBq/m². This dosing scheme is based on phase 1 trials with the compound, indicating a dose limiting toxicity in the kidneys above 7.4 GBq/m² after a short follow-up of 150 days and partly without kidney protection by amino acid infusion (76). Longer follow-up of the patients by the other phase 1 trials did show the benefit of dosimetry guided therapy or, as a second option, to use lower administrated activities per treatment cycle (58, 61, 63). By lowering the activity per treatment cycle the total BED will decrease to the kidneys and thus reduce the risk of renal toxicity.

For ^{177}Lu -DOTA-octreotate the most commonly used fixed dosing scheme is based on the protocol used by Kwekkeboom et al.: 4 treatment cycles of 7.4 GBq (29). Originally some patients were excluded from getting the 4th treatment cycle, as they would otherwise exceed the conservative kidney dose limit of 23 Gy. This same limit of 23 Gy is used in the dosimetry guided treatment schedule used by Sandström et al.: the 200 patients in this study were treated by consecutive cycles of 7.4 GBq, until the 23 Gy was reached; 50% of the patients got more than 4 cycles, ranging between 2 and 10 (65).

A treatment schedule based on dosimetry should be focusing on both the absorbed dose to the kidneys and to the bone marrow. Volume delineation of the renal cortex is not a straightforward procedure and time-consuming when done manually. The exact volume is not needed when using the average activity concentrations over a volume inside a representative sample of the kidney (65). The QSPECT method uses this same principle, but also transforms the activity concentration to a standard uptake value (SUV) by scaling with the total body uptake measured at 40-60 min after the ^{177}Lu therapeutic dose before any void (77). This same method is also used for determining the absorbed dose in a section of the patient's spine as a representative sample for the bone marrow.

Patients that are retreated with 2 additional cycles of ^{177}Lu -DOTA-octreotate PRRT after relapse following the first treatment do not show renal toxicity (78, 79). Considering the variance observed in the kidney dosimetry the cumulative activity of 44 GBq could lead to a kidney BED between 11 and 90 Gy, according to the range reported in 200 patients by Sandström (65).

5 COMBINATION OF PRRT WITH OTHER TREATMENTS

Interesting combination treatments include PRRT as adjuvant treatment after surgery, as this approach might prevent development of tumor lesions after spread of tumor cells during surgery, or eradicate micro-metastases that already developed prior to surgery. This PRRT approach was studied in a preclinical model, mimicking perioperative tumor spill by injection of SSTR-positive tumor cells into the portal vein. In this study ^{177}Lu -DOTATATE treatments significantly reduced or prevented tumor development (80). PRRT can also be applied as neoadjuvant treatment to achieve tumor size reduction enabling curative surgery. This has been successfully performed recently in two patients suffering from pancreatic NETs (81, 82).

Another option to improve anti-tumor response is the combination of PRRT with chemotherapeutics; the latter may be applied for radiosensitization of the tumor cells based on cellular and molecular interaction, like enhancing DNA damage and repair, cell-cycle synchronization, enhanced apoptosis, tumor cell re-oxygenation or inhibition of cell proliferation. Radiosensitizing agents are commonly used in combination with external beam radiation therapy (EBRT). Drugs with radiosensitizing effects based on cellular and molecular interactions include camptothecin, gemcitabine, and 5-FU or its prodrug capecitabine (Cap). The radiosensitizing effect of camptothecin is due to its effect of preventing DNA relegation by binding to topoisomerase I, which inhibits repair of single stranded breaks caused by radiation. Gemcitabine causes accumulation of tumor cells in the radiosensitive G2/M phase, making the tumor cells more sensitive for PRRT. Cap not only abrogates DNA replication because of insertion of chain-stopping nuclides, it also is a thymidine synthetase inhibitor causing depletion of thymidine. Besides radiosensitizing effects, Cap has also been described to deplete the tumor cell's methylguanine DNA methyl transferase (MGMT), an enzyme responsible for the repair of DNA damage caused by the DNA alkylating agent temozolomide

(TMZ) (50). In their clinical study Claringbold et al. used a treatment scheme based on these findings (83). This scheme existed of 14 days of Cap treatment, starting 5 days before radiopeptide administration, and the administration of TMZ during the last 5 days of Cap treatment (83).

Until now the radiosensitizing effects as described above have been the main focus for clinical application of combinations of PRRT with chemotherapeutics (83-86). Some challenges have to be faced during such studies though. So, during PRRT tumor uptake of radionuclides depends on both tumor vascularization and SSTR-expression, which both can be affected by anticancer therapeutics (87-89).

In our preclinical study in mice an increased tumor perfusion was measured after TMZ treatment for 14 days. This resulted in an increased uptake of radiopeptide after TMZ treatment (89).

Considering SSTR expression, Fueger et al. examined the possible influence of cytotoxic or cytostatic agents on binding characteristics of an SST ligand *in vitro* (87). They found a reduced expression of high-affinity DOTA-LAN binding sites in response to the incubation with gemcitabine, camptotecin, mitomycin C and doxorubicin (DOX) (Table 1). In case of gemcitabine, a 4-day recovery eventually resulted in a significant up-regulation of SSTR. This was confirmed in a study by Nayak et al. (90), in which uptake of ^{177}Lu -DOTATOC in cells in culture was 1.5-3 times increased 4 days after gemcitabine exposure compared to that in untreated control cells. Besides an SSTR up-regulation the treated cells also showed cell cycle modulation; most of the viable cells were in the radiosensitive G2/M phase. These effects resulted in a synergistic effect of gemcitabine and ^{177}Lu -DOTATOC (90).

As RAD001 or everolimus has been shown to be effective against pancreatic NETs (91), a combination of PRRT with RAD001 could be another promising option for PRRT combination therapy. In a preclinical study however, the combination of RAD001 and PRRT was less effective compared to PRRT-only (68). As RAD001 has been shown to cause a G1 arrest (92), Pool et al. suggested this to be a possible explanation for the reduced tumor response to the combination of mTOR-inhibitor everolimus (RAD001) with ^{177}Lu -DOTATATE (93). Because NET cells have a peak of radio-resistance during early G1 phase (48), the tumor cells may have been less sensitive to ^{177}Lu -DOTATATE when administered after start of RAD001 treatment.

Considering the clinical application of combining PRRT with other anticancer agents, currently only phase II clinical trials have been reported. In these studies PRRT using ^{177}Lu -DOTATATE has been combined with 5-FU or Cap whether or not supplemented with TMZ. 5-FU combined with high-dose ^{111}In -octreotide appeared to be safe in a study with 21 patients, but did not add to therapeutic response rates compared to ^{111}In -octeotide treatments-only (94). Administration of 5-FU or Cap + PRRT was reported to be safe based on the studies of Barber et al. (84) and Van Essen et al. (85). The study reported by Van Essen et al. was continued by a two-armed, randomized, prospective study in which the combination of ^{177}Lu -DOTATATE with Cap is being

Table 1: combination of PRRT with other therapeutic agents

Therapeutic agent:	Mechanism of action:	Studies:	Results:	References:
Gemcitabine	Chain stopper and ribonuclease reductase inhibitor -> Chromosome aberration -> Cell cycle synchronization	In vitro study	SSTR expression was down regulated during exposure, which turned over in an up regulation 4 days after exposure, resulting in synergism with ¹⁷⁷ Lu-DOTATATE	(87, 90)
Camptothecin	Binds to Topoisomerase I and DNA complex, preventing DNA relegation -> Enhanced apoptosis -> Cell cycle arrest	In vitro study	SSTR expression was down regulated during camptothecin exposure	(87)
Mitomycin C	Crosslinking DNA	In vitro study	SSTR expression was down regulated during Mitomycin C exposure	(87)
Cisplatin	Crosslinking DNA -> Repair inhibition	In vivo study	Cisplatin + ¹⁷⁷ Lu-DOTATOC was 23% more effective compare to ¹⁷⁷ Lu-DOTATOC alone	(87)
Doxorubicin	Intercalating with DNA -> Cell cycle arrest	In vivo study	Doxorubicin + ¹⁷⁷ Lu-DOTATOC was 14% more effective compared to ¹⁷⁷ Lu-DOTATOC alone	(87)
RAD001 (everolimus)	mTOR inhibitor -> Cell cycle arrest	In vivo study	RAD001 + ¹⁷⁷ Lu-DOTATATE was less effective compared to ¹⁷⁷ Lu-DOTATATE alone	(93)
5-Fluouracil or its prodrug capecitabine	Chain stopper and thymidine synthetase inhibitor -> Repair inhibition -> Cell cycle arrest	Phase II clinical trial	Combination with ¹⁷⁷ Lu-DOTATATE appeared to be safe	(84-86)
Temozolomide	DNA alkylating agent	Phase II clinical trial	Combination with Capecitabine and ¹⁷⁷ Lu-DOTATATE appeared to be safe	(83)

compared with ^{177}Lu -DOTATATE-only. Claringbold et al. (86), (83) concluded that both Cap and the combination of Cap and TMZ could be safely combined with PRRT. After their study combining Cap and TMZ with PRRT in 35 patients, the authors reported that response rates and progression free survival (PFS) times appeared to exceed results with ^{177}Lu -DOTATATE as a single agent (83). In their study GEP-NETs showed better responses than enteric NETs. Therefore, the overall response rate seen in GP NETs almost certainly reflected the synergistic effect of TMZ, whereas partial responses seen in enteric NET patients was attributable to the radiopeptide component of the multimodality therapy. This suggests that for each subtype of NET the optimal combination of PRRT and chemotherapy should be selected.

CONCLUDING REMARKS

Despite PRRT being a most promising therapy for NET patients for whom curative surgery is not an option anymore, there is still room for improvement as discussed in this review.

The increased tumor uptake of radionuclides reported for radiolabelled SSTR antagonists or i.a. administration is promising. More clinical studies should follow to establish the value of these approaches.

Regarding the combined use of ^{90}Y and ^{177}Lu , there is a clear need for comparative studies before effectiveness of this combination can be evaluated. Alpha-emitters have promising features; the first studies have just been performed and longer follow-up periods are needed now to investigate potential long-term toxicity.

Considering individual dosimetry, a large percentage of patients might receive additional treatment cycles before reaching dose-limiting toxicity as has been determined in kidneys and bone marrow. Whether or not additional cycles will have a major influence on tumor response however, is not known yet.

Combinations of PRRT with other anticancer therapies have appeared to be safe, but until now only phase II clinical trials have been reported. In addition, only a small number of anticancer agents have been combined with PRRT, leaving numerous possible options for further research.

We conclude that currently several directions to improve PRRT effects have been indicated, but additional preclinical and especially translational and clinical research is needed to obtain further proof of value.

REFERENCES

1. Hemminki, K. and X. Li, *Incidence trends and risk factors of carcinoid tumors: a nationwide epidemiologic study from Sweden*. *Cancer*, 2001. **92**(8): p. 2204-10.
2. Modlin, I.M., K.D. Lye, and M. Kidd, *A 5-decade analysis of 13,715 carcinoid tumors*. *Cancer*, 2003. **97**(4): p. 934-59.
3. Yao, J.C., et al., *One hundred years after "carcinoid": epidemiology of and prognostic factors for neuroendocrine tumors in 35,825 cases in the United States*. *J Clin Oncol*, 2008. **26**(18): p. 3063-72.
4. Modlin, I.M., et al., *Therapeutic options for gastrointestinal carcinoids*. *Clin Gastroenterol Hepatol*, 2006. **4**(5): p. 526-47.
5. Kwekkeboom, D.J., et al., *Peptide receptor radionuclide therapy in patients with gastroenteropancreatic neuroendocrine tumors*. *Semin Nucl Med*, 2010. **40**(2): p. 78-88.
6. Bodei, L., et al., *Peptide receptor radionuclide therapy with (1)(7)(7)Lu-DOTATATE: the IEO phase I-II study*. *Eur J Nucl Med Mol Imaging*, 2011. **38**(12): p. 2125-35.
7. van Essen, M., et al., *Peptide receptor radionuclide therapy with 177Lu-octreotate in patients with foregut carcinoid tumours of bronchial, gastric and thymic origin*. *Eur J Nucl Med Mol Imaging*, 2007. **34**(8): p. 1219-27.
8. Waldherr, C., et al., *The clinical value of (90Y-DOTA)-D-Phe1-Tyr3-octreotide (90Y-DOTATOC) in the treatment of neuroendocrine tumours: a clinical phase II study*. *Ann Oncol*, 2001. **12**(7): p. 941-5.
9. Taniyama, Y., et al., *Systemic distribution of somatostatin receptor subtypes in human: an immunohistochemical study*. *Endocr J*, 2005. **52**(5): p. 605-11.
10. Reubi, J.C., et al., *Detection of somatostatin receptors in surgical and percutaneous needle biopsy samples of carcinoids and islet cell carcinomas*. *Cancer research*, 1990. **50**(18): p. 5969-77.
11. Reubi, J.C., et al., *Somatostatin receptor sst1-sst5 expression in normal and neoplastic human tissues using receptor autoradiography with subtype-selective ligands*. *Eur J Nucl Med*, 2001. **28**(7): p. 836-46.
12. Patel, Y.C., *Somatostatin and its receptor family*. *Front Neuroendocrinol*, 1999. **20**(3): p. 157-98.
13. Krenning, E.P., et al., *Somatostatin receptor scintigraphy with (111In-DTPA-D-Phe1)- and (123I-Tyr3)-octreotide: the Rotterdam experience with more than 1000 patients*. *Eur J Nucl Med*, 1993. **20**(8): p. 716-31.
14. Kwekkeboom, D.J., et al., *(177Lu-DOTAOTyr3)octreotate: comparison with (111In-DTPAo)octreotide in patients*. *Eur J Nucl Med*, 2001. **28**(9): p. 1319-25.
15. Rosenberg, J.M., *Octreotide: a synthetic analog of somatostatin*. *Drug Intell Clin Pharm*, 1988. **22**(10): p. 748-54.
16. Rinke, A., et al., *Placebo-controlled, double-blind, prospective, randomized study on the effect of octreotide LAR in the control of tumor growth in patients with metastatic neuroendocrine midgut tumors: a report from the PROMID Study Group*. *J Clin Oncol*, 2009. **27**(28): p. 4656-63.
17. Ambrosini, V., et al., *(6)(8)Ga-labelled peptides for diagnosis of gastroenteropancreatic NET*. *Eur J Nucl Med Mol Imaging*, 2012. **39** **Suppl 1**: p. S52-60.

18. Hubalewska-Dydejczyk, A., et al., *^{99m}Tc-EDDA/HYNIC-octreotate scintigraphy, an efficient method for the detection and staging of carcinoid tumours: results of 3 years' experience.* Eur J Nucl Med Mol Imaging, 2006. **33**(10): p. 1123-33.
19. Sepulveda-Mendez, J., et al., *Specificity and sensitivity of (9)(9)mTc-EDDA/HYNIC-Tyr(3)-octreotide ((9)(9)mTc-TOC) for imaging neuroendocrine tumors.* Nucl Med Commun, 2012. **33**(1): p. 69-79.
20. Bombardieri, E., et al., *¹¹¹In-pentetreotide scintigraphy: procedure guidelines for tumour imaging.* Eur J Nucl Med Mol Imaging, 2010. **37**(7): p. 1441-8.
21. Gabriel, M., et al., *⁶⁸Ga-DOTA-Tyr3-octreotide PET in neuroendocrine tumors: comparison with somatostatin receptor scintigraphy and CT.* J Nucl Med, 2007. **48**(4): p. 508-18.
22. Hofmann, M., et al., *Biokinetics and imaging with the somatostatin receptor PET radioligand (68)Ga-DOTATOC: preliminary data.* Eur J Nucl Med, 2001. **28**(12): p. 1751-7.
23. Rosch, F. and R.P. Baum, *Generator-based PET radiopharmaceuticals for molecular imaging of tumours: on the way to THERANOSTICS.* Dalton Trans, 2011. **40**(23): p. 6104-11.
24. Valkema, R., et al., *Phase I study of peptide receptor radionuclide therapy with (In-DTPA)octreotide: the Rotterdam experience.* Semin Nucl Med, 2002. **32**(2): p. 110-22.
25. Anthony, L.B., et al., *Indium-111-pentetreotide prolongs survival in gastroenteropancreatic malignancies.* Semin Nucl Med, 2002. **32**(2): p. 123-32.
26. Waldherr, C., et al., *Tumor response and clinical benefit in neuroendocrine tumors after 7.4 GBq (90)Y-DOTATOC.* J Nucl Med, 2002. **43**(5): p. 610-6.
27. Bodei, L., et al., *Receptor-mediated radionuclide therapy with ⁹⁰Y-DOTATOC in association with amino acid infusion: a phase I study.* Eur J Nucl Med Mol Imaging, 2003. **30**(2): p. 207-16.
28. Valkema, R., et al., *Survival and response after peptide receptor radionuclide therapy with (90Y-DOTA0,Tyr3)octreotide in patients with advanced gastroenteropancreatic neuroendocrine tumors.* Semin Nucl Med, 2006. **36**(2): p. 147-56.
29. Kwekkeboom, D.J., et al., *Treatment with the radiolabeled somatostatin analog (177 Lu-DOTA 0,Tyr3)octreotate: toxicity, efficacy, and survival.* J Clin Oncol, 2008. **26**(13): p. 2124-30.
30. Fani, M., H.R. Maecke, and S.M. Okarvi, *Radiolabeled peptides: valuable tools for the detection and treatment of cancer.* Theranostics, 2012. **2**(5): p. 481-501.
31. Teunissen, J.J., et al., *Nuclear medicine techniques for the imaging and treatment of neuroendocrine tumours.* Endocrine-related cancer, 2011. **18 Suppl 1**: p. S27-51.
32. Ginj, M., et al., *Radiolabeled somatostatin receptor antagonists are preferable to agonists for in vivo peptide receptor targeting of tumors.* Proc Natl Acad Sci U S A, 2006. **103**(44): p. 16436-41.
33. Cescato, R., et al., *Evaluation of ¹⁷⁷Lu-DOTA-sst2 antagonist versus ¹⁷⁷Lu-DOTA-sst2 agonist binding in human cancers in vitro.* Journal of nuclear medicine : official publication, Society of Nuclear Medicine, 2011. **52**(12): p. 1886-90.

34. Wild, D., et al., *First clinical evidence that imaging with somatostatin receptor antagonists is feasible*. Journal of nuclear medicine : official publication, Society of Nuclear Medicine, 2011. **52**(9): p. 1412-7.
35. Putzer, D., et al., *Somatostatin receptor PET in neuroendocrine tumours: 68Ga-DOTA0,Tyr3-octreotide versus 68Ga-DOTA0-lanreotide*. Eur J Nucl Med Mol Imaging, 2013. **40**(3): p. 364-72.
36. Virgolini, I., et al., *Comparative somatostatin receptor scintigraphy using in-111-DOTA-lanreotide and in-111-DOTA-Tyr3-octreotide versus F-18-FDG-PET for evaluation of somatostatin receptor-mediated radionuclide therapy*. Ann Oncol, 2001. **12 Suppl 2**: p. S41-5.
37. Reubi, J.C., *Peptide receptors as molecular targets for cancer diagnosis and therapy*. Endocr Rev, 2003. **24**(4): p. 389-427.
38. Wang, X., et al., *Comprehensive evaluation of a somatostatin-based radiolabelled antagonist for diagnostic imaging and radionuclide therapy*. Eur J Nucl Med Mol Imaging, 2012. **39**(12): p. 1876-85.
39. Tulipano, G., et al., *Characterization of new selective somatostatin receptor subtype-2 (sst2) antagonists, BIM-23627 and BIM-23454. Effects of BIM-23627 on GH release in anesthetized male rats after short-term high-dose dexamethasone treatment*. Endocrinology, 2002. **143**(4): p. 1218-24.
40. Fani, M., et al., *PET of somatostatin receptor-positive tumors using 64Cu- and 68Ga-somatostatin antagonists: the chelate makes the difference*. J Nucl Med, 2011. **52**(7): p. 1110-8.
41. O'Donoghue, J.A., M. Bardies, and T.E. Wheldon, *Relationships between tumor size and curability for uniformly targeted therapy with beta-emitting radionuclides*. J Nucl Med, 1995. **36**(10): p. 1902-9.
42. de Jong, M., et al., *Combination radionuclide therapy using 177Lu- and 90Y-labeled somatostatin analogs*. Journal of nuclear medicine : official publication, Society of Nuclear Medicine, 2005. **46 Suppl 1**: p. 13S-7S.
43. Kunikowska, J., et al., *Clinical results of radionuclide therapy of neuroendocrine tumours with 90Y-DOTATATE and tandem 90Y/177Lu-DOTATATE: which is a better therapy option?* Eur J Nucl Med Mol Imaging, 2011. **38**(10): p. 1788-97.
44. Villard, L., et al., *Cohort study of somatostatin-based radiopeptide therapy with ((90)Y-DOTA)-TOC versus ((90)Y-DOTA)-TOC plus ((177)Lu-DOTA)-TOC in neuroendocrine cancers*. J Clin Oncol, 2012. **30**(10): p. 1100-6.
45. Savolainen, S., et al., *Radiation dosimetry is a necessary ingredient for a perfectly mixed molecular radiotherapy cocktail*. Eur J Nucl Med Mol Imaging, 2012. **39**(3): p. 548-9.
46. Nayak, T.K., et al., *Somatostatin-receptor-targeted alpha-emitting 213Bi is therapeutically more effective than beta(-)-emitting 177Lu in human pancreatic adenocarcinoma cells*. Nuclear medicine and biology, 2007. **34**(2): p. 185-93.
47. Miederer, M., et al., *Preclinical evaluation of the alpha-particle generator nuclide 225Ac for somatostatin receptor radiotherapy of neuroendocrine tumors*. Clin Cancer Res, 2008. **14**(11): p. 3555-61.
48. Dodson, H., S.P. Wheatley, and C.G. Morrison, *Involvement of centrosome amplification in radiation-induced mitotic catastrophe*. Cell Cycle, 2007. **6**(3): p. 364-70.

49. Giesel, F., et al., *Monitoring of perfusion changes after systemic versus selective arterial ¹⁷⁷Lu/⁹⁰Y-DOTATOC and ²¹³Bi-DOTATOC radiopeptide therapy using contrast-enhanced ultrasound in liver metastatic neuroendocrine cancer*. European journal of nuclear medicine and molecular imaging, 2011. **38**(Suppl. 2): p. S117.
50. Kulke, M.H., et al., *O⁶-methylguanine DNA methyltransferase deficiency and response to temozolomide-based therapy in patients with neuroendocrine tumors*. Clin Cancer Res, 2009. **15**(1): p. 338-45.
51. Limouris, G.S., et al., *Selective hepatic arterial infusion of In-111-DTPA-Phe1-octreotide in neuroendocrine liver metastases*. Eur J Nucl Med Mol Imaging, 2008. **35**(10): p. 1827-37.
52. Kratochwil, C., et al., *Hepatic arterial infusion enhances DOTATOC radiopeptide therapy in patients with neuroendocrine liver metastases*. Endocrine-related cancer, 2011. **18**(5): p. 595-602.
53. Pool, S.E., B. Kam, and W.A.P. Breeman, *Increasing intrahepatic tumour uptake of ¹¹¹In-DTPA-octreotide by loco regional administration*. Eur J Nucl Med Mol Imaging, 2009. **36**: p. S427.
54. Kratochwil, C., et al., *Intraindividual comparison of selective arterial versus venous ⁶⁸Ga-DOTATOC PET/CT in patients with gastroenteropancreatic neuroendocrine tumors*. Clin Cancer Res, 2010. **16**(10): p. 2899-905.
55. Imhof, A., et al., *Response, survival, and long-term toxicity after therapy with the radiolabeled somatostatin analogue (⁹⁰Y-DOTA)-TOC in metastasized neuroendocrine cancers*. J Clin Oncol. **29**(17): p. 2416-23.
56. Sabet, A., et al., *Long-Term Hematotoxicity After Peptide Receptor Radionuclide Therapy with ¹⁷⁷Lu-Octreotate*. J Nucl Med.
57. Rolleman, E.J., et al., *Safe and effective inhibition of renal uptake of radiolabelled octreotide by a combination of lysine and arginine*. Eur J Nucl Med Mol Imaging, 2003. **30**(1): p. 9-15.
58. Barone, R., et al., *Patient-specific dosimetry in predicting renal toxicity with (⁹⁰Y-DOTATOC: relevance of kidney volume and dose rate in finding a dose-effect relationship*. J Nucl Med, 2005. **46 Suppl 1**: p. 99S-106S.
59. Wessels, B.W., et al., *MIRD pamphlet No. 20: the effect of model assumptions on kidney dosimetry and response--implications for radionuclide therapy*. J Nucl Med, 2008. **49**(11): p. 1884-99.
60. Valkema, R., et al., *Long-term follow-up of renal function after peptide receptor radiation therapy with (⁹⁰Y-DOTA(0),Tyr(3)-octreotide and (¹⁷⁷Lu-DOTA(0), Tyr(3)-octreotate*. J Nucl Med, 2005. **46 Suppl 1**: p. 83S-91S.
61. Bodei, L., et al., *Long-term evaluation of renal toxicity after peptide receptor radionuclide therapy with ⁹⁰Y-DOTATOC and ¹⁷⁷Lu-DOTATATE: the role of associated risk factors*. Eur J Nucl Med Mol Imaging, 2008. **35**(10): p. 1847-56.
62. Guerriero, F., et al., *Kidney dosimetry in (¹)(⁷)(⁷)Lu and (⁹)(⁰)Y peptide receptor radionuclide therapy: influence of image timing, time-activity integration method, and risk factors*. Biomed Res Int. **2013**: p. 935351.
63. Jamar, F., et al., *⁸⁶Y-DOTA(0)-D-Phe1-Tyr3-octreotide (SMT487)--a phase 1 clinical study: pharmacokinetics, biodistribution and renal protective effect of different regimens of amino acid co-infusion*. Eur J Nucl Med Mol Imaging, 2003. **30**(4): p. 510-8.

64. Garkavij, M., et al., *¹⁷⁷Lu-(DOTA₀,Tyr₃) octreotate therapy in patients with disseminated neuroendocrine tumors: Analysis of dosimetry with impact on future therapeutic strategy.* Cancer. **116**(4 Suppl): p. 1084-92.
65. Sandstrom, M., et al., *Individualized dosimetry of kidney and bone marrow in patients undergoing ¹⁷⁷Lu-DOTA-octreotate treatment.* J Nucl Med. **54**(1): p. 33-41.
66. De Jong, M., et al., *Inhomogeneous localization of radioactivity in the human kidney after injection of ((111)In-DTPA)octreotide.* J Nucl Med, 2004. **45**(7): p. 1168-71.
67. Konijnenberg, M., et al., *Radiation dose distribution in human kidneys by octreotides in peptide receptor radionuclide therapy.* J Nucl Med, 2007. **48**(1): p. 134-42.
68. Baechler, S., et al., *Three-dimensional radiobiological dosimetry of kidneys for treatment planning in peptide receptor radionuclide therapy.* Med Phys. **39**(10): p. 6118-28.
69. Forrer, F., et al., *Bone marrow dosimetry in peptide receptor radionuclide therapy with (¹⁷⁷Lu-DOTA(0),Tyr(3))octreotate.* Eur J Nucl Med Mol Imaging, 2009. **36**(7): p. 1138-46.
70. Hindorf, C., et al., *EANM Dosimetry Committee guidelines for bone marrow and whole-body dosimetry.* Eur J Nucl Med Mol Imaging. **37**(6): p. 1238-50.
71. Lassmann, M., et al., *EANM Dosimetry Committee series on standard operational procedures for pre-therapeutic dosimetry I: blood and bone marrow dosimetry in differentiated thyroid cancer therapy.* Eur J Nucl Med Mol Imaging, 2008. **35**(7): p. 1405-12.
72. Walrand, S., et al., *Experimental facts supporting a red marrow uptake due to radiometal transchelation in ⁹⁰Y-DOTATOC therapy and relationship to the decrease of platelet counts.* Eur J Nucl Med Mol Imaging. **38**(7): p. 1270-80.
73. Arvold, N.D., et al., *Pancreatic neuroendocrine tumors with involved surgical margins: prognostic factors and the role of adjuvant radiotherapy.* Int J Radiat Oncol Biol Phys. **83**(3): p. e337-43.
74. Pauwels, S., et al., *Practical dosimetry of peptide receptor radionuclide therapy with (⁹⁰Y)-labeled somatostatin analogs.* J Nucl Med, 2005. **46 Suppl 1**: p. 92S-8S.
75. Ezziddin, S., et al., *Early prediction of tumour response to PRRT. The sequential change of tumour-absorbed doses during treatment with ¹⁷⁷Lu-octreotate.* Nuklearmedizin. **52**(5).
76. Otte, A., et al., *Yttrium-90 DOTATOC: first clinical results.* Eur J Nucl Med, 1999. **26**(11): p. 1439-47.
77. Beauregard, J.M., et al., *Quantitative (¹⁷⁷Lu) SPECT (QSPECT) imaging using a commercially available SPECT/CT system.* Cancer Imaging. **11**: p. 56-66.
78. Sabet, A., et al., *Outcome and toxicity of salvage therapy with Lu-octreotate in patients with metastatic gastroenteropancreatic neuroendocrine tumours.* Eur J Nucl Med Mol Imaging.
79. van Essen, M., et al., *Salvage therapy with (¹⁷⁷Lu)-octreotate in patients with bronchial and gastroenteropancreatic neuroendocrine tumors.* J Nucl Med. **51**(3): p. 383-90.

80. Breeman, W.A., et al., *Anti-tumor effect and increased survival after treatment with (177Lu-DOTA0,Tyr3)octreotate in a rat liver micrometastases model*. Int J Cancer, 2003. **104**(3): p. 376-9.
81. Kaemmerer, D., et al., *Neoadjuvant peptide receptor radionuclide therapy for an inoperable neuroendocrine pancreatic tumor*. World J Gastroenterol, 2009. **15**(46): p. 5867-70.
82. Stoeltzing, O., et al., *Staged surgery with neoadjuvant 90Y-DOTATOC therapy for down-sizing synchronous bilobular hepatic metastases from a neuroendocrine pancreatic tumor*. Langenbecks Arch Surg, 2010. **395**(2): p. 185-92.
83. Claringbold, P.G., R.A. Price, and J.H. Turner, *Phase I-II study of radiopeptide 177Lu-octreotate in combination with capecitabine and temozolomide in advanced low-grade neuroendocrine tumors*. Cancer Biother Radiopharm, 2012. **27**(9): p. 561-9.
84. Barber, T.W., et al., *The potential for induction peptide receptor chemoradionuclide therapy to render inoperable pancreatic and duodenal neuroendocrine tumours resectable*. Eur J Surg Oncol, 2012. **38**(1): p. 64-71.
85. van Essen, M., et al., *Report on short-term side effects of treatments with 177Lu-octreotate in combination with capecitabine in seven patients with gastroenteropancreatic neuroendocrine tumours*. Eur J Nucl Med Mol Imaging, 2008. **35**(4): p. 743-8.
86. Claringbold, P.G., et al., *Phase II study of radiopeptide 177Lu-octreotate and capecitabine therapy of progressive disseminated neuroendocrine tumours*. Eur J Nucl Med Mol Imaging, 2011. **38**(2): p. 302-11.
87. Fueger, B.J., et al., *Effects of chemotherapeutic agents on expression of somatostatin receptors in pancreatic tumor cells*. J Nucl Med, 2001. **42**(12): p. 1856-62.
88. Jain, R.K., *Normalizing tumor microenvironment to treat cancer: bench to bedside to biomarkers*. J Clin Oncol, 2013. **31**(17): p. 2205-18.
89. S.M. Bison, J.C.H., S.J. Koelewijn, H.C. Groen, S. Berndsen, M. Melis, M.R. Bernsen, M. de Jong, *Optimization of combination of peptide receptor radionuclide therapy (PRRT) and temozolomide therapy using SPECT/CT and MRI in mice*. 2013.
90. Nayak, T.K., et al., *Enhancement of somatostatin-receptor-targeted (177Lu-(DOTA(0)-Tyr(3))-octreotide therapy by gemcitabine pretreatment-mediated receptor uptake, up-regulation and cell cycle modulation*. Nuclear medicine and biology, 2008. **35**(6): p. 673-8.
91. Yao, J.C., et al., *Everolimus for advanced pancreatic neuroendocrine tumors*. The New England journal of medicine, 2011. **364**(6): p. 514-23.
92. Fingar, D.C. and J. Blenis, *Target of rapamycin (TOR): an integrator of nutrient and growth factor signals and coordinator of cell growth and cell cycle progression*. Oncogene, 2004. **23**(18): p. 3151-71.
93. Pool, S.E., et al., *mTOR inhibitor RAD001 promotes metastasis in a rat model of pancreatic neuroendocrine cancer*. Cancer research, 2012.
94. Hubble, D., et al., *177Lu-octreotate, alone or with radiosensitising chemotherapy, is safe in neuroendocrine tumour patients previously treated with high-activity 111In-octreotide*. European journal of nuclear medicine and molecular imaging, 2010. **37**(10): p. 1869-75.

CHAPTER 3

mTOR inhibitor RAD001 promotes metastasis in a rat model of pancreatic neuroendocrine cancer.

Pool SE, Bison SM, Koelewijn SJ, van der Graaf LM, Melis M, Krenning EP, de Jong M.

Published in Cancer Res. 2013 Jan 1;73(1):12-8.

ABSTRACT

Herein we report that mTOR (mammalian target of rapamycin) inhibition by Everolimus (RAD001), administered twice weekly for 4.5 weeks, resulted in the occurrence of distant metastasis in a rat pancreatic neuroendocrine tumor model. RAD001 treatment was given as a single treatment or combined with (^{177}Lu -DOTA,Tyr³)octreotate (^{177}Lu -DOTATATE), the latter targeting the somatostatin receptor subtype 2 (sst₂). RAD001 alone resulted in minor anti-tumor effects. The combination of ^{177}Lu -DOTATATE and RAD001 was much more effective than RAD001 alone, but this combination did not show a better antitumor effect in comparison to ^{177}Lu -DOTATATE alone. Unexpectedly, tumor metastasis was found in 77 % of animals treated with RAD001 or RAD001 plus ^{177}Lu -DOTATATE. Metastasis was not found in control and ^{177}Lu -DOTATATE-treated animals, not even if the primary tumor was surgically removed when tumor size was > 4 cm³ to save the animals for further follow up. The metastasizing potential of RAD001 could be induced by of the treatment itself or of the discontinued treatment. Clinically this observation is of great importance for non-compliant patients or patients which have to stop RAD001 therapy because of adverse effects.

INTRODUCTION

Gastroenteropancreatic neuro-endocrine tumors (GEPNETs) are usually slow growing and most patients present with already metastasized disease at time of diagnosis. As published by Missiaglia et al. (1) in many PNETs the mTOR signal transduction pathway is up regulated. This pathway plays a key role in regulating cell growth, metabolism, proliferation and angiogenesis. Inhibition of the mTOR signal transduction pathway in PNETs by RAD001 has shown promising results with a clinical benefit of 76%, given as a single treatment (n=115), and of 82%, given in combination with octreotide-LAR (n=45) (2). The RADIANT-3 study, a randomized, double blind, placebo-controlled, multicenter Phase III trial of 10 mg RAD001 daily in PNET-patients (n=410) has been finished recently. Median progression-free survival for RAD001 plus best supportive care was 11 months versus 4.6 months in the placebo group ($p < 0.001$) with acceptable toxicity (3). Most recently the FDA approved RAD001 for the treatment of PNET patients.

Since the late 1990s clinical Peptide Receptor Radionuclide Therapy (PRRT) studies have been performed with radiolabeled somatostatin analogs, such as ^{177}Lu -DOTATATE and (^{90}Y -DOTA,Tyr³)octreotide (^{90}Y -DOTATOC, Onalta™), targeting sst_2 overexpressed on most GEPNETs. These studies have shown very promising results with regard to tumor response, overall survival, and quality of life (4, 5).

Considering the promising results of both RAD001 and PRRT for the treatment of GEPNETs, we combined these two therapies in the CA20948 syngeneic pancreatic tumor model in the rat. This radiosensitive model is commonly used for preclinical PRRT experiments and also showed to be susceptible to RAD001 treatment (6). For comparison, studies were also performed in the xenograft H69 tumor model in nude mice. The aim of the current study was to investigate the therapeutic effects of combined treatment with RAD001 and ^{177}Lu -DOTATATE versus those of the two mono treatments.

MATERIALS AND METHODS

Cell lines

The CA20948 rat pancreatic tumor cell line (derived from a rat pancreas at our institution) is of acinar origin (7) and has high sst_2 expression and was cultured as reported before (8). The cells were passaged for a maximum of 20 times and checked for mycoplasma infection and sst_2 expression every 3 months.

The H69 tumor cell line is a human small cell lung carcinoma (ATCC, Wesel, Germany), has high sst_2 expression, was passaged for a maximum of 10 times and was cultured according to the suppliers (ATCC) protocol.

Tumor models

The animal studies were in agreement with the Animal Welfare Committee requirements of our institution and conducted following generally accepted guidelines. For the first

two experiments male Lewis rats (Harlan, Horst, the Netherlands) were used with a mean body weight of 275 g. For tumor induction, 10^7 CA20948 tumor cells in 0.5 ml ice cold PBS/animal were injected subcutaneously in the lower flank. Monitoring body weight and tumor size by caliper measurements were performed by a technician blinded for the treatment groups. Tumor volume was calculated according to $0.4 \times \text{length} \times \text{width} \times \text{height}$. In the first study (fig. 1), animals were euthanized when tumor size had reached a volume of more than 4 cm^3 or when a tumor was bleeding due to skin penetration. In the second study the primary subcutaneous tumors were surgically removed when tumor volume exceeded 4 cm^3 or when the tumor was bleeding due to skin penetration, saving the animals for follow-up. Animals were euthanized when $>10\%$ loss of body weight was detected.

For the third experiment 24 male NMRI Nu/Nu mice with a mean body weight of 35 grams xenotransplanted sst_2 expressing H69 cells were used. Animals were euthanized when tumor size reached a volume of more than 2 cm^3 , when a tumor was bleeding due to skin penetration, or when $>10\%$ loss of body weight was detected.

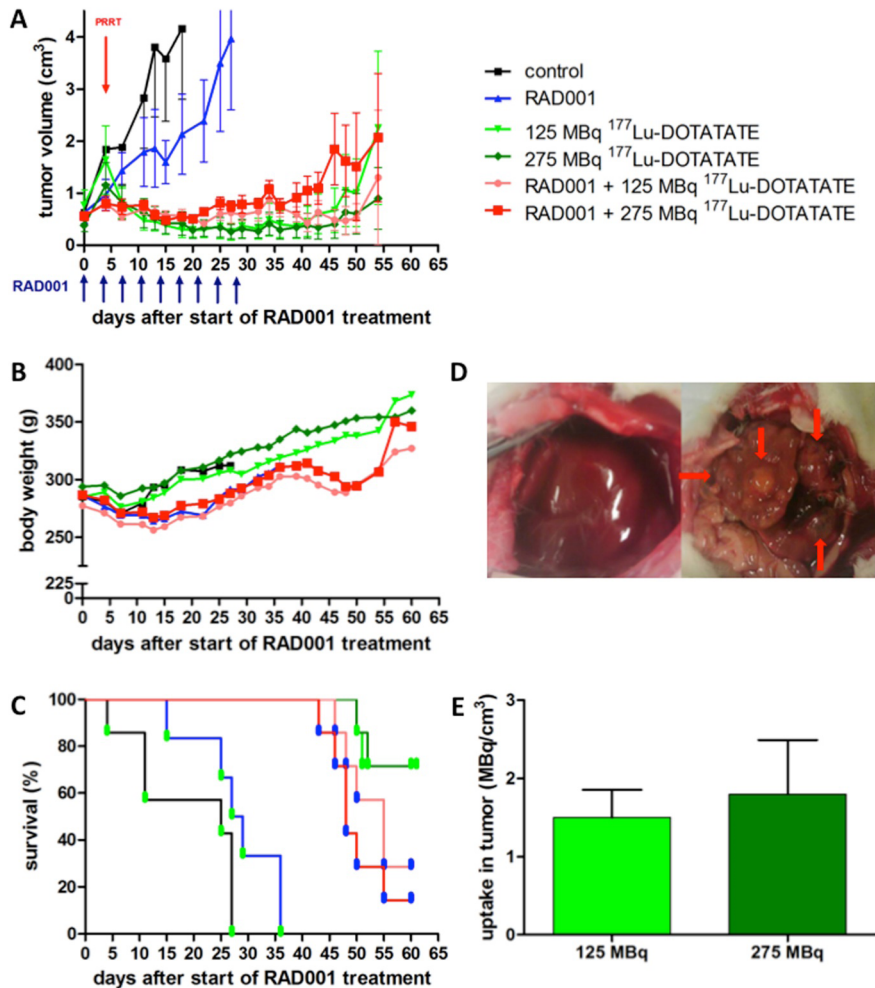
RAD001

In the first experiment, RAD001 (kind gift from Novartis, Basel, Switzerland) and placebo was prepared according to the manufacturers protocol. In the second and third experiment RAD001 powder (LC laboratories, Woburn, USA) was dissolved in 2 ml ethanol and further diluted to the appropriate concentration in 5% (w/v) glucose solution. RAD001 was administered orally by gavage with a blunt needle.

Radionuclides and peptides

DOTA, Tyr^3 -octreotate was obtained from Mallinckrodt, St Louis, MO. $^{177}\text{LuCl}_3$ was obtained from NRG, Petten, the Netherlands and was distributed by IDB-Holland, Baarle-Nassau, the Netherlands. ^{177}Lu -DOTA, Tyr^3 -octreotate was locally prepared as described before (9) in a specific activity of $125 \text{ MBq}/3.4 \mu\text{g}$ peptide. Labeling of ^{111}In -DTPA-octreotide (Octreoscan (Tyco Health Care, Petten, the Netherlands)) in a specific activity of $30 \text{ MBq } ^{111}\text{InCl}_3 / 0.5 \mu\text{g}$ DTPA-octreotide was performed as previously described (10). For the mice experiments a specific activity of $30 \text{ MBq } ^{111}\text{InCl}_3 / 0.1 \mu\text{g}$ DTPA-octreotide was used.

In vitro autoradiography and HE staining
As previously described in detail (11).



(Right) Figure 1. Anti-tumor effect by RAD001 + ¹⁷⁷Lu-DOTATATE combination treatment did not lead to better anti-tumor effects compared to ¹⁷⁷Lu-DOTATATE alone and unexpectedly resulted in distant metastasis. Fig. 1A; Subcutaneous CA20948 tumor size after treatment with vehicle of RAD001 (control), RAD001 (5 mg/kg), ¹⁷⁷Lu-DOTATATE (125 MBq or 275 MBq) or a combination of RAD001 plus ¹⁷⁷Lu-DOTATATE (Table 1). The red arrow depicts the administration of ¹⁷⁷Lu-DOTATATE. The blue arrows depict RAD001 administrations. Data are presented as mean ± sem. Fig. 1B; Mean body weight per treatment group from start of RAD001 treatment. Both combination treatment groups showed loss of body weight beyond day 40. Data are presented as mean. Fig. 1C; Survival curves of the different treatment groups, a green dot represents sacrifice of at least one animal because of subcutaneous tumor size > 4 cm³ or a ruptured tumor. A blue dot represents sacrifice of at least one animal because of loss of body weight or poor condition, correlating with metastasis. Fig. 1D; Animals with (right) and without (left) metastases in the liver as indicated by the red arrows. Fig. 1E; ¹⁷⁷Lu-DOTATATE uptake in subcutaneous primary CA20948 tumors after different doses of ¹⁷⁷Lu-DOTATATE (125 MBq/3.4 ug and 275 MBq/7.5 ug) as quantified by SPECT.

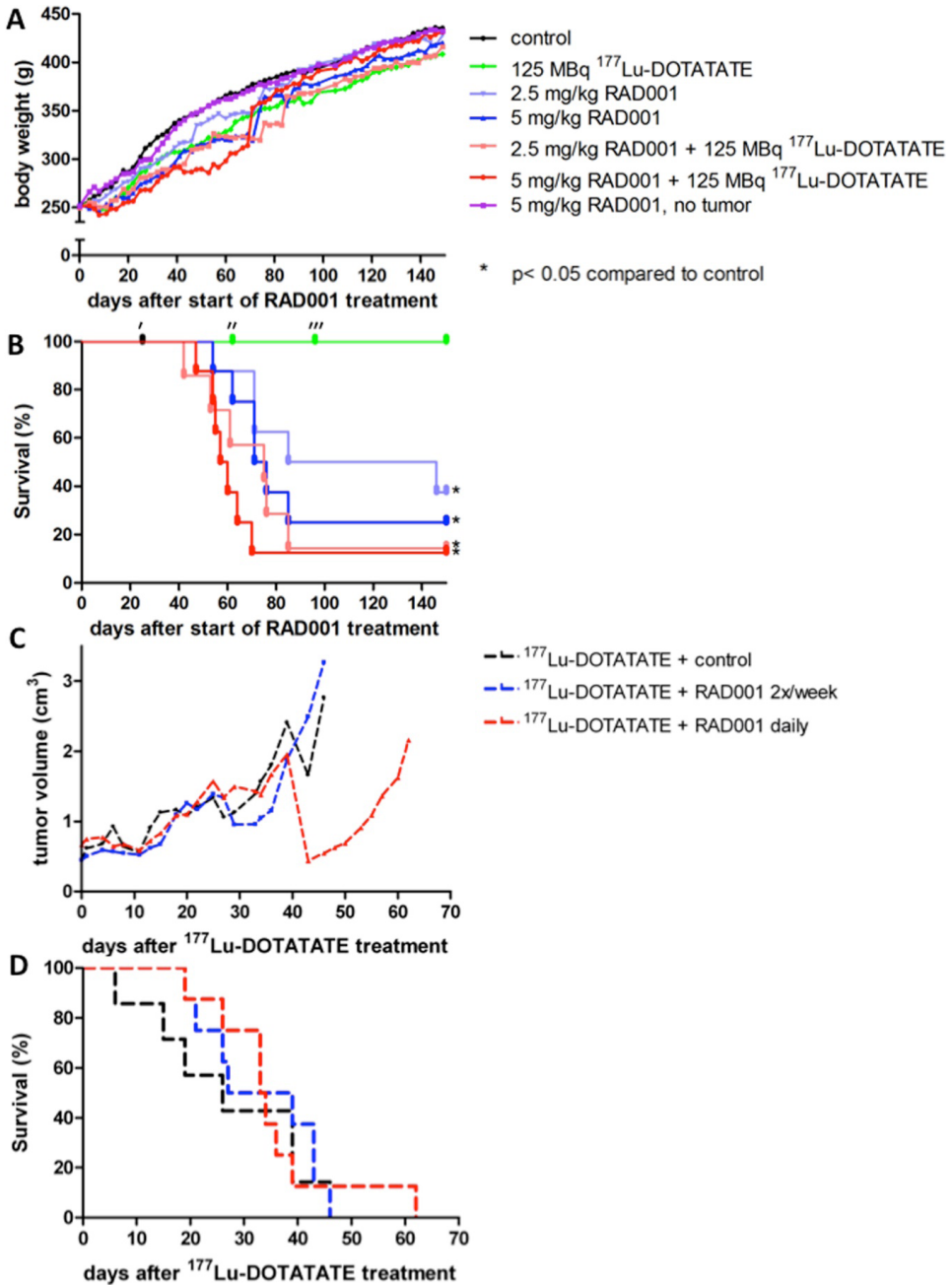


Figure 2. RAD001 treatment (with or without ¹⁷⁷Lu-DOTATATE) resulted in the occurrence of distant metastasis. **Fig. 2A**; Mean body weight per group from start of RAD001 treatment. Again the dip in body weight in the RAD001-treated animals is observed; from day 40 on in the high-dose RAD001 group, from day 60 on in the low-dose RAD001 group. **Fig. 2B**; Survival curve, censored for metastasis-unrelated death. All RAD001 treatment groups

had significantly lower survival rate compared to control and PRRT-only groups. ' Animal found death in cage, no metastases upon autopsy. " Animal did not survive subcutaneous tumor surgical resection, no metastasis upon autopsy. □ Animal with macroscopically visible tumor spill during subcutaneous tumor surgical resection. **Fig. 2C**; Subcutaneous H69 tumor size in NMRI Nu/Nu mice was monitored after treatment with ¹⁷⁷Lu-DOTATATE in combination with vehicle of RAD001(control), RAD001 (5 mg/kg, twice a week) and RAD001 (5 mg/kg, daily). At day 21 a second ¹⁷⁷Lu-DOTATATE treatment was given for reduction of subcutaneous H69 tumor size facilitating a longer follow-up. No additional therapeutic effect of RAD001 on ¹⁷⁷Lu-DOTATATE treatment is seen in this tumor model. Data are presented as mean. **Fig. 2D**; Survival curve showing no significant difference between combination treatment of ¹⁷⁷Lu-DOTATATE with vehicle RAD001 (control), RAD001 administered twice weekly or RAD001 administered daily.

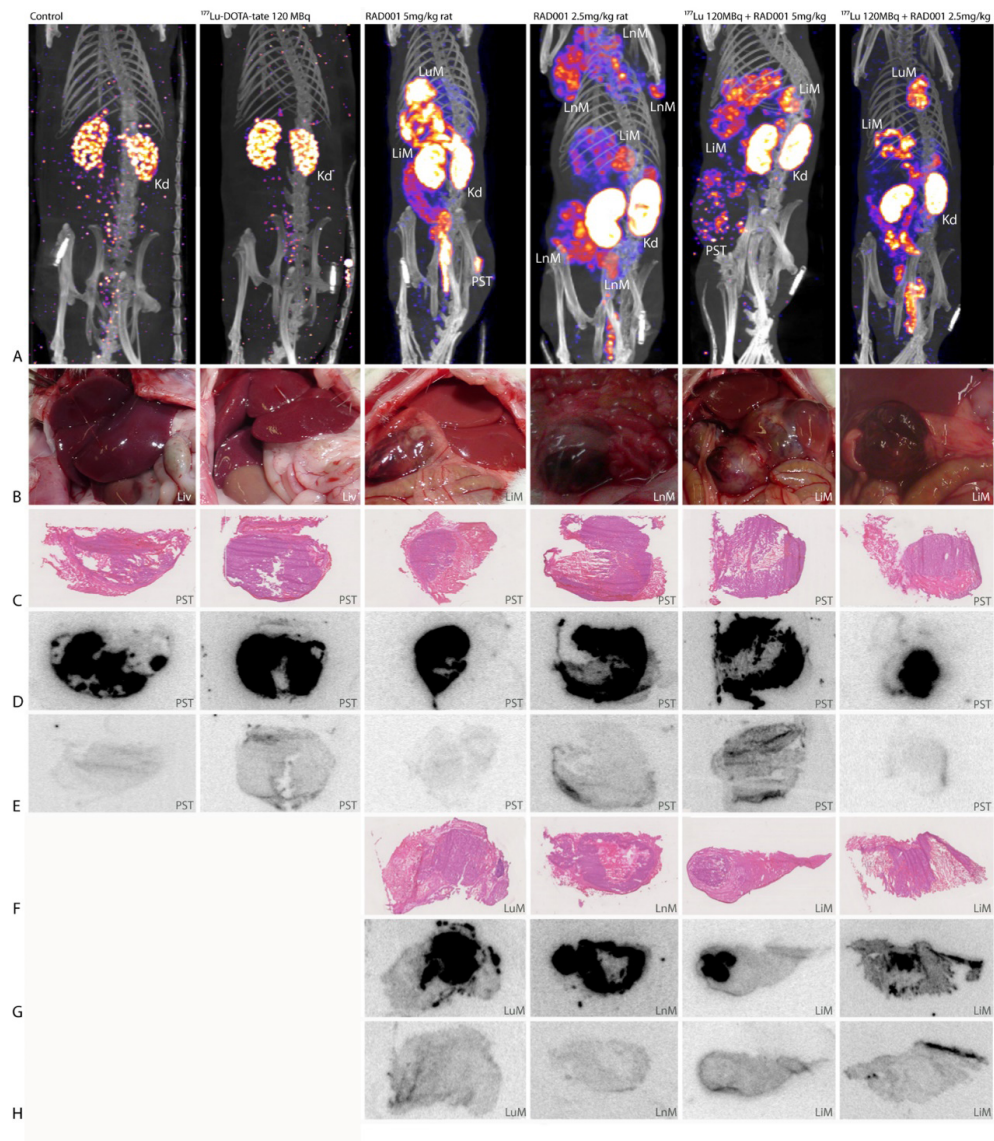


Figure 3. RAD001 treatment resulted in the occurrence of distant metastasis, shown by $^{111}\text{In-DTPA-octreotide}$ SPECT/CT and in vitro autoradiography. **Fig. 3A**; SPECT/CT of animals representing all treatment groups. The SPECT/CT of control and $^{177}\text{Lu-DOTATATE}$ treated animals were performed at the end of the experiment at day 150 and only show uptake in kidneys. The SPECT/CTs of the other animals were made just before euthanasia because of tumor growth and show clear uptake in tumor tissue and kidneys. Kd = kidney, LuM = lung metastasis, LiM = liver metastasis, LnM = lymph node metastasis, PST = primary subcutaneous tumor. **Fig. 3B**; autopsy images. Healthy livers (Liv) in control and $^{177}\text{Lu-DOTATATE}$ treated animals. Distant metastasis in the liver (LvM) in RAD001

treated animals. **Fig. 3C**; Hematoxylin/eosin sections of primary subcutaneous tumors (PST) **Fig. 3D**; corresponding ^{111}In -DTPA-octreotide in vitro autoradiography images **Fig. 3E**; corresponding ^{111}In -DTPA-octreotide in vitro autoradiography images with addition of a 1000 x excess of unlabeled DTPA-octreotide. **Fig. 3F**; Hematoxylin/eosin sections of distant metastasis in RAD001 treated animals. **Fig. 3G**; corresponding ^{111}In -DTPA-octreotide in vitro autoradiography images **Fig. 3H**; corresponding ^{111}In -DTPA-octreotide in vitro autoradiography images with block.

Experimental setup

In experiment 1, ten days after tumor inoculation RAD001 treatment was started, followed by ^{177}Lu -DOTATATE injection. Animals were randomized into matching treatment groups with regard to tumor size at the start of treatment. Six treatment groups were created using one dose of RAD001 (5 mg/kg BW twice a week) and two doses of ^{177}Lu -DOTATATE, 125 or 278 MBq, either as mono treatment or in combination (Table 1). Experiment 1 ended at day 60. To keep animal discomfort as low as possible and for practical reasons RAD001 was administered twice weekly. Experiment 2 was essentially similar as experiment 1, variations were 2.5 next to 5 mg/kg BW dose of RAD001, alone or combined with 125 MBq ^{177}Lu -DOTATATE (Table 1). The most important difference in comparison to experiment 1 was the resection of the subcutaneous tumor when tumor size > 4 cm³. Experiment 2 was terminated at day 150. All animals still alive at the end of the experiment were checked for distant metastases by ^{111}In -DTPA-octreotide SPECT/CT and autopsy.

In experiment 3, NMRI Nu/Nu mice bearing subcutaneous H69 tumors were first treated with 28 MBq ^{177}Lu -DOTATATE injected intraperitoneally. Four days later three combination treatment groups were created ad random. The first group received RAD001 (5mg/kg BW) daily, the second group received RAD001 (5mg/kg BW) twice a week with placebo treatment daily for the rest of the week and the third group received placebo treatment daily. RAD001/placebo treatment was given for a total of four weeks. Three weeks after the first ^{177}Lu -DOTATATE treatment a second 25 MBq ^{177}Lu -DOTATATE treatment was given to all animals as an alternative for surgical removal of the primary tumor. When subcutaneous tumor size exceeded 2 cm³ the animal was checked for distant metastases by ^{111}In -DTPA-octreotide SPECT/CT and autopsy.

Surgical procedure

During all surgical procedures isoflurane/O₂ anesthesia was applied and animals were kept warm using a heating pad. After shaving and disinfection an incision was made just beside the tumor. The capsule surrounding the tumor was carefully dissected from surrounding tissue. The wound was closed by absorbable sutures.

Table 1. Treatment groups in studies 1 and 2.

Group	Treatment	n	tumor volume > 4 cm ³
Study 1			
1 Control	Vehicle only	7	†
2 RAD001	RAD001 (2x/week, 5 mg/kg bw)	6	†
3 Combination of low dose ¹⁷⁷ Lu-DOTATATE with RAD001	RAD001 (2x/week, 5 mg/kg bw) and 125 MBq ¹⁷⁷ Lu-DOTATATE	7	†
4 Combination of high dose ¹⁷⁷ Lu-DOTATATE with RAD001	RAD001 (2x/week, 5 mg/kg bw) and 275 MBq ¹⁷⁷ Lu-DOTATATE	7	†
5 Low dose ¹⁷⁷ Lu-DOTATATE	125 MBq ¹⁷⁷ Lu-DOTATATE	6	†
6 High dose ¹⁷⁷ Lu-DOTATATE	275 MBq ¹⁷⁷ Lu-DOTATATE	7	†
Study 2			
7 Control	Vehicle only	8	Surgery
8 Low dose RAD001	RAD001 (2x/week, 2,5 mg/kg bw)	8	Surgery
9 High dose RAD001	RAD001 (2x/week, 5 mg/kg bw)	8	Surgery
10 Combination of low dose RAD001 with ¹⁷⁷ Lu-DOTATATE	RAD001 (2x/week, 2,5 mg/kg bw) + 125 MBq ¹⁷⁷ Lu-DOTATATE	7	Surgery
11 Combination of high dose RAD001 with ¹⁷⁷ Lu-DOTATATE	RAD001 (2x/week, 5 mg/kg bw) + 125 MBq ¹⁷⁷ Lu-DOTATATE	8	Surgery
12 ¹⁷⁷ Lu-DOTATATE	125 MBq ¹⁷⁷ Lu-DOTATATE	8	Surgery
13 RAD001, no tumor	RAD001 (2x/week, 5 mg/kg bw)	7	n.a.

BW = body weight, † = euthanasia, n.a. = not applicable. All animals were bearing CA20948 tumors, except for animals in group 13.

SPECT/CT scanning

24 (experiment 1) or 48 h (experiment 2) after intravenous (i.v.) injection of ¹⁷⁷Lu-DOTATATE, a helical SPECT scan was acquired covering the tumor region using the four-headed NanoSPECT/CT system (Bioscan) using Nucline software (v2.01, Mediso) for quantification of ¹⁷⁷Lu-DOTATATE tumor uptake. Just before euthanizing an animal, a whole body SPECT/CT scan was made 4 – 24 hours after i.v. injection of ¹¹¹In-DTPA-octreotide for detection of distant metastasis.

RESULTS AND DISCUSSION

Our first study, described in table 1 (group 1 – 6), showed CA20948 tumor growth inhibition by RAD001 mono therapy as was previously found by Boulay et al. as well (6). Also in clinical studies mTOR inhibition generally seems to elicit a cytostatic rather than a cytotoxic response (15, 16). Boulay et al. also showed twice weekly

administration of RAD001 to be as effective as daily administration in this tumor model (6). All animals in the control and the RAD001-only group had to be euthanized within 36 days post start of treatment because of tumor growth beyond 4 cm³ or a ruptured tumor. As expected, all animals receiving ¹⁷⁷Lu-DOTATATE with or without RAD001 exhibited significant antitumor response compared to controls ($p \leq 0.05$). However ¹⁷⁷Lu-DOTATATE in combination with RAD001 did not show to be more effective than ¹⁷⁷Lu-DOTATATE alone (Fig. 1A). A dose effect relationship for the low and high dose ¹⁷⁷Lu-DOTATATE was not found, which is in agreement with similar levels of ¹⁷⁷Lu-DOTATATE tumor uptake in these two groups 24 hours after injection, as quantified based on SPECT (Fig. 1E). Partial saturation of the sst₂ receptors on the tumor cells in the high dose group could play a role in this respect.

Strikingly, from day 40 post start of treatment, most animals in the combination therapy groups showed unexpected decrease in body weight (Fig. 1B). Tumor metastasis to the liver and occasionally to the lung was found in these animals upon autopsy (Fig. 1D). In the combination treatment groups 11 out of 14 animals had to be euthanized because of loss of body weight and apparent metastasis (Fig. 1C). Metastases could be visualized after injection of ¹¹¹In-DTPA-octreotide by SPECT/CT, indicating sst₂ expression. ¹⁷⁷Lu-DOTATATE-only treated animals did not show loss of body weight and were all free of metastasis, confirmed by negative ¹¹¹In-DTPA-octreotide SPECT/CT scans and negative autopsies (Figure 1D). The occurrence of spontaneous metastasis in the subcutaneous CA20948 tumor model has not been described before, despite the fact that this model has often been used in PRRT studies with long follow-up periods (12). We therefore hypothesize that RAD001, alone or in combination with ¹⁷⁷Lu-DOTATATE, or the discontinuation of RAD001 treatment might be the cause of the metastasis. Unfortunately the RAD001 mono therapy treatment group in this study did not survive long enough to develop or to be tested for metastases by SPECT.

For further investigation, a second study was performed (Table 1, group 7-13) in which a subcutaneous tumor reaching a volume of 4 cm³ was surgically removed to allow long term follow-up. Furthermore, in this experiment also a 2.5 mg/kg BW dose of RAD001 was applied next to the earlier used 5 mg/kg BW, combined with 125 MBq ¹⁷⁷Lu-DOTATATE (Table 1). In an additional group (group 13) 5 mg/kg BW of RAD001 was given to control rats without tumor.

The therapeutic effects obtained in this second study were in agreement with the first study, without significant difference using the lower RAD001 dose. PRRT resulted in complete response of the CA20948 tumor in 3 out of 7 animals, whereas in all other animals the subcutaneous tumor had to be removed surgically. In one animal treated with ¹⁷⁷Lu-DOTATATE, clear tumor spill into the wound bed was observed during the surgical procedure resulting in tumor regrowth in the wound bed and metastasis in an ipsi lateral lymph node in the groin. Therefore this animal was not included in our analysis. The decrease in body weight seen in the RAD001 + PRRT animals in study 1 was less explicit in study 2 (Fig. 2B) probably because of earlier intervention.

Again distant metastasis developed in animals receiving RAD001, either in high or low dose, or in combination with ^{177}Lu -DOTATATE. (Fig. 2A), whereas control and ^{177}Lu -DOTATATE treated animals remained metastasis free. When development of distant metastasis was suspected based on loss of body weight, ^{111}In -DTPA-octreotide was injected and 4-24 hours later a SPECT/CT scan (Fig. 3A) was acquired. When a distant metastasis could be visualized, the animal was euthanized, followed by autopsy as illustrated by photographic images (Fig. 3B). Of tumor tissue collected, frozen sections were prepared and used for hematoxylin eosin staining (Fig. 3C + F) and ^{111}In -DTPA-octreotide *in vitro* autoradiography with (Fig. 3E + H) or without (Fig. 3D + G) a 1000 x excess of unlabeled octreotide (block). All metastasis appeared to be sst₂-positive, in agreement with the receptor status of the primary subcutaneous tumors. In a third study, RAD001 administered daily/twice weekly combined with PRRT in a suboptimal dose did again not show any significant additional therapeutic effect on subcutaneous human H69 xenografts in nude mice compared to placebo combined with PRRT (Fig. 2C + D). In this experiment no distant metastasis was found after RAD001 therapy. A possible explanation could be the slow growth rate of the H69 tumor; longer follow up and surgical removal of the primary subcutaneous tumor as performed in the rat experiment 2 was preferred, this was not allowed according to the animal ethical protocol for this study though.

An explanation of the mechanism of action leading to the unexpected metastases in lung, liver and lymph nodes in the rat model cannot be given, based on these studies. Understanding the pathways involved and how they are interconnected is needed to explain the current findings. As recently discussed by Ebos et al. (13) sustained suppression of the VEGF pathway may lead to a rebound in tumor growth, once discontinued. Comparable to our findings with RAD001, acceleration of metastasis was found in preclinical models after short-term treatment with the VEGFR/PDGFR kinase inhibitor sunitinib (14). The fact that in our studies RAD001 treatment was discontinued after 4.5 weeks may have resulted in such rebound effect via VEGFR as well. The twice weekly administration of RAD001 could also have resulted in an incomplete inhibition resulting in a (twice weekly repeated) upregulation of growth pathways. Discontinued mTOR inhibition could also have stimulated glucose uptake, glycolysis and de novo lipid biosynthesis, which are considered hallmarks of cancer and cancer metastasis. A possible explanation for the higher therapeutic effects found for ^{177}Lu -DOTATATE only treatment compared to the combination treatment of RAD001 and ^{177}Lu -DOTATATE could be the fact that in the combination treatment the tumor cell proliferation rate is lowered by RAD001, resulting in a decreased radio sensitivity. The acceleration of metastasis could be caused by an effect on the immune system that could be unique to this particular preclinical CA20948 tumor model. Therefore comparable experiments with other preclinical tumor models, such as the H69 mice model with surgical removal of the primary subcutaneous tumor, will have to be performed. If the results of our studies can be translated to humans, mTOR inhibition treatment should be closely watched especially after discontinuation of this therapy because of adverse effects or in non-compliant patients, despite the positive therapeutic results of mTOR inhibition in different kinds of tumors.

REFERENCES

1. Missiaglia E, Dalai I, Barbi S, Beghelli S, Falconi M, della Peruta M, et al. Pancreatic endocrine tumors: expression profiling evidences a role for AKT-mTOR pathway. *Journal of clinical oncology : official journal of the American Society of Clinical Oncology*. 2010;28:245-55.
2. Yao JC, Lombard-Bohas C, Baudin E, Kvols LK, Rougier P, Ruzsniwski P, et al. Daily oral everolimus activity in patients with metastatic pancreatic neuroendocrine tumors after failure of cytotoxic chemotherapy: a phase II trial. *J Clin Oncol*. 2010;28:69-76.
3. Yao JC, Shah MH, Ito T, Bohas CL, Wolin EM, Van Cutsem E, et al. Everolimus for advanced pancreatic neuroendocrine tumors. *N Engl J Med*. 2011;364:514-23.
4. Pool SE, Krenning EP, Koning GA, van Eijck CH, Teunissen JJ, Kam B, et al. Preclinical and clinical studies of peptide receptor radionuclide therapy. *Semin Nucl Med*. 2010;40:209-18.
5. Kwekkeboom DJ, de Herder WW, Kam BL, van Eijck CH, van Essen M, Kooij PP, et al. Treatment with the radiolabeled somatostatin analog (177 Lu-DOTA 0,Tyr3) octreotate: toxicity, efficacy, and survival. *J Clin Oncol*. 2008;26:2124-30.
6. Boulay A, Zumstein-Mecker S, Stephan C, Beuvink I, Zilbermann F, Haller R, et al. Antitumor efficacy of intermittent treatment schedules with the rapamycin derivative RAD001 correlates with prolonged inactivation of ribosomal protein S6 kinase 1 in peripheral blood mononuclear cells. *Cancer Res*. 2004;64:252-61.
7. Longnecker DS, Lilja HS, French J, Kuhlmann E, Noll W. Transplantation of azaserine-induced carcinomas of pancreas in rats. *Cancer Lett*. 1979;7:197-202.
8. Bernard BF, Krenning E, Breeman WA, Visser TJ, Bakker WH, Srinivasan A, et al. Use of the rat pancreatic CA20948 cell line for the comparison of radiolabelled peptides for receptor-targeted scintigraphy and radionuclide therapy. *Nucl Med Commun*. 2000;21:1079-85.
9. Kwekkeboom DJ, Bakker WH, Kooij PP, Konijnenberg MW, Srinivasan A, Erion JL, et al. (177Lu-DOTA0,Tyr3)octreotate: comparison with (111In-DTPA0)octreotide in patients. *Eur J Nucl Med*. 2001;28:1319-25.
10. Breeman WA, Kwekkeboom DJ, Kooij PP, Bakker WH, Hofland LJ, Visser TJ, et al. Effect of dose and specific activity on tissue distribution of indium-111-pentetreotide in rats. *Journal of nuclear medicine : official publication, Society of Nuclear Medicine*. 1995;36:623-7.
11. Melis M, Forrer F, Capello A, Bijster M, Bernard BF, Reubi JC, et al. Up-regulation of somatostatin receptor density on rat CA20948 tumors escaped from low dose (177Lu-DOTA0,Tyr3)octreotate therapy. *Q J Nucl Med Mol Imaging*. 2007;51(4):324-33
12. de Jong M, Breeman WA, Bernard BF, Bakker WH, Schaar M, van Gameren A, et al. (177Lu-DOTA(0),Tyr3) octreotate for somatostatin receptor-targeted radionuclide therapy. *Int J Cancer*. 2001;92:628-33.
13. Ebos JM, Kerbel RS. Antiangiogenic therapy: impact on invasion, disease progression, and metastasis. *Nat Rev Clin Oncol*. 2011;8:210-21.

CHAPTER 3

14. Ebos JM, Lee CR, Cruz-Munoz W, Bjarnason GA, Christensen JG, Kerbel RS. Accelerated metastasis after short-term treatment with a potent inhibitor of tumor angiogenesis. *Cancer Cell*. 2009;15:232-9.
15. Yecies JL, Manning BD. mTOR links oncogenic signaling to tumor cell metabolims. *J Mol Med* 2011;89:221-8.
16. Blay JY. Updating progress in sarcoma therapy with mTOR inhibitors. *Annals Oncol: Offi J Eur Soc Med Oncol/ESMO* 2011;22:280-7.

CHAPTER 4

Peptide Receptor Radionuclide Therapy (PRRT) with (^{177}Lu -DOTA⁰,Tyr³)octreotate in combination with RAD001 treatment; further investigations on tumor metastasis and response in the rat pancreatic CA20948 tumor model

Bison SM, Pool SE, Koelewijn SJ, van der Graaf LM, Groen HC, Melis M, de Jong M

Published in EJNMMI Research 2014, 4:21

ABSTRACT

Previously we reported on the unexpected development of distant metastases in the subcutaneous rat pancreas CA20948 tumor model after 4.5 weeks treatment with RAD001-only or in combination with ($^{177}\text{Lu-DOTA}^0, \text{Tyr}^3$)octreotate ($^{177}\text{Lu-DOTATATE}$) (1). Moreover, the combination therapy was less effective compared to $^{177}\text{Lu-DOTATATE}$ -only. In the current study we address the following questions; 1) Why was the combination therapy less effective? Is $^{177}\text{Lu-DOTATATE}$ tumor uptake affected by pretreatment with RAD001? 2) Could sudden cessation of RAD001 therapy cause the development of distant metastases? 3) Is $^{177}\text{Lu-DOTATATE}$ an effective treatment option for these metastases?

Methods Lewis rats (HanHsd or SsNHsd substrain with a slight difference in immune response) bearing subcutaneous CA20948 tumors were treated with either 125 or 275 MBq $^{177}\text{Lu-DOTATATE}$, RAD001 or their combination. RAD001 was given twice a week for 4.5 or 12 weeks, $^{177}\text{Lu-DOTATATE}$ was given as a single injection. When combined, RAD001 was started either 3 days prior to or 3 days post administration of $^{177}\text{Lu-DOTATATE}$. SPECT/CT was performed to quantify $^{177}\text{Lu-DOTATATE}$ tumor uptake. Where indicated, primary tumors were surgically removed when tumor size > 6000 mm³ to enable monitoring for possible metastasis. If metastases were suspected an $^{111}\text{In-DTPA}$ -octreotide SPECT/CT scan was performed. Seven rats with metastases were treated with 400 MBq $^{177}\text{Lu-DOTATATE}$.

Results $^{177}\text{Lu-DOTATATE}$ tumor uptake was not significantly affected by RAD001 pre-treatment. The occurrence of metastases after RAD001 treatment was not dose dependent in the dose range tested, nor was it related to the duration of RAD001 treatment. In the experiment in which the LEW/SsNsd substrain was used only 12.5% of RAD001 treated rats showed complete response (CR), compared to 50% tumor regression in the control group. Re-treatment with a high dose of $^{177}\text{Lu-DOTATATE}$ resulted in CR in only two out of seven animals.

Conclusion Less effective anti-tumor effects after the combination of RAD001 + $^{177}\text{Lu-DOTATATE}$ could not be explained by reduced $^{177}\text{Lu-DOTATATE}$ tumor uptake after RAD001. Our current data support RAD001 induced immune suppression as the reason for this observation. No evidence was found that cessation of RAD001 treatment caused development of metastases. Metastases appeared to be less sensitive to $^{177}\text{Lu-DOTATATE}$ treatment than primary tumors.

Keywords: RAD001, Everolimus, Affinitor, Metastasis, $^{177}\text{Lu-DOTATATE}$

INTRODUCTION

Neuroendocrine tumors (NETs) consist of a heterogeneous group of neoplasms originating from cells characterized by the synthesis and release of amines/peptides (2). Since 1973, the incidence of NETs has been increasing, in which genetic factors might play a role (3) and in addition improved diagnostics contributed to a higher registered incidence of NETs (2). Because NETs are slowly proliferating tumors, the prevalence of NETs is much higher than the incidence, resulting in a relatively high percentage of NET patients in the population of cancer patients (4). In >50% of the patients, NETs are diagnosed at a relatively late stage, often with metastatic spread (3), which leaves little chance for curative surgery. As a consequence of the slow proliferation rate, most NETs are relatively resistant to chemotherapeutics. Most NETs are characterized by overexpression of somatostatin receptors, mainly subtype 2 (sst2). Targeting these receptors by administration of somatostatin analogs radiolabeled with, e.g., beta particle-emitting radionuclides, such as ^{177}Lu or ^{90}Y , allows peptide receptor radionuclide therapy (PRRT) of NET patients. This therapeutic approach is being performed since more than 10 years and has proven to be an effective treatment option in patients with inoperable disease. Therapeutic responses result in a significantly longer overall survival time compared to other treatments such as chemotherapy or external beam radiation therapy (5-7). PRRT also improves patient's self-assessed quality of life (8). Although PRRT is a successful therapy, complete remissions (CR) in patients with metastasized disease are still rare, so there is an urgent need for improvement. The combination of PRRT with the mammalian target of rapamycin (mTOR) inhibitor everolimus or RAD001 could be promising in this respect. Everolimus (RAD001) has recently received FDA approval for the treatment of pancreatic NETs. RAD001 has been reported to show anti-tumor and anti-angiogenic activity both *in vitro* as well as *in vivo*, since both tumor proliferation and tumor angiogenesis are regulated by mTOR (9). The clinical RADIANT III trial, a randomized, double-blind, placebo-controlled, multicenter phase III trial in pancreatic neuroendocrine tumor (PNET) patients, showed a median progression-free survival of 11 months after daily administration of 10 mg RAD001 plus best supportive care versus 4.6 months in the placebo group (3). Since it was shown that RAD001 may act as radiosensitizer in various tumor models (10), RAD001 and PRRT could have a synergistic effect. Antitumor efficacies of RAD001 treatment schedules in the CA20948 tumor model have been reported before by Boulay et al. (11). In this study, comparable anti-tumor effects were shown for twice weekly and daily RAD001 administration. We have performed a combination study of the two treatments in the sst2-expressing CA20948 tumorbearing rat model on which we recently reported the first data (1). In this study, we compared either ^{177}Lu -DOTATATE, RAD001, or their combination for treatment of tumor-bearing rats. RAD001 was administered orally twice a week for 4.5 weeks, and a suboptimal dose of ^{177}Lu -DOTATATE (leaving room for additional effect of RAD001) was given once. Unexpectedly, we observed that the majority (77%) of rats treated with RAD001 (single treatment or combined with PRRT) developed metastases. We have used this subcutaneous CA20948 tumor model in many PRRT studies for more than 10 years, and metastases never occurred before.

We have hypothesized that a rebound effect after stopping the RAD001 treatment after 4.5 weeks initiated a metastasizing process. Furthermore, we observed that rats treated with the combination of RAD001 and ^{177}Lu -DOTATATE showed less impressive anti-tumor effects compared to those treated with ^{177}Lu -DOTATATE-only. In the current studies, we performed additional in vivo experiments in the same rat model and obtained additional results from the previous studies. To find an explanation for the lower therapeutic effect of the combination vs. single ^{177}Lu -DOTATATE therapy, ^{177}Lu -DOTATATE tumor uptake was quantified in tumors with and without RAD001 pretreatment. Moreover, in LEW/ SsNsd rats, we studied the effects of longer, i.e., 12 instead of 4.5 weeks.

Table 1. Overview of the research questions and setup of the subsequent studies

Research question (rat strain)	Study	Groups	N	^{177}Lu -TATE (MBq)	RAD001 (dose, period)
A) Potential synergistic effect of RAD001 in combination with ^{177}Lu-DOTATATE (LEW/HanHsd)	1	Control	7	-	placebo
		RAD only	6	-	5.0 mg/kg, 4.5w
		^{177}Lu -TATE low dose	7	125	placebo
		^{177}Lu -TATE high dose	7	275	placebo
		RAD + ^{177}Lu -TATE low dose	7	125	5.0 mg/kg, 4.5w
		RAD + ^{177}Lu -TATE high dose	7	275	5.0 mg/kg, 4.5w
B) Prolonged follow up of potential development of distant metastasis (LEW/HanHsd)	2	control	8	-	placebo
		low dose RAD	8	-	2.5 mg/kg, 4.5w
		high dose RAD	8	-	5.0 mg/kg, 4.5w
		^{177}Lu -TATE	7	125	placebo
		^{177}Lu -TATE + low dose RAD	8	125	2.5 mg/kg, 4.5w
		^{177}Lu -TATE + high dose RAD	7	125	5.0 mg/kg, 4.5w
C) Influence of RAD001 on tumor uptake of ^{177}Lu-DOTATATE (LEW/HanHsd)	1 + 2	^{177}Lu -TATE	21	125 or 275	placebo
		RAD + ^{177}Lu -TATE	29	125 or 275	2.5 mg/kg or 5.0 mg/kg, 4.5w

Table 1 continues

D) Effects of prolonged RAD001 treatment (LEW/SsNHsd)	3	control	8	-	Placebo
		RAD	8	-	5.0 mg/kg, 4.5w
		¹⁷⁷ Lu-TATE + RAD	8	125	5.0 mg/kg, 4.5w
		RAD prolonged treatment	8	-	5.0 mg/kg, 12w
		¹⁷⁷ Lu-TATE + RAD prolonged treatment	8	125	5.0 mg/kg, 12w
E) Effects of PRRT on growth of metastases (LEW/SsNHsd)	3	High dose ¹⁷⁷ Lu-TATE after diagnosis of metastases	7	400	-

¹⁷⁷Lu-TATE: ¹⁷⁷Lu-DOTA⁰,Tyr³-octreotate, RAD: RAD001, PRRT: peptide receptor radionuclide therapy, w: weeks.

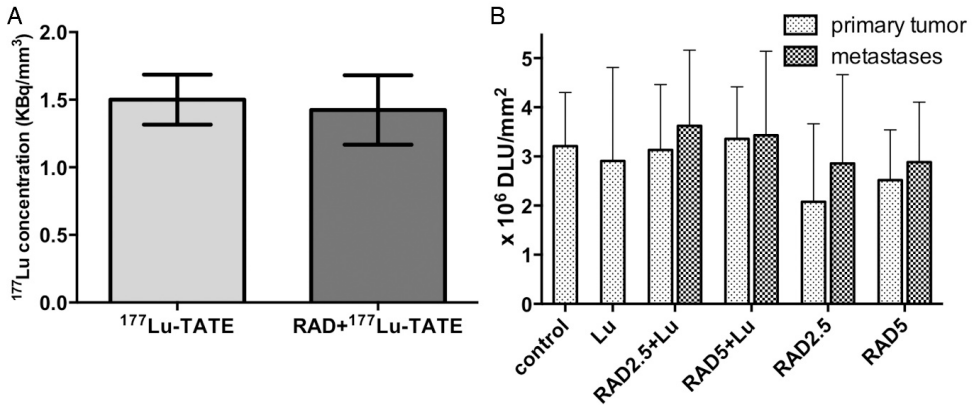


Figure 1. A) Tumor concentration of ¹⁷⁷Lu-DOTATATE in rats receiving ¹⁷⁷Lu-DOTATATE-only (light grey bar) and groups receiving ¹⁷⁷Lu-DOTATATE 4 days after RAD001 therapy was started (dark grey bar). B) Quantification of sst₂ expression in primary tumors and metastases based on in vitro autoradiography. (¹⁷⁷Lu-TATE: ¹⁷⁷Lu-DOTA⁰,Tyr³-octreotate, RAD: RAD001 2.5 or 5 mg/kg, DLU: digital light unit)

MATERIALS AND METHODS

Tumor Cell Lines

The rat sst₂-expressing pancreatic tumor CA20948 cell line (12) was cultured in Dulbecco's modified Eagle's medium (DMEM, Gibco, Invitrogen Corp., Breda, the Netherlands) supplemented with 10% heat-inactivated fetal bovine serum.

Animals and tumor model

The animal ethics committee of our institution has approved all experiments. Male Lewis rats (250 to 300 g) were obtained from Harlan (Heerlen, the Netherlands). We used LEW/HanHsd Lewis rats, and where indicated, we also included rats from the LEW/SsNHsd substrain. In the LEW/SsNHsd substrain, the immune system shows an enhanced CD4+ and CD8+ T cell (auto)-immune response (13-17). This autoimmunity is linked to an increased tumor immunity (18, 19). One week after arrival, rats were inoculated subcutaneously with 10^7 CA20948 cells in 0.5 ml HBSS. For all experiments, animals were randomized into matching treatment groups with regard to tumor size at the start of treatment. A person blinded for the treatment measured tumor size using a calliper and weighed the rats three times a week. Tumor volume was calculated using the formula: $0.4 \times \text{length} \times \text{width} \times \text{height}$. Tumor response was defined as follows: partial response (PR) as >50% reduction of tumor volume and complete response (CR) as 100% reduction of tumor volume. Tumors were allowed to develop until a maximum of 4 to 6 cm³ and were surgically removed where indicated. Rats were euthanized when >10% loss of body weight (BW) was registered.

Anesthesia

2.5% Isoflurane/O₂ gas anesthesia was used at 0.5 ml/min during tumor cell inoculation, administration of ¹⁷⁷LuDOTATATE, scanning, or surgery.

Surgical procedure to remove the primary tumor

When primary tumors were >4 to 6 cm³, surgical tumor resection was performed where indicated. During surgery, a heating pad was used to maintain body temperature. Routine shaving and disinfecting of the skin was performed. The tumor including the tumor capsule was carefully dissected from the surrounding tissue. After tumor resection, the skin was closed using individual sutures (vicryl 3/0).

RAD001

RAD001 and its placebo, kindly provided by Novartis Pharmaceuticals, Basel, Switzerland, were used for study 1 and prepared according to the manufacturer's protocol. For the next experiments, RAD001 powder from LC laboratories, Woburn, USA, was dissolved in 2 ml ethanol and diluted with 5% glucose solution in water to obtain 3 or 6 mg/ml. RAD001 was administered orally by gavage in a volume of 0.2 ml; thus, 0.8 or 1.6 mg/rat or 2.5/5 mg/kg BW was administered depending on treatment group. For each administration, RAD001 was prepared freshly from powder.

Radionuclides and peptides

DOTA⁰, Tyr³-octreotate was obtained from Mallinckrodt, St. Louis, MO, USA, and ¹⁷⁷LuCl₃ was obtained from IDB, Baarle-Nassau, the Netherlands. ¹⁷⁷Lu-DOTATATE was

prepared as described before (20), with a specific activity of 100 MBq/2.75 µg peptide, and injected iv via the tail vein under anesthesia. Labeling of ¹¹¹In-DTPA-octreotide (OctreoScan, Covidien, Petten, the Netherlands) in a specific activity of 30 MBq/0.5 µg DTPA-octreotide was performed as described previously (21).

SPECT/CT scanning

Forty-eight hours after injection of ¹⁷⁷Lu-DOTATATE, helical single-photon emission computed tomography/ computed tomography (SPECT/CT) scanning of the tumor region was performed with the four-headed NanoSPECT/CT system (BioScan, Washington DC, USA). Multi-pinhole rat collimators with nine pinholes (diameter 2.5 mm) per head were used: 24 projections, 90 s per projection, were applied. SPECT scans were reconstructed iteratively on a 256 × 256 matrix, using HiSPECT NG software (Scivis GmbH, Göttingen Germany) and ordered subset expectation maximization (OSEM). The total amount of radioactivity (MBq) in the tumor was quantified by drawing a sufficiently large volume of interest (VOI) around the tumor using InVivoScope software (IVS, Bioscan, Washington DC, USA). To achieve accurate quantification, the camera was calibrated by scanning a 20-ml polypropylene tube rat phantom filled with a known amount of ¹⁷⁷Lu activity. The in vivo tumor volume was assessed by setting the lower threshold to 90% of the maximum voxel intensity of the tumor using the IRW program (Siemens, Erlangen, Germany). Before euthanasia, a whole-body SPECT/CT scan of rats was acquired 24 h after intravenous injection of ¹¹¹In-DTPA-octreotide (50 MBq ¹¹¹In/0.5 µg DTPA-octreotide) to detect CA20948 metastases. During scanning, the rat body temperature was maintained using a heated bed.

***In vitro* autoradiography**

Autoradiography was performed on primary tumors as well as metastases. Frozen sections of 10 µm (Cryo-Star HM 560 M; Microm, Walldorf, Germany) were mounted on Superfrost plus slides (Menzel, Braunschweig, Germany) and incubated with 10⁻¹⁰M ¹¹¹In-DTPA-octreotide with and without an excess (10⁻⁶M) of unlabelled octreotide. Adjacent sections were used for Hematoxylin/Eosin staining. Tumor sections were exposed to SR phosphor imaging screens (Packard Instruments Co., Meriden, USA) in X-ray cassettes. After 48 h exposure, screens were read by a Cyclone phosphor imager and analysed using OptiQuant 03.00 (Perkin Elmer, Groningen, the Netherlands).

Statistics

Prism software version 5.0 (Graph Pad) was used to analyse tumor growth and determine statistical significance between groups. An unpaired T-test was used for statistical analysis of tumor uptake (Figure 1). Results are given as mean +/-SD. A log rank test was performed for curve comparison in Figures 2A and 2B. Body weight data in Figure 2C are expressed as mean values.

Experimental design

An overview of the different research questions (A-E) and treatment groups in all studies (1-3) is given in Table 1 and described below.

A) Potential synergistic effect of RAD001 in combination with ^{177}Lu -DOTATATE

To study whether RAD001 has an additional anti-tumoral effect on ^{177}Lu -DOTATATE, 6 different study groups were included with 6-7 rats per group. Besides the control group and the RAD001-only therapy groups (5 mg/kg twice a week for 4.5 weeks), 2 groups received ^{177}Lu -DOTATATE as a single therapy in different doses (125 or 275 MBq), and 2 groups received the same doses of ^{177}Lu -DOTATATE combined with RAD001 treatment (5 mg/kg twice a week for 4.5 weeks starting 3 days prior to PRRT)¹. Rats were euthanized when tumor size exceeded 4 cm³.

B) Prolonged follow up of potential development of distant metastasis in all groups after surgical resection of the primary tumor

Six additional groups of rats were included in the next study with 7-8 rats in each group. To enable prolonged follow up, in this experiment primary tumors were surgically removed when >4 cm³. This enabled longer follow up to study the development of metastases in relation to the combination of ^{177}Lu -DOTATATE and RAD001 or RAD001-only. 2.5 or 5.0 mg/kg RAD001 was administered twice weekly for 4.5 weeks, either alone or 3 days prior to 125 MBq ^{177}Lu -DOTATATE,

C) Influence of RAD001 on tumor uptake of ^{177}Lu -DOTATATE ^{177}Lu -DOTATATE-uptake in tumors was quantified based on SPECT/CT scans acquired 48 hours after administration of ^{177}Lu -DOTATATE in experiment 1 and 2 to examine if previous RAD001 treatment results in reduced ^{177}Lu -retention in CA20948 tumors.

D) Effects of prolonged RAD001 treatment Five groups of 8 rats were included. 5 mg/kg RAD001 therapy was started 4 days after 125 MBq ^{177}Lu -DOTATATE. RAD001 was administered twice a week and continued for either 4.5 or 12 weeks. Surgical resection was performed if tumors reached a volume of 6 cm³.

E) Effects of PRRT retreatment on metastases If rats in experiment 3 showed lethargy or a >10% body weight loss, SPECT/CT was performed using ^{111}In -DTPA-octreotide. If metastases could be discriminated, 400MBq/10.8µg ^{177}Lu -DOTATATE PRRT was given. 24h after ^{177}Lu -DOTATATE injections, SPECT/CT was performed to image ^{177}Lu -DOTATATE uptake in metastases. Therapeutic effect was monitored by follow-up of body weight and ^{111}In -DTPA-octreotide SPECT/CT when ongoing decrease in body weight was registered.

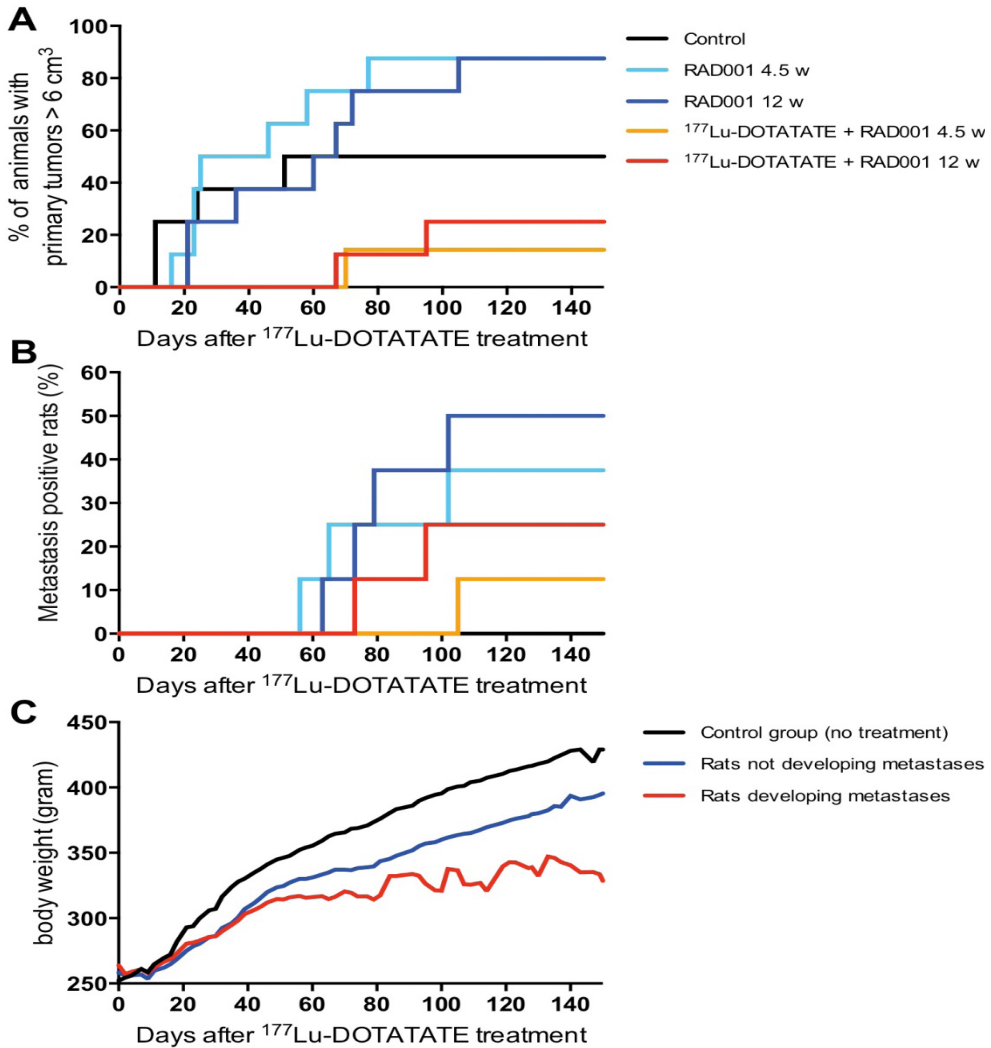


Figure 2. A) Percentage of (LEW/SsNHsd Lewis) rats with primary tumors that reached the max. size > 6 cm³ and underwent surgery afterwards to remove the tumor. The control group received saline. RAD001 therapy started at day 4 (5 mg/kg administered twice weekly). ¹⁷⁷Lu-DOTATATE (125 MBq) was administered at day 1. B) Percentage of (LEW/SsNHsd Lewis) rats developing metastases in each group. C) Mean body weight of animals in the control group (black line) and of the rats treated with either RAD001 or a combination of RAD001 and ¹⁷⁷Lu-DOTATATE that did not develop metastases (blue line) versus the body weight of rats treated with RAD001 or a combination of RAD001 and ¹⁷⁷Lu-DOTATATE that developed metastases (red line).

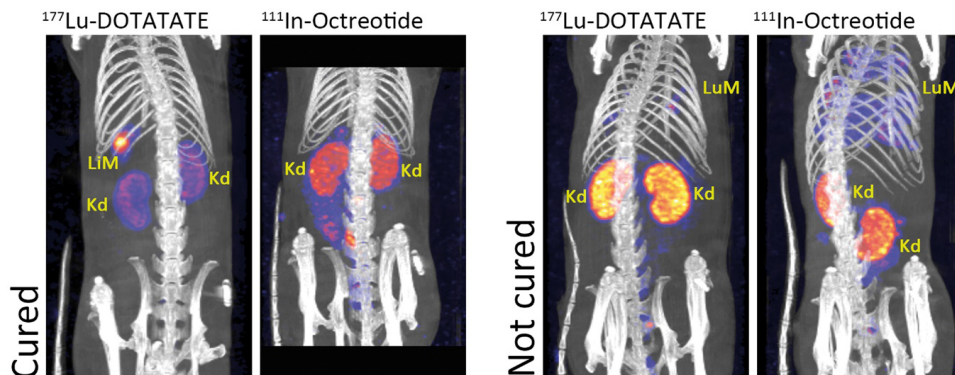


Figure 3. Two representative sets of SPECT/CT scans of rats before and after retreatment with ^{177}Lu -DOTATATE. The two images at the left represent a rat with liver metastasis; the lesion was not detectable anymore on the scan with ^{111}In -DTPA-octreotide made 8 days after ^{177}Lu -DOTATATE PRRT. The two images at the right represent a rat treated for lung metastases. On the right scan after injection of ^{111}In -DTPA-octreotide made before euthanasia of the rat because of on-going weight loss. (LuM = lung metastases, LiM = liver metastases, Kd = kidney)

RESULTS

A) Potential synergistic effect of RAD001 in combination with ^{177}Lu -DOTATATE

In experiment 1 treatment with RAD001-only did not result in any complete or partial anti-tumor responses (According to our definitions in this preclinical study: Partial response (PR): > 50% reduction of tumor volume, but no CR (100% reduction of tumor volume) (Table 2). Groups treated with ^{177}Lu -DOTATATE-only showed 57% CRs after 125 MBq ^{177}Lu -DOTATATE and 71% after 275 MBq ^{177}Lu -DOTATATE. Combination of ^{177}Lu -DOTATATE and RAD001 however, resulted in only 29% CR after 125 MBq ^{177}Lu -DOTATATE + RAD001 and 14% after 275 MBq ^{177}Lu -DOTATATE + RAD001. So, in contrast to our hypothesis, no additive effect with regard to tumor response could be achieved by combining RAD001 and ^{177}Lu -DOTATATE. Moreover, unexpectedly, all rats treated with the combination of RAD001 and ^{177}Lu -DOTATATE and not showing CR eventually developed metastases as was reported earlier¹.

B) Prolonged follow up of potential development of distant metastasis in all groups after surgical resection of the primary tumor

Prolonged monitoring after primary tumor removal, the majority (77%) of rats treated with RAD001 (either 5.0 mg/kg or 2.5 mg/kg), developed metastases that resulted in mean body weight loss around 43 days after start of treatment. For these two doses no clear dose dependence on RAD001 was found (Table 2).

C) Influence of RAD001 on tumor uptake of ^{177}Lu -DOTATATE The ^{177}Lu -tumor uptake in ^{177}Lu -DOTATATE-only treated rats was $1.51 \pm 0,07 \text{ kBq/mm}^3$, while this was

$1.42 \pm 0,07$ kBq/mm³ in rats pre-treated with RAD001. Thus no significant different values between the groups ($p=0.50$, Figure 1A) were found.

D) Effects of prolonged RAD001 treatment In contrast to previous experiments 50% of the rats in the control group showed a CR. The rats from the combination groups (¹⁷⁷Lu-DOTATATE + RAD001 for 4.5weeks resp. ¹⁷⁷Lu-DOTATATE + RAD001 for 12 weeks) showed a CR in 87.5% resp. 75% (not significantly different; $p=0.63$) of the animals, in comparison to only 12.5% of rats in both RAD001-only therapy groups. Within these 2 RAD001-only groups, there was no significant difference regarding both the number of animals that needed surgery as well as the time until surgery.

With regard to development of metastases, at day 150 p.t. no metastases were detected in untreated rats (Figure 2B). Also the time of appearance of the metastases in the combination group was later; 61 d p.t. vs. 91 p.t, respectively.

Monitoring the body weight of rats revealed the effects of treatment and the development of metastases. Rats in the control group showed a normal gain in body weight over time (Figure 2C). Rats treated with ¹⁷⁷Lu-DOTATATE + RAD001 or RAD001-only not developing metastases, also showed gain in body weight over time, although at a slower rate. However, the mean body weight of rats developing metastases stabilized as a result of their poor condition.

E) Effects of PRRT on growth of metastases Although SPECT/CT confirmed significant uptake of ¹⁷⁷Lu-DOTATATE in metastases (Figure 3), in only two of the seven rats there was CR after retreatment with high dose ¹⁷⁷Lu-DOTATATE. The average survival time of the non-responsive rats after detection and treatment of the metastases varied between 8 and 37 days, with an average of 27 days. One rat with CR recovered from a liver metastasis that was clearly visualized after administration of ¹⁷⁷Lu-DOTATATE. Eight days later there was no sign of this lesion as shown in the ¹¹¹In-octreotide scan, which was confirmed after dissection. On the other hand, a rat suffering from lung metastases did not respond to ¹⁷⁷Lu-DOTATATE. 8 days after re-treatment further loss in body weight was measured and the ¹¹¹In-DTPA-octreotide SPECT/CT still showed extended lung metastases, also found at autopsy. Determination of sst₂-density on CA20948 primary tumors and metastases using in vitro autoradiography revealed no significant differences (Figure 1B).

DISCUSSION

We previously reported on the disappointing results of the combination of mTOR inhibitor RAD001 with ¹⁷⁷Lu-DOTATATE PRRT in the CA20948 rat tumor model. No hypothesised synergistic effect was found; the combination treatment appeared even less effective than ¹⁷⁷Lu-DOTATATE-only. This observation cannot be explained by reduced ¹⁷⁷Lu-DOTATATE uptake in the subcutaneous CA20948 tumors after RAD001 treatment as we demonstrated here. (Figure 1A).

Even more striking was the fact that the majority of RAD001 treated animals developed tumor metastasis to lymph nodes, liver and/or lung. RAD001 initially has been introduced as an immunosuppressive to protect patients from rejecting allografts after organ transplantation (22). In 2005 Law et al. (23) reviewed the immunosuppressive effects of RAD001 in relation to its anti-tumor effects, and discussed immune suppression by RAD001 to be tumor growth accentuating. Therefore the application of RAD001 as an anti-tumor agent should be monitored carefully in the clinic, but to the best of our knowledge as yet no tumor accentuating effects in patients have been reported. Recently, after the publication of our Priority Report on our first findings, RAD001 has received FDA approval for the treatment of advanced NETs and is commonly used in clinical practice nowadays. Although we must consider the fact that RAD001 is used in patients with already advanced (metastasized) disease, so far no reports on accelerated metastasis in patients related to RAD001 treatment have been published. We earlier hypothesized multiple reasons for the occurrence of metastases: the twice-weekly dose regimen instead of daily dosing as is applied in clinical therapy, effects of RAD001 on the immune system and/or tumor microenvironment, or the discontinuation of RAD001 treatment at 4.5-weeks after start of treatment. In the current studies we compared 4.5-weeks of RAD001 treatment with 12-weeks twice-weekly RAD001 treatment. This prolonged RAD001 treatment (with or without ^{177}Lu -DOTATATE therapy) did not reduce the number of rats developing metastases and in addition no delay in the occurrence of metastasis was seen. In fact, comparison of the 4.5-weeks RAD001 groups versus 12-weeks RAD001 groups showed a higher percentage of rats developing metastasis in the 12-weeks RAD001 groups, namely, 38% vs. 25% ($p=0.45$) in the 4.5-weeks RAD001 groups. The average time until detection of metastases was also not significantly different between groups receiving RAD001 for 4.5-weeks (82 days p.t.) versus 12-weeks (78 day p.t.). Moreover, in 67% of the rats developing metastases in the 12-weeks treatment groups, metastases were diagnosed while rats were still receiving RAD001. Therefore it is unlikely that the occurrence of metastases is due to cessation of RAD001 administration. Potentially the twice-weekly administration could lead to a repetitive on-off effect on the mTOR pathway with repetitive up regulation/rebound effects of the mTOR pathway with varying plasma concentration levels of RAD001 in a twice weekly dose regimen(24) . In future experiments a daily RAD001 dose regimen will have to be compared to the twice-weekly dose regimen as was used in the current studies.

Compared to a treatment with RAD001-only, less animals receiving a combination of ^{177}Lu -DOTATATE and RAD001 developed metastases and mean time to diagnosis for those metastases was 30 days later compared to the rats receiving RAD001-only. Results from the combination therapy groups with ^{177}Lu -DOTATATE administered 4 days before RAD001 therapy suggested that ^{177}Lu -DOTATATE administered prior to RAD001 therapy reduced both incidence and time of onset of metastases in comparison to the reverse order combination. When ^{177}Lu -DOTATATE was administered 4 days after RAD001 therapy however, there was no reduction in the percentage of rats developing metastases in the combination therapy groups, indicating that rats with (some) tumor reduction already induced by PRRT were less likely to develop

metastases than rats not treated with PRRT. This is in agreement with the fact that animals that showed CRs after PRRT or PRRT plus RAD001 did not develop metastases during follow up.

Table 2. Overview of tumor responses.

Experiment	Group	CR (%)	PR (%)	% rats with metastases	n
1	Control*	0	0	0	7
	RAD 5mg/kg*	0	0	0	6
	¹⁷⁷ Lu-TATE 125 MBq	57	29	0	7
	¹⁷⁷ Lu-TATE 278 MBq	71	29	0	7
	RAD 5mg/kg + ¹⁷⁷ Lu-TATE 125 MBq	29	57	71	7
	RAD 5mg/kg+ ¹⁷⁷ Lu-TATE 278 MBq	14	57	86	7
2	Control**	0	0	0	8
	RAD 5.0 mg/kg**	0	13	75	8
	RAD 2.5 mg/kg**	13	0	63	8
	¹⁷⁷ Lu-TATE 125 MBq**	43	57	0	7
	¹⁷⁷ Lu-TATE 125 MBq+ RAD 5.0 mg/kg**	0	63	88	8
	¹⁷⁷ Lu-TATE 125 MBq + RAD 2.5 mg/kg**	14	43	86	7
3	Control **	50	0	0	8
	RAD 4½ weeks**	12.5	12.5	37.5	8
	RAD 12 weeks**	12.5	25	50	8
	¹⁷⁷ Lu-TATE 125 MBq + RAD 4½ weeks**	87.5	12.5	12.5	8
	¹⁷⁷ Lu-TATE 125 MBq + RAD 12 weeks**	75	25	25	8

*rats did not survive until 42 – 14⁶ days post start of treatment (p.t.), the time frame in which metastases became apparent in the other groups, because rats had to be euthanized when primary tumor size was > 4-6 cm³. **Primary tumors were surgically removed when tumor size was >4-6cm³. CR, complete response (100% reduction of tumor size); PR, partial response (> 50% reduction of tumor volume but no CR); n: number of animals/group, ¹⁷⁷Lu-TATE: ¹⁷⁷Lu-DOTA⁰, Tyr³-octreotate, RAD: RAD001.

In studies 1 and 2 we used a syngeneic tumor model in rats with an uncompromised immune system. A significant role for T lymphocytes in the immune response to tumors after or during ionizing radiation therapy has been described, the latter resulting in upregulation of tumor-specific antigens(25-29). As immune suppression by RAD001 has been proven to be mainly due to suppression of T-lymphocyte activation and proliferation(30, 31), to our opinion immune suppression by RAD001 is a likely explanation for reduced tumor response to PRRT in combination with RAD001 as observed in our study. In studies 1 and 2 LEW/HanHsd rats were used, whereas in study 3 the LEW/SsNHsd substrain was used, providing the opportunity to test the hypothesis mentioned above. In this substrain the immune system is more active

compared to the HanHsd strain and shows an enhanced (auto)-immune response (13-17). In these rats 50% of tumors in the control group went into spontaneous regression after reaching an average tumor volume of $\approx 3\text{cm}^3$, probably due to an immune response against the growing tumor. In such rats treated with RAD001 (4.5 or 12 weeks) only 12.5% of the tumors went into regression. In a mouse model on rejection of an allogeneic subcutaneous tumor as created by Hammond-McKribben et al. (22), another mTOR inhibitor, the rapamycin derivative SDZ RAD, was used to prevent rejection of allogeneic tumors. So, immune suppression by RAD001 might have caused the reduced tumor response in our study with ^{177}Lu -DOTATATE administered after RAD001 as well.

Contrary to our results, a combination of ionizing radiation (IR) with rapamycin has been proven to be more effective than IR-only in preclinical studies (10, 32, 33). These studies however have been performed in xenograft models using immunodeficient mice lacking T-cells.

As discussed in our priority report, reduced cell proliferation rate caused by a G1 arrest could also be an explanation for the reduced tumor response to ^{177}Lu -DOTATATE in rats treated with the combination of RAD001 and ^{177}Lu -DOTATATE. RAD001 treatment has been shown to cause a G1 arrest, as mTOR is being linked to phosphatidylinositol 3-kinase (PI3K) pathways (34). Within 24 h after RAD001 administration a significant increase of cells in G1 phase has been described (35, 36). As cells with a long cycling time, including NET cells, have a peak of radioresistance during early G1 phase (37), tumor cells may have been less sensitive to ^{177}Lu -DOTATATE when administered 4 d after the start of RAD001 treatment. Since clinical trials combining RAD001 and PRRT are being performed (38), to our opinion the decreased antitumor response in our study when RAD001 was administered prior to ^{177}Lu -TATE is rather relevant. Also in a clinical situation the combination of both therapies might be less effective compared to just PRRT.

For re-treatment of the rats with metastases we used a dose of 400MBq ^{177}Lu -DOTATATE, which is remarkably higher compared to the initial 125 or 275 MBq treatment doses. Still only 2 out of 7 rats with metastases were cured, suggesting metastases in our model to be more resistant to PRRT compared to the primary tumor. As it is quite complex to study responses of metastases in a preclinical model, there have not been many preclinical studies on therapies in metastatic models. However, to be able to get more solid information on sensitivity of metastases to PRRT in a preclinical model, certainly more studies in different models are necessary. The current CA20948 metastatic tumor model after RAD001 treatment could be a more realistic metastasis model for future experiments compared to often applied metastasis-tumor models in which tumor cell suspensions are injected intravenously.

Concluding remarks: Results described here confirmed and provided more information on development of metastasis after RAD001 treatment in our in vivo rat tumor model. The impaired tumor response to the combination of RAD001 and ^{177}Lu -DOTATATE in

comparison with that after ^{177}Lu -DOTATATE-only could not be attributed to a reduced tumor uptake of ^{177}Lu -DOTATATE in rats after RAD001 treatment. Moreover, the occurrence of metastases could not be attributed to the sudden cessation of RAD001 treatment, as we observed treatment for 12-weeks did not result in a lower metastasis rate compared to treatment for 4.5-weeks. Immune suppression by RAD001 could be a good explanation for reduced tumor response after RAD001 as well as for development of metastasis. More studies in different tumor models are needed now to provide proof and give detailed information on the translational value of these findings to the clinic.

REFERENCES

1. Pool SE, Bison S, Koelewijn SJ, van der Graaf LM, Melis M, Krenning EP, et al. mTOR inhibitor RAD001 promotes metastasis in a rat model of pancreatic neuroendocrine cancer. *Cancer research*. 2012. Epub 2012/11/15.
2. Modlin IM, Moss SF, Gustafsson BI, Lawrence B, Schimmack S, Kidd M. The archaic distinction between functioning and nonfunctioning neuroendocrine neoplasms is no longer clinically relevant. *Langenbeck's archives of surgery*. 2011;396(8):1145-56. Epub 2011/04/28.
3. Yao JC, Shah MH, Ito T, Bohas CL, Wolin EM, Van Cutsem E, et al. Everolimus for advanced pancreatic neuroendocrine tumors. *The New England journal of medicine*. 2011;364(6):514-23. Epub 2011/02/11.
4. Yao JC, Hassan M, Phan A, Dagohoy C, Leary C, Mares JE, et al. One hundred years after "carcinoid": epidemiology of and prognostic factors for neuroendocrine tumors in 35,825 cases in the United States. *Journal of clinical oncology : official journal of the American Society of Clinical Oncology*. 2008;26(18):3063-72. Epub 2008/06/21.
5. van Essen M, Krenning EP, Kam BL, de Jong M, Valkema R, Kwekkeboom DJ. Peptide-receptor radionuclide therapy for endocrine tumors. *Nature reviews Endocrinology*. 2009;5(7):382-93. Epub 2009/06/03.
6. Kwekkeboom DJ, de Herder WW, van Eijck CH, Kam BL, van Essen M, Teunissen JJ, et al. Peptide receptor radionuclide therapy in patients with gastroenteropancreatic neuroendocrine tumors. *Semin Nucl Med*. 2010;40(2):78-88. Epub 2010/02/02.
7. Bodei L, Cremonesi M, Grana CM, Fazio N, Iodice S, Baio SM, et al. Peptide receptor radionuclide therapy with (1)(7)(7)Lu-DOTATATE: the IEO phase I-II study. *European journal of nuclear medicine and molecular imaging*. 2011;38(12):2125-35. Epub 2011/09/06.
8. Teunissen JJ, Kwekkeboom DJ, Krenning EP. Quality of life in patients with gastroenteropancreatic tumors treated with (177Lu-DOTA0,Tyr3)octreotate. *Journal of clinical oncology : official journal of the American Society of Clinical Oncology*. 2004;22(13):2724-9. Epub 2004/07/01.
9. Seeliger H, Guba M, Kleespies A, Jauch KW, Bruns CJ. Role of mTOR in solid tumor systems: a therapeutic target against primary tumor growth, metastases, and angiogenesis. *Cancer metastasis reviews*. 2007;26(3-4):611-21. Epub 2007/08/24.
10. Manegold PC, Paringer C, Kulka U, Krimmel K, Eichhorn ME, Wilkowski R, et al. Antiangiogenic therapy with mammalian target of rapamycin inhibitor RAD001 (Everolimus) increases radiosensitivity in solid cancer. *Clinical cancer research : an official journal of the American Association for Cancer Research*. 2008;14(3):892-900. Epub 2008/02/05.
11. Boulay A, Zumstein-Mecker S, Stephan C, Beuvink I, Zilbermann F, Haller R, et al. Antitumor efficacy of intermittent treatment schedules with the rapamycin derivative RAD001 correlates with prolonged inactivation of ribosomal protein S6 kinase 1 in peripheral blood mononuclear cells. *Cancer research*. 2004;64(1):252-61. Epub 2004/01/20.

12. Bernard BF, Krenning E, Breeman WA, Visser TJ, Bakker WH, Srinivasan A, et al. Use of the rat pancreatic CA20948 cell line for the comparison of radiolabelled peptides for receptor-targeted scintigraphy and radionuclide therapy. *Nuclear medicine communications*. 2000;21(11):1079-85. Epub 2001/02/24.
13. Cutler LS, Greiner DL, Rozenski D. Experimental autoallergic sialadenitis in the LEW rat. II. Target antigens are associated with cell surface and intracellular particulate fractions derived from the submandibular gland. *Cellular immunology*. 1991;135(2):346-53. Epub 1991/07/01.
14. Greiner DL, Angelillo M, Wayne AL, Fitzgerald KM, Rozenski D, Cutler LS. Experimental autoallergic sialadenitis in the LEW rat. III. Role of CD4+ T cells in EAS induction. *Cellular immunology*. 1991;135(2):354-9. Epub 1991/07/01.
15. Perlik F, Zidek Z. The susceptibility of several inbred strains of rats to adjuvant-induced arthritis and experimental allergic encephalomyelitis. *Zeitschrift fur Immunitatsforschung, experimentelle und klinische Immunologie*. 1974;147(2):191-3. Epub 1974/06/01.
16. Gasser DL, Palm J, Gonatas NK. Genetic control of susceptibility to experimental allergic encephalomyelitis and the Ag-B locus of rats. *J Immunol*. 1975;115(2):431-3. Epub 1975/08/01.
17. Friedman I, Ron N, Laufer A, Davies AM. Experimental myocarditis: enhancement by the use of pertussis vaccine in Lewis rats. *Experientia*. 1970;26(10):1144-5. Epub 1970/10/15.
18. Gridley G, McLaughlin JK, Ekblom A, Klareskog L, Adami HO, Hacker DG, et al. Incidence of cancer among patients with rheumatoid arthritis. *Journal of the National Cancer Institute*. 1993;85(4):307-11. Epub 1993/02/17.
19. Sakaguchi S, Takahashi T, Yamazaki S, Kuniyasu Y, Itoh M, Sakaguchi N, et al. Immunologic self tolerance maintained by T-cell-mediated control of self-reactive T cells: implications for autoimmunity and tumor immunity. *Microbes and infection*. 2001;3(11):911-8. Epub 2001/09/21.
20. Kwekkeboom DJ, Bakker WH, Kooij PP, Konijnenberg MW, Srinivasan A, Erion JL, et al. (177Lu-DOTAOTyr3)octreotate: comparison with (111In-DTPA)octreotide in patients. *Eur J Nucl Med*. 2001;28(9):1319-25. Epub 2001/10/05.
21. Breeman WA, Kwekkeboom DJ, Kooij PP, Bakker WH, Hofland LJ, Visser TJ, et al. Effect of dose and specific activity on tissue distribution of indium-111-pentetreotide in rats. *Journal of nuclear medicine : official publication, Society of Nuclear Medicine*. 1995;36(4):623-7. Epub 1995/04/01.
22. Hammond-McKibben D, Saulnier M, Zhang J, Risher N, Lake P, Weetall M. Immunologic pathways in a quantitative model of immunosuppression based on rejection of an allogeneic or xenogeneic tumor graft. *Transplantation*. 2005;79(8):889-96. Epub 2005/04/26.
23. Law BK. Rapamycin: an anti-cancer immunosuppressant? *Critical reviews in oncology/hematology*. 2005;56(1):47-60. Epub 2005/07/26.
24. Tanaka C, O'Reilly T, Kovarik JM, Shand N, Hazell K, Judson I, et al. Identifying optimal biologic doses of everolimus (RAD001) in patients with cancer based on the modeling of preclinical and clinical pharmacokinetic and pharmacodynamic data. *Journal of clinical oncology : official journal of the American Society of Clinical Oncology*. 2008;26(10):1596-602. Epub 2008/03/12.

25. North RJ. Gamma-irradiation facilitates the expression of adoptive immunity against established tumors by eliminating suppressor T cells. *Cancer immunology, immunotherapy* : CII. 1984;16(3):175-81. Epub 1984/01/01.
26. Stone HB, Peters LJ, Milas L. Effect of host immune capability on radiocurability and subsequent transplantability of a murine fibrosarcoma. *Journal of the National Cancer Institute*. 1979;63(5):1229-35. Epub 1979/11/01.
27. Demaria S, Formenti SC. Role of T lymphocytes in tumor response to radiotherapy. *Frontiers in oncology*. 2012;2:95. Epub 2012/09/01.
28. Lorimore SA, Coates PJ, Scobie GE, Milne G, Wright EG. Inflammatory-type responses after exposure to ionizing radiation in vivo: a mechanism for radiation-induced bystander effects? *Oncogene*. 2001;20(48):7085-95. Epub 2001/11/13.
29. Apetoh L, Tesniere A, Ghiringhelli F, Kroemer G, Zitvogel L. Molecular interactions between dying tumor cells and the innate immune system determine the efficacy of conventional anticancer therapies. *Cancer research*. 2008;68(11):4026-30. Epub 2008/06/04.
30. Wiederrecht GJ, Sabers CJ, Brunn GJ, Martin MM, Dumont FJ, Abraham RT. Mechanism of action of rapamycin: new insights into the regulation of G1-phase progression in eukaryotic cells. *Progress in cell cycle research*. 1995;1:53-71. Epub 1995/01/01.
31. Wicker LS, Boltz RC, Jr., Matt V, Nichols EA, Peterson LB, Sigal NH. Suppression of B cell activation by cyclosporin A, FK506 and rapamycin. *European journal of immunology*. 1990;20(10):2277-83. Epub 1990/10/11.
32. Kim KW, Moretti L, Mitchell LR, Jung DK, Lu B. Combined Bcl-2/mammalian target of rapamycin inhibition leads to enhanced radiosensitization via induction of apoptosis and autophagy in non-small cell lung tumor xenograft model. *Clinical cancer research : an official journal of the American Association for Cancer Research*. 2009;15(19):6096-105. Epub 2009/09/24.
33. Eshleman JS, Carlson BL, Mladek AC, Kastner BD, Shide KL, Sarkaria JN. Inhibition of the mammalian target of rapamycin sensitizes U87 xenografts to fractionated radiation therapy. *Cancer research*. 2002;62(24):7291-7. Epub 2002/12/25.
34. Fingar DC, Blenis J. Target of rapamycin (TOR): an integrator of nutrient and growth factor signals and coordinator of cell growth and cell cycle progression. *Oncogene*. 2004;23(18):3151-71. Epub 2004/04/20.
35. Loehberg CR, Strissel PL, Dittrich R, Strick R, Dittmer J, Dittmer A, et al. Akt and p53 are potential mediators of reduced mammary tumor growth by cloroquine and the mTOR inhibitor RAD001. *Biochemical pharmacology*. 2012;83(4):480-8. Epub 2011/12/07.
36. Sukumari-Ramesh S, Singh N, Dhandapani KM, Vender JR. mTOR inhibition reduces cellular proliferation and sensitizes pituitary adenoma cells to ionizing radiation. *Surgical neurology international*. 2011;2:22. Epub 2011/03/24.
37. Dodson H, Wheatley SP, Morrison CG. Involvement of centrosome amplification in radiation-induced mitotic catastrophe. *Cell Cycle*. 2007;6(3):364-70. Epub 2007/02/14.
38. Turner JH. Australian Experience of Radiopetide Therapy of NET. *World J Nucl Med*. 2011;1:52.

CHAPTER 5

Optimization of combined temozolomide and peptide receptor radionuclide therapie (PRRT) in mice after multimodality molecular imaging studies

Bison SM, Haeck JC, Bol K, Koelewijn SJ, Groen HC, Melis M, Veenland J, Bernsen MR, de Jong M

Published in European Journal of Nuclear Medicine and Molecular Imaging research. 2015 Dec; 5:62 DOI 10.1186/s13550-015-0142-y

INTRODUCTION

Systemic internal radiation therapy using radiolabelled peptides, specifically targeting receptors overexpressed on tumour cells, is an attractive cancer treatment. A high absorbed radiation dose is being delivered to tumours with a tolerable toxicity in normal non-targeted tissues. This so-called "peptide receptor radionuclide therapy" (PRRT) has been shown to be a most effective treatment option for patients with SSTR-expressing NETs (1-3).

Most NETs are slowly proliferating tumours, making them relatively resistant to most chemotherapeutics. In more than 50% of the patients, NETs are diagnosed at a relatively late stage, often with metastatic spread (4), which leaves little chance for curative surgery. Then, PRRT with radiolabelled SST-analogues appeared to be an attractive cancer treatment. A high absorbed radiation dose is being delivered to tumours with a tolerable toxicity in normal non-targeted tissues (1-3). Radiolabelled SST-analogues, such as ^{111}In -DTPA-octreotide (^{111}In -octreotide) or ^{177}Lu -DOTA,Tyr³-octreotate (^{177}Lu -TATE), show a high binding affinity for the somatostatin receptor type 2 (SSTR2), which is overexpressed on the vast majority of neuroendocrine tumours (NETs) (5).

PRRT has proven to be an effective therapy in most patients with NETs (1, 6). Nevertheless, despite the improvement of progression free survival and quality of life, complete remissions after PRRT are still rare. A combination of PRRT with radio-sensitizing chemotherapeutics, such as capecitabine (5-fluorouracil) or temozolomide (TMZ), might induce synergistic effects (7-9). Currently, phase II clinical trials combining PRRT, using ^{177}Lu -TATE, and capecitabine or both capecitabine and TMZ are ongoing. The first analyses showed promising results (8, 10).

When PRRT with chemotherapeutics are being combined, also potential negative interactions between the two therapies should be taken into consideration. Chemotherapy might affect the SSTR2 expression on tumour cells, on which PRRT depends for targeting of radionuclides, for example (11-12). Moreover, tumour vasculature might be affected by chemotherapy whereas efficient/adequate tumour perfusion is required for local delivery of ^{177}Lu -TATE (13). To obtain an optimal therapeutic scheme for the combination of PRRT and TMZ, information on afore mentioned tumour characteristics during treatment is required, which was the aim of this preclinical study using an H69-tumour-bearing mouse model. Tumour perfusion was monitored by dynamic contrast enhanced (DCE)-MRI and SSTR expression by ^{111}In -octreotide SPECT. The results from these imaging studies were applied in the design of different therapeutic schemes to stratify maximum therapeutic efficacy using TMZ and PRRT.

MATERIALS AND METHODS

Experimental setup

We have started a pilot study in which H69 tumour-bearing mice were treated with increasing amounts of ^{177}Lu -TATE to determine which dose resulted in clear tumour responses, but without complete cure to allow detection of additional effects during combination therapy. Three groups (n=7) of H69-tumour bearing mice were treated with 10, 20 or 30 MBq ^{177}Lu -TATE and compared with untreated control animals. Monitoring of body weight and tumour size was performed until d28 after start of treatment.

For TMZ treatment different dosing schedules have been reported, including a total administered dose of >1000 mg/kg (14) or the administration of one or more cycles during 5d, in which a dose of 50 or 120 mg/kg/d was administered (15) (16) . Since we planned to administer only one cycle, we used a dose of 50 mg/kg/d for 2 weeks, to study the effects of TMZ treatment in the H69 model, supplemented with investigations into combination of PRRT and TMZ. In this study the earlier determined optimal dose of 30 MBq ^{177}Lu -TATE was used.

Imaging studies to determine tumour characteristics during PRRT or TMZ treatment

Three groups of mice were included in this imaging study (Table 1). The PRRT group received a single dose of 50MBq ^{177}Lu -TATE on d1 and the TMZ group was treated with 50mg/kg TMZ administered orally for 2 weeks, starting at d1. The control group received saline. The timeline for these studies is shown in Figure 1a.

Table 1. Overview experimental groups in imaging study (figure 1a)

Group	Number of mice	Treatment	Imaging
^{177}Lu -TATE	4	30MBq ^{177}Lu -TATE i.v.	7 x MRI, 1 x SPECT/CT
TMZ	10	TMZ 50 mg/kg p.o. for 14d	6 x MRI, 7 x SPECT/CT
Control	3	Saline	4 x MRI

PRRT group

Mice (n=4) received a baseline DCE-MRI scan 1d prior to administration of 50 MBq ^{177}Lu -TATE. During follow-up of the therapy, MRI scans were acquired on d4, 7, 10, 14, 20 and 28. Moreover, a SPECT/CT scan to determine the tumour uptake of ^{177}Lu -TATE was performed 24h after administration.

TMZ group

Mice (n=7) received one baseline DCE-MRI scan 2d prior start of TMZ treatment, which was repeated once weekly during and after TMZ treatment until d28. To determine the level of radiopeptides uptake, ^{111}In -octreotide SPECT/CT scanning was performed 1d prior start of TMZ treatment and repeated once weekly for 4 weeks during and after TMZ.

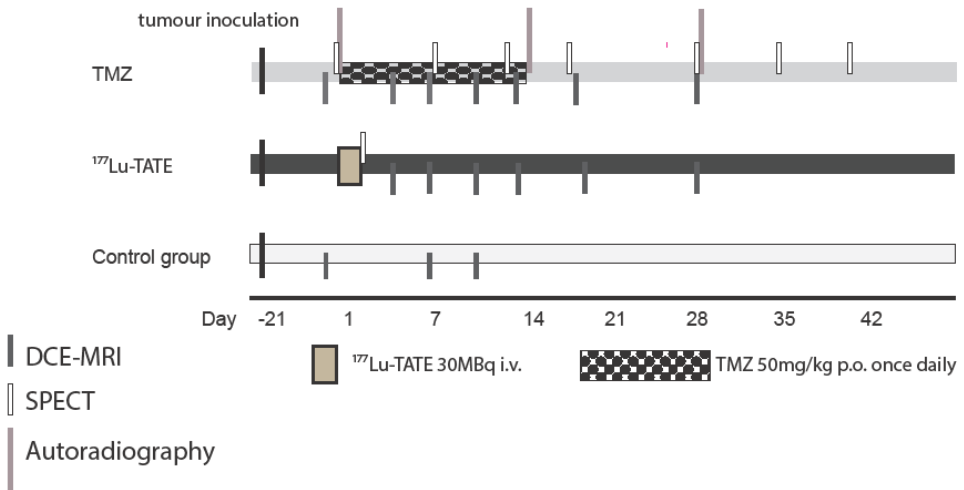


Figure 1a. Time-line imaging studies.

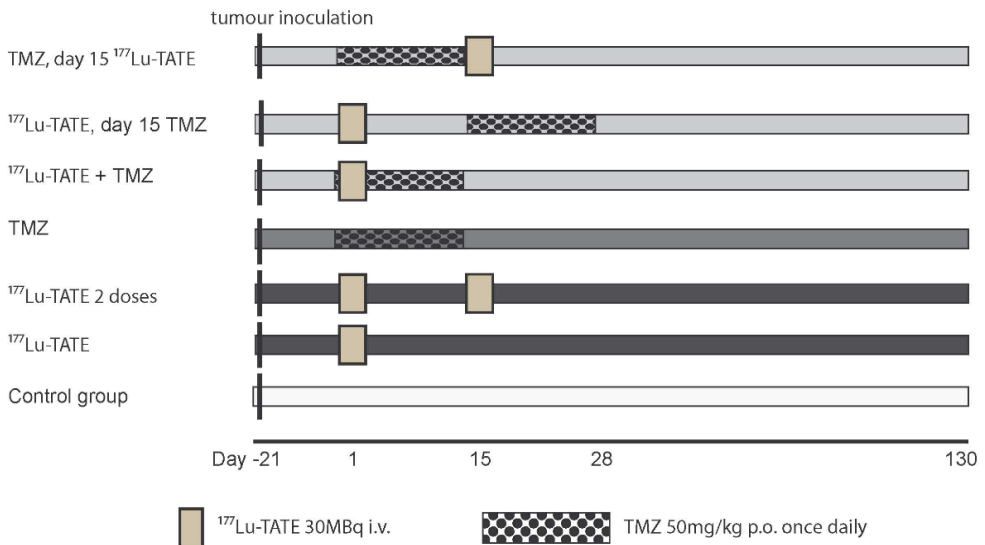


Figure 1b. Time-line for combination therapy studies
 (^{177}Lu -TATE = ^{177}Lu -DOTA, Tyr³-octreotate, TMZ= temozolomide)

At d-1 (before TMZ), d15 (after TMZ) and d28, when tumours showed maximal response, three mice were sacrificed to collect the H69 xenograft to determine the level of SSTR expression by in vitro autoradiography using ^{111}In -octreotide.

Control group

Non-treated mice (n=3) received four DCE-MRI scans; at d-1, 4, 7 and 11.

Combination therapy of PRRT and TMZ

Seven groups of mice were included to compare H69 responses after different combination treatment schedules, including a placebo control group (Table 2). Uptake of ^{177}Lu -TATE was quantified in 3-5 tumours of each group after PRRT by SPECT imaging. The timeline for these studies is shown in Figure 1b.

Table 2. Overview treatment experimental groups in therapy study

Group	^{177}Lu -TATE	Treatment TMZ	Number of mice
Control	-	Placebo	5
1: PRRT single	30MBq d1	Placebo	8
2: PRRT double	30MBq d1, 30MBq d15	Placebo	8
3: TMZ	-	50mg/kg for 14d from d1	9
4: PRRT + TMZ at d15	30MBq d1	50mg/kg for 14d from d15	8
5: PRRT + TMZ	30MBq d1	50mg/kg for 14d from d1	8
6: TMZ + PRRT at d15	30MBq d15	50mg/kg for 14d from d1	10

Tumour cell line

The SSTR2-expressing human small cell lung cancer cell line H69 was obtained from ECACC (Salisbury, UK) and grown in RPMI medium (Gibco, Invitrogen Corp., Breda, The Netherlands) supplemented with 10% heat-inactivated fetal bovine serum.

Animals and tumour model

All animal experiments have been conducted with prior approval of the animal ethics committee of our institution, and performed in accordance with Dutch laws. Male NMRI nu/nu mice (body weight ~33g) were obtained from Harlan (Heerlen, the Netherlands). One week after arrival, mice were inoculated subcutaneously with 10^7 H69 cells in 0.2 ml HBSS. For all experiments, animals were randomized into matching treatment groups regarding tumour size at the start of treatment. Three times a week, mice were weighed and tumour size was measured using a calliper by a person blinded for the treatment. Tumour volume was calculated using the formula: $0.5(\text{length} \times \text{width})^{1.5}$. Mice were euthanized when > 10% loss of body weight (BW) since start of

the experiment was observed or when tumour volume exceeded 1800mm³.

Chemotherapeutics

Temozolomide was obtained from Sun Pharmaceutical Industries Europe B.V. (Hoofddorp, The Netherlands). In the pilot study TMZ was dissolved as 8 mg/ml 50% glucose jelly and 200 µl was administered orally. For the imaging and final therapy studies a 8 mg/ml solution TMZ was prepared in Oraplus (Paddock laboratories, Inc. Minneapolis USA) and 200µl aliquots were administered by oral gavage 5 days a week for 2 weeks resulting in a dose of 50mg/kg/d TMZ.

Radionuclides and peptides

DOTA,Tyr³-octreotate was obtained from Mallinckrodt, St Louis, MO and ¹⁷⁷LuCl₃ was obtained from NRG Petten, The Netherlands. ¹⁷⁷Lu-TATE was prepared as described previously (17) with a specific activity of 100MBq/2.75µg peptide, and 10-30MBq was injected intravenously (i.v.) in a volume of 200µl via the tail vein. Labelling of ¹¹¹In-DTPA-octreotide (OctreoScan, Covidien, Petten, The Netherlands) was performed as described at a specific activity of 30 MBq/1.0µg DTPA-octreotide (17).

SPECT/CT

During scanning experiments 2.0% isoflurane/O₂ gas anaesthesia was applied at 0.5 ml/min. Twenty-four hours after injection of ¹⁷⁷Lu-TATE or ¹¹¹In-octreotide helical SPECT/CT of the tumour region was performed with a four-headed NanoSPECT/CT system (BioScan, Washington DC USA) with 9 pinhole mice collimators (diameter 1.4 mm) per head. The scans were obtained using 24 projections of 120 sec per projection and a quality factor of 0.7. SPECT scans were reconstructed iteratively on a 256x256 matrix, using HiSPECT NG software (Scivis, GmbH Göttingen Germany) and ordered subset expectation maximization (OSEM). The total amount of radioactivity (MBq) in the tumour was quantified by 3D quantification using InVivoScope software (IVS, Bioscan, Washington DC USA). To achieve accurate quantification, the camera was calibrated by scanning a 20mL polypropylene tube phantom filled with a known amount of ¹⁷⁷Lu or ¹¹¹In radioactivity. During scanning, body temperature of the mice was maintained using a heated bed.

MRI

Imaging was performed on a pre-clinical 7.0T scanner (Discovery MR901, Agilent technologies/GE Healthcare) with the standard imaging gradient set (300 mT/m, slew rate of 1000 mT/m/ms – rise time = 300 µs). A 150 mm transmit coil and 4-channel surface coil (5cm FOV) were used to acquire all images.

DCE-MRI data were acquired following a bolus i.v. injection of Gadobutrol (Gadovist; Bayer Healthcare, Germany). The acquisition parameters used were: TR =10 ms, TE = 2 ms, flip angle 12°, matrix size=116'116 and slice thickness=0.8 mm with a total

imaging volume of $50 \times 50 \times 32 \text{ mm}^3$ (x, y, z). Four k-space segments were acquired using a segmented readout sequence called TRICKS (18). This resulted in a temporal resolution of 4.7 seconds. 4-5 time points were acquired before contrast administration to obtain the baseline signal intensity. Prior to acquiring the DCE-MRI image series, a saturation recovery T1 map was acquired using a spin echo sequence with varying repetition times (TRs), settings: echo time (TE) = 8 ms, TR = 200, 400, 800, 1600 ms. T2 maps were also acquired with a spin echo sequence varying the TE, settings: TR = 1200 ms, TE = 8, 16, 25, 35 ms. All mapping images were acquired with slice thickness 0.8 mm, 5 cm FOV and 256×256 matrix.

Image analysis

For analysis of the DCE-MRI data we used two methods: semi-quantitative and quantitative analysis. All calculations were performed using Matlab (Mathworks co.). In semi-quantitative analysis the signal-intensity time curves were used to determine the time to peak (TTP), maximum signal enhancement (Smax), and the area under the curve (AUC) for the total curve and also for the first 60 seconds (AUC60). The AUC and AUC60 were calculated using a triangulation algorithm. Furthermore, the wash-in was calculated as a linear slope from the first point before contrast enhancement to the first maximum. The wash-out was calculated from the slope of the first maximum to the measurement at 60 seconds after injection. The wash-out curve was not necessarily linear in shape, but using this method we were able to discriminate the wide variety in wash-out kinetics. In order to calculate quantitative parameters from the DCE-MRI data, the signal-intensity time curves were converted to contrast-concentration time curves using a T1-map calibration. A pharmacokinetic compartment model could be fitted to these contrast-concentration time curves. Quantitative analysis consisted of calculation of K^{trans} and k_{ep} , calculated according to Tofts perfusion model (19). A population-based average arterial input function (AIF) obtained from Weidensteiner (20) was used for consistency in the results. For the response to therapy comparison of the tumor-perfusion parameters was performed; regions of interest were drawn around the tumors and mean parameter values were calculated.

***In vitro* autoradiography on tumours treated with TMZ during the imaging study**

Sections of 10 μm were sliced from frozen tumours (Cryo-Star HM 560 M; Microm, Walldorf, Germany), mounted on Superfrost plus slides (Menzel, Braunschweig, Germany) and incubated with 10^{-9} M ^{111}In -octreotide with and without an excess (10^{-6} M) of unlabelled octreotide. Adjacent sections were stained with Hematoxylin/Eosin. Tumour sections were exposed to SR phosphor imaging screens (Packard Instruments Co., Meriden, USA) in X-ray cassettes. After 48 h exposure, screens were read by a Cyclone phosphor imager and analysed using OptiQuant 03.00 (Perkin Elmer, Groningen, The Netherlands).

Statistics

Prism software version 5.0 (Graph Pad) was used to analyse tumour growth and determine statistical significance between groups. An one way ANOVA was used for statistical analysis of tumour uptake and results are given as mean \pm SD. A log rank test was performed for curve comparison.

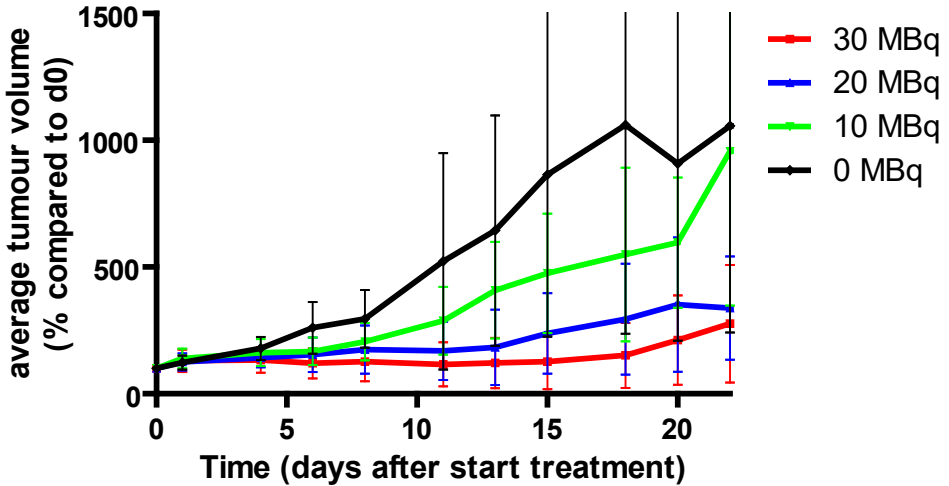


Figure 2. Dose finding. H69 tumour volume after treatment with different amounts of $^{177}\text{Lu-DOTA,Tyr}^3\text{-octreotate}$, 6 mice/group.

RESULTS

$^{177}\text{Lu-TATE}$ dose-response study

All three $^{177}\text{Lu-TATE}$ groups showed delay of tumour growth compared to the control group (Figure 2). As expected most significant tumour growth suppression was found in the 30MBq group, although complete response was not reached in any mouse.

IMAGING STUDIES

Effect of single agent treatment on tumour growth

Treatment with either $^{177}\text{Lu-TATE}$ or TMZ resulted in transient reduction in tumour size/volume, confirming previous results. However, the kinetics of the tumour response after the two treatments differed (Figure 3a).

The average ^{177}Lu -tumour uptake in the PRRT group was $1.71 \pm 0.11 \text{ kBq/mm}^3$ at 24h

after administration of 50 MBq ^{177}Lu -TATE. Maximum reduction of tumour volume was reached at ~d14, after which the tumours increased in size again. After an average of 43d, euthanasia was needed because the maximal allowed tumour size (1800 mm³) was reached.

In mice treated with TMZ, the tumour volumes increased until d9 reaching maximum tumour sizes, after which decrease of tumour sizes was observed. At d51, at the end of the imaging study, the average tumour volume increased again, however at that time none of the tumours exceeded a volume of 1800 mm³.

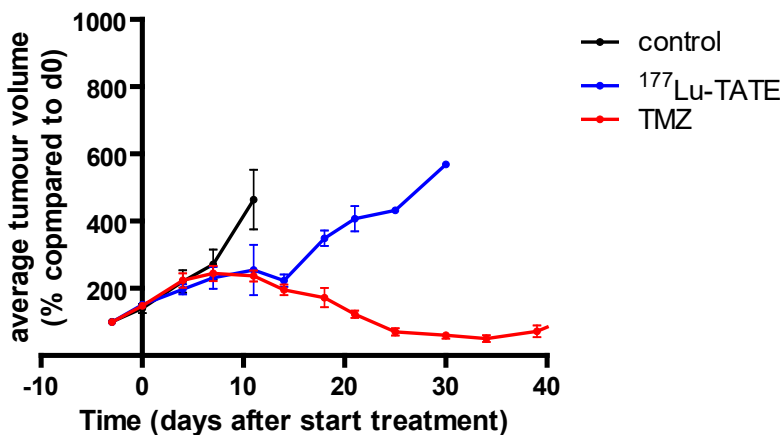


Figure 3a. Effect on H69 tumour volume of single agent treatment. The control group (black line) received saline, the PRRT group was treated with 30MBq ^{177}Lu -DOTA, Tyr^3 -octreotate (^{177}Lu -TATE) (blue line) on d1 and the temozolomide (TMZ) group (red line) was treated for 14d with orally administered TMZ at a dose of 50mg/kg/d. # mice/group

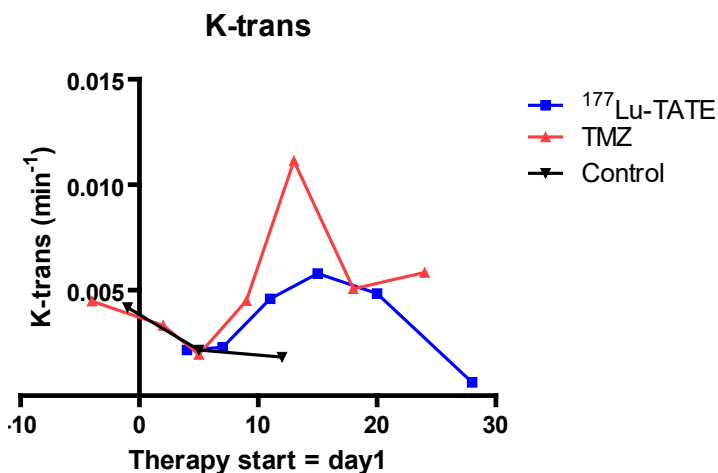


Figure 3b. Tumour perfusion in ^{177}Lu -DOTA, Tyr^3 -octreotate (^{177}Lu -TATE) (30 MBq) and temozolomide (TMZ) (50 mg/kg/day for 14 days) treated mice.

Tumour perfusion during ^{177}Lu -TATE or TMZ treatment

MRI-based determination of tumour perfusion was expressed as the median perfusion parameter k^{trans} /min. Perfusion appeared to be relatively low in untreated H69 with even minor decrease during the twelve days of measurements when tumours increased in size (Figure 3b). Tumours subjected to TMZ and ^{177}Lu -TATE initially showed a fast decrease in k^{trans} , reaching minimum values at d4 (0.0022 +/- 0.0019 min^{-1} for ^{177}Lu -TATE) or 5 (0.0020 +/- 0.0012 min^{-1} for TMZ). When tumour size decreased due to therapeutic effects an increase in k^{trans} was measured. The local maximum in k^{trans} values was reached ~2 weeks after (start of) treatment. Tumours in the group receiving TMZ showed the highest k^{trans} values at d13 (0.0111 min^{-1} +/- 0.0006); a 5-fold increase compared to d5 ($p=0.05$). The ^{177}Lu -TATE group's maximum k^{trans} value was reached at d15 (0.0058 +/- 0.0018 min^{-1}), being 2.75 times higher than at d4 ($p=0.27$). During further follow up the k^{trans} values decreased again in both the TMZ and ^{177}Lu -TATE group.

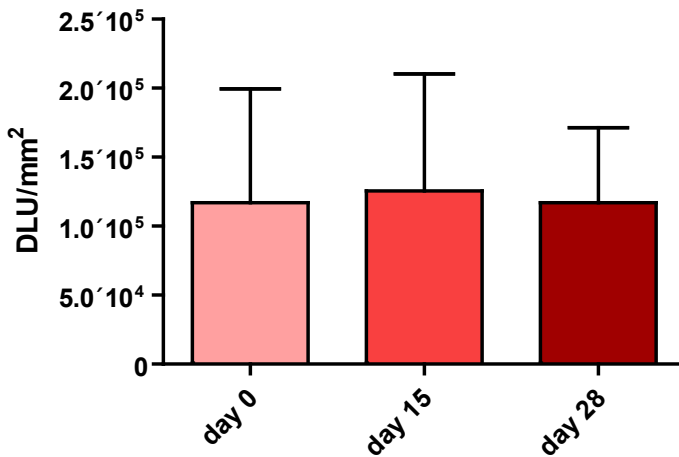


Figure 4a: SSTR expression of H69 tumours treated with temozolomide (TMZ).

Quantification of Somatostatin receptor (SSTR) density in frozen sections of H69 tumours as determined by ^{111}In -octreotide in vitro autoradiography. The amount of radioactivity is expressed in density light units (DLU)/mm². SSTR expression was quantified at d0, d15 (one day after TMZ treatment), and d28 when tumours reached a minimal volume after TMZ treatment. 3 tumours/day examined.

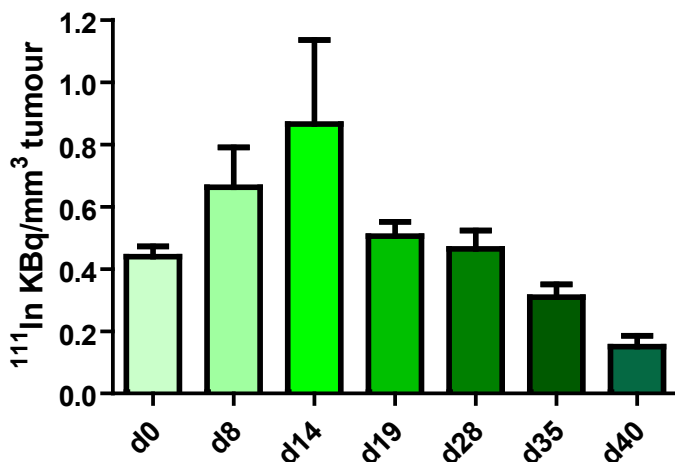


Figure 4b. Tumour uptake of ^{111}In -octreotide in mice treated with temozolomide (TMZ). Based on SPECT images, the average tumour concentration of ^{111}In -octreotide was determined 24h after administration. Mice were treated with TMZ from d1 until d 14.

SSTR2 expression and uptake of ^{111}In -octreotide before and after TMZ treatment

In vitro autoradiography results showed no difference in SSTR2 expression of H69 xenografts before (d0) or after (d15 and d28) TMZ treatment (Figure 4a). Yet, SPECT imaging showed that at d0 (average tumour volume 456 mm³) the average ^{111}In -tumour uptake was 0.44 ± 0.12 kBq/mm³ H69 xenograft, while after 14d of TMZ treatment this was increased until 0.87 ± 0.27 kBq/mm³ (average tumour volume 442 mm³) ($p=0,015$). When the administration of TMZ was discontinued, the ^{111}In -H69 uptake dropped again to 0.50 ± 0.15 kBq/mm³ at d19 and 0.46 ± 0.16 kBq/mm³ at d28, further declining until d40 (Figure 4b).

THERAPY STUDY

Responses to the different treatment schedules

As expected all mice in the control group had to be euthanized due to excessive tumour growth, this was also true for the mice in the single treatment groups with ^{177}Lu -TATE- (group 1 and 2) or TMZ (group 3), albeit with a significant delay of 20-50 days (Figure 5b). The median survival time (MST) to reach the maximum tumour size of 1800 mm³ was 32d for the mice in the control group versus 53d for the single ^{177}Lu -TATE group (1) and 74d for the double ^{177}Lu -TATE group (2). The single TMZ group 3 reached an extended MST of 81d.

In all three groups treated with a combination of ^{177}Lu -TATE and TMZ an additive effect of the two treatments was determined. Since in several mice complete tumour response was reached MST could not be determined. Regarding survival, the difference

between the best performing single therapy group 3 (TMZ) and group 4 (TMZ 14d after ^{177}Lu -TATE) was significant ($p=0.046$), whereas the other combination groups performed even better. Thus, the applied treatment schedules in these three groups had a striking impact on tumour response. In group 4 still 57% of tumours reached a volume of 1800mm^3 before the end of the study at d123. When ^{177}Lu -TATE and TMZ were combined from the start (group 5) only 25% of tumours reached this maximum size. By far the best result was obtained in group 6 with ^{177}Lu -TATE administered after 14d TMZ treatment. Only one tumour (10%) escaped from treatment, whereas the other tumours showed complete response.

Tumour uptake of ^{177}Lu -TATE

The uptake of ^{177}Lu -TATE in H69 tumors was quantified 24h after administration of 30 MBq ^{177}Lu -TATE based on SPECT/CT imaging. As reference, the average ^{177}Lu -tumour uptake was 1.73 ± 0.17 kBq/ mm^3 without previous treatment. When after 14d a second dose of ^{177}Lu -TATE was given, a comparable ^{177}Lu -tumour concentration of 1.68 ± 0.09 kBq/ mm^3 was found. However, in mice receiving ^{177}Lu -TATE on d15 after initial TMZ for 14d a significantly higher uptake of 2.24 ± 0.46 kBq/ mm^3 was determined ($p=0.013$) (Figure 5c).

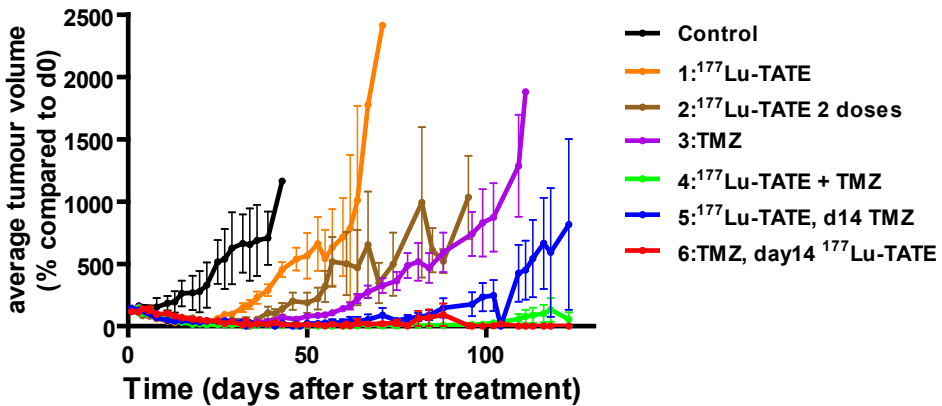


Figure 5a. Average H69 tumour volume for each treatment group.

The control group was treated with placebo, 30MBq ^{177}Lu -DOTA, Tyr^3 -octreotate (^{177}Lu -TATE) was i.v. administered at d1 to mice in groups 1, 4 and 5, at d15 for group 6, and both at d 1 and d15 for group 2. Temozolomide (TMZ) was administered orally once daily for 14d at a dose of 50mg/kg from d1 to mice in group 3, 4 and 6, starting at d14 for group 5. 8-10 mice/group

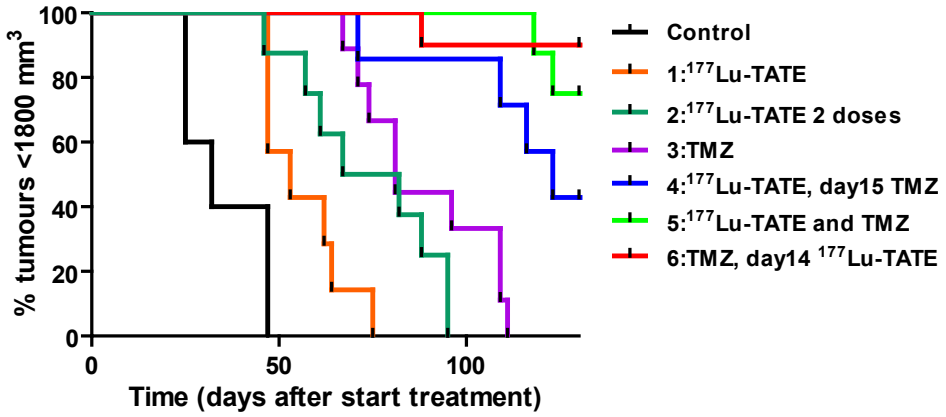


Figure 5b. Survival curve, with percentage of animals with tumours <1800mm³ per treatment group. (TMZ= temozolomide, (¹⁷⁷Lu-TATE= ¹⁷⁷Lu-DOTA,Tyr³-octreotate)

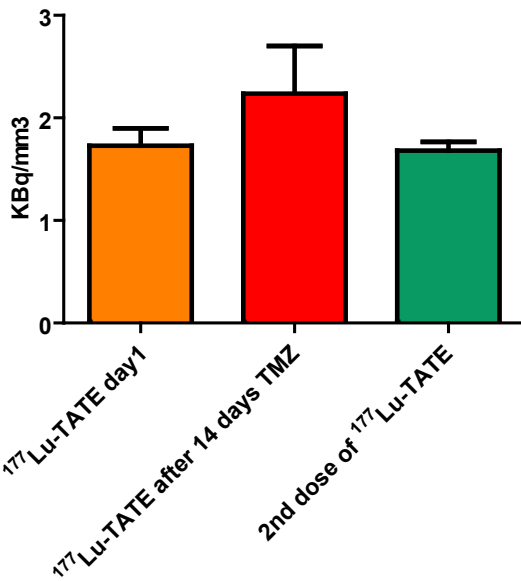


Figure 5c. Average tumour radioactivity at 24h after administration of ¹⁷⁷Lu-DOTA,Tyr³-octreotate (¹⁷⁷Lu-TATE), (TMZ= temozolomide). Orange bar: group 1, 2 (first dose), 4, 5 Red bar: group 6 Blue bar: group 2 (second dose). # resp. 14, 6 and 6 mice/group

DISCUSSION

Despite the fact that significant tumour response rates have been reported after treatment of NET patients with ^{177}Lu -TATE or (90Y-DOTA)-D-Phe1-Tyr3-octreotide (90Y-DOTATOC) (21-22), complete responses are still rare, urging for improvements of PRRT protocols. TMZ is currently being applied in combination with radiotherapy for treatment of glioblastoma patients (23). TMZ (+ Cap) is also effective in NET patients (24-25). Therefore we examined in mice if this alkylating agent offered synergistic effects when combined with ^{177}Lu -TATE PRRT.

In this preclinical study we aimed to elucidate the most effective treatment schedule of the TMZ and PRRT combination. We applied a TMZ dose of 50 mg/kg daily for two weeks, which appeared to be an effective dose in our H69 model not resulting in complete responses. The same was true for a dose of 30MBq ^{177}Lu -TATE leading to a significant delay of H69-tumour size increase.

The human small cell lung cancer (SCLC) H69 cell line, used in our studies expresses SSTR2 in high densities. As a subtype of NETs SCLC accounts for about 20% of all lung cancers (26) and shows a 5 year survival rate of only 20% (26). For this type of cancer there is a clear need to find therapeutic methods resulting in better survival. Several chemotherapeutics, including TMZ, are being used to treat SCLC (27), making the H69 cell line a suitable model for preclinical in vivo PRRT research using radiolabelled SST analogues (28). To study dosimetry and tumour response, Schmitt et al. applied several activity doses of ^{177}Lu -TATE for PRRT of H69 tumour-bearing mice (29-30). In their study tumours showed a significantly higher uptake of radioactivity compared to all normal organs (28). In a therapy study, using substantially larger tumours than in our study (resp. 1000 and 2000 mm³ at day 0), increasing growth delays using doses of 45, 60 and 120 MBq or two fractions of 45 MBq ^{177}Lu -TATE were found (30).

In the clinical trials in which PRRT was combined with Capecitabine and TMZ, the focus mainly has been on the radiosensitizing effects of the chemotherapeutics (8, 31), not considering other effects these agents might have on tumour characteristics. To our opinion, the potential influence of chemotherapeutics on tumour perfusion and SSTR2 expression is of major importance as well, to determine an optimal scheme for the combination of PRRT with chemotherapeutics.

In this study we report a significant increase of H69-tumor perfusion after TMZ treatment. The highest values were measured after 14 days of TMZ treatment, coinciding with a peak in the uptake of radiolabelled octreotide. The latter observation was confirmed during therapy, as ^{177}Lu -uptake in H69 tumours after ^{177}Lu -TATE administration was significantly higher when mice were pre-treated for 14d with TMZ. This was not the case when pre-treatment consisted of an additional dose of ^{177}Lu -TATE.

This increased tumour uptake/retention of radioactivity after TMZ treatment can be explained by different phenomena. A relation between tumour volume and concentration of radioactivity has been described, indicating an increased concentration of radioactivity in smaller tumours (28). In our studies however the average tumour size was in the same range at d0 or at d14, resp. a mean tumour volume of $456 \pm 122 \text{ mm}^3$ versus $442 \pm 66 \text{ mm}^3$, demonstrating that the peak of radioactivity uptake at d14 was not influenced by tumour volume. At later time points, when tumour sizes continued to decrease as a result of TMZ treatment, also the concentration of ^{111}In -octreotide decreased.

An increased level of SSTR2 expression might also explain the peak of radiopeptide uptake after 14d of TMZ. Using *in vitro* studies, Fueger et al. showed increased SSTR2 expression in pancreatic tumour cells four days after exposure to several chemotherapeutics, not including TMZ (11, 32). This phenomenon could not explain our findings in the current study, however, as we found no differences in SSTR2 expression prior to or after TMZ treatment, when *in vivo* H69-uptake of ^{111}In -octreotide peaked.

Therefore, increased tumour perfusion caused by TMZ treatment offers the best explanation for the raised levels of ^{111}In and ^{177}Lu tumour-uptake, as was explored and confirmed by application of measurement of perfusion parameters by DCE-MRI. In multiple studies TMZ, when administered in a metronomic (repetitive, low dose) schedule, has been demonstrated to have anti-angiogenic effects that may result in normalized tumour vasculature depending on the administered TMZ dose (33-34). Therefore, direct or indirect anti-angiogenic effects of chemotherapeutics can improve tumour perfusion and reduce the interstitial pressure (35), enabling enhanced delivery to the tumour of therapeutic compounds, including radiolabelled peptides. Our measurements with DCE-MRI support the suggestion that there is an important relationship between functional vasculature and radiopeptide uptake (36).

Considering the anti-tumour response, a small, but not significant ($p=0.28$) difference was found between group 5 (concurrent ^{177}Lu -TATE and TMZ) and group 6 (^{177}Lu -TATE after 14d TMZ treatment) regarding CR; with 75% versus 90% CR, respectively. However, when we compare group 6 with group 4 (the group in which ^{177}Lu -TATE was administered at d1 and TMZ treatment started at d15), a striking and significant difference ($p=0.046$) between those groups was found, in agreement with the fact that TMZ potentiates the effect of ^{177}Lu -TATE.

Therefore, the optimal response found in the group receiving ^{177}Lu -TATE after TMZ treatment might be based on a combination of factors:

Increased uptake of ^{177}Lu -TATE because of enhanced perfusion resulting in a higher absorbed tumour radiation dose and therefore an increased anti-tumour response (37).

Increased radiosensitivity induced by TMZ. The cytotoxicity of TMZ is primarily due to alkylation at the O6 position of guanine combined with an additional alkylation at the N7 position. TMZ has been reported to act synergistically with radiation therapy, as alkylated guanine has been reported to be radiosensitizing (9), as was shown in multiple types of cancer cells (9, 38). As the half-life of ^{177}Lu is 6.7 days (28), also the group receiving ^{177}Lu -TATE at the same day that TMZ treatment was started might have had some benefit from the radiosensitizing effects of TMZ.

Increased oxygenation might have contributed to improved therapeutic responses as was demonstrated for radiation therapy (39). After beta-particle radiation DNA damage occurs as a result of the creation of free oxygen radicals (40), so the effect of ^{177}Lu -TATE treatment might be enhanced when tumour oxygenation is improved. The mice receiving ^{177}Lu -TATE 14 days prior to TMZ treatment did not have this benefit.

CONCLUSIONS

Multimodality imaging enabled to determine the optimal schedule for the combination of PRRT and TMZ in H69-xenografted nude mice. Improved perfusion due to TMZ pre-treatment, as determined by DCE-MRI, resulted in increased uptake of ^{177}Lu -TATE as proven by SPECT/CT, which was confirmed by the induced therapeutic effects observed.

REFERENCES

1. Kwekkeboom, D.J., et al., Peptide receptor radionuclide therapy in patients with gastroenteropancreatic neuroendocrine tumors. *Semin Nucl Med*, 2010. **40**(2): p. 78-88.
2. Laverman, P., et al., Radiolabelled peptides for oncological diagnosis. *Eur J Nucl Med Mol Imaging*, 2012. **39 Suppl 1**: p. S78-92.
3. Krenning, E.P., et al., Radiolabelled somatostatin analogue(s) for peptide receptor scintigraphy and radionuclide therapy. *Ann Oncol*, 1999. **10 Suppl 2**: p. S23-9.
4. Yao, J.C., et al., One hundred years after "carcinoid": epidemiology of and prognostic factors for neuroendocrine tumors in 35,825 cases in the United States. *J Clin Oncol*, 2008. **26**(18): p. 3063-72.
5. Reubi, J.C., et al., Detection of somatostatin receptors in surgical and percutaneous needle biopsy samples of carcinoids and islet cell carcinomas. *Cancer Res*, 1990. **50**(18): p. 5969-77.
6. Bodei, L., et al., Peptide receptor radionuclide therapy with (1)(7)(7)Lu-DOTATATE: the IEO phase I-II study. *Eur J Nucl Med Mol Imaging*, 2011. **38**(12): p. 2125-35.
7. Rich, T.A., R.C. Shepard, and S.T. Mosley, Four decades of continuing innovation with fluorouracil: current and future approaches to fluorouracil chemoradiation therapy. *J Clin Oncol*, 2004. **22**(11): p. 2214-32.
8. Claringbold, P.G., R.A. Price, and J.H. Turner, Phase I-II study of radiopeptide ¹⁷⁷Lu-octreotate in combination with capecitabine and temozolomide in advanced low-grade neuroendocrine tumors. *Cancer Biother Radiopharm*, 2012. **27**(9): p. 561-9.
9. Bobola, M.S., et al., Minimally cytotoxic doses of temozolomide produce radiosensitization in human glioblastoma cells regardless of MGMT expression. *Mol Cancer Ther*, 2010. **9**(5): p. 1208-18.
10. van Essen, M., et al., Report on short-term side effects of treatments with ¹⁷⁷Lu-octreotate in combination with capecitabine in seven patients with gastroenteropancreatic neuroendocrine tumours. *Eur J Nucl Med Mol Imaging*, 2008. **35**(4): p. 743-8.
11. Fueger, B.J., et al., Effects of chemotherapeutic agents on expression of somatostatin receptors in pancreatic tumor cells. *J Nucl Med*, 2001. **42**(12): p. 1856-62.
12. Nayak, T.K., et al., Enhancement of somatostatin-receptor-targeted (¹⁷⁷Lu-(DOTA(0)-Tyr(3))-octreotide therapy by gemcitabine pretreatment-mediated receptor uptake, up-regulation and cell cycle modulation. *Nuclear medicine and biology*, 2008. **35**(6): p. 673-8.
13. Pasquier, E., et al., Concentration- and schedule-dependent effects of chemotherapy on the angiogenic potential and drug sensitivity of vascular endothelial cells. *Angiogenesis*, 2013. **16**(2): p. 373-86.
14. Hirst, T.C., et al., Systematic review and meta-analysis of temozolomide in animal models of glioma: was clinical efficacy predicted? *Br J Cancer*, 2013. **108**(1): p. 64-71.

15. Palma, J.P., et al., ABT-888 confers broad in vivo activity in combination with temozolomide in diverse tumors. *Clin Cancer Res*, 2009. **15**(23): p. 7277-90.
16. Kitange, G.J., et al., Induction of MGMT expression is associated with temozolomide resistance in glioblastoma xenografts. *Neuro Oncol*, 2009. **11**(3): p. 281-91.
17. Breeman W., d.E.a.K.E., Effects of quenchers on the radiochemical purity of ¹¹¹In-labeled peptides *J Nucl Med.* , 2007. **2007; 48 (Supplement 2):73P**.
18. Korosec, F.R., et al., Time-resolved contrast-enhanced 3D MR angiography. *Magn Reson Med*, 1996. **36**(3): p. 345-51.
19. Tofts, P.S., et al., Estimating kinetic parameters from dynamic contrast-enhanced T(1)-weighted MRI of a diffusable tracer: standardized quantities and symbols. *J Magn Reson Imaging*, 1999. **10**(3): p. 223-32.
20. Weidensteiner, C., et al., Quantitative dynamic contrast-enhanced MRI in tumor-bearing rats and mice with inversion recovery TrueFISP and two contrast agents at 4.7 T. *J Magn Reson Imaging*, 2006. **24**(3): p. 646-56.
21. van Essen, M., et al., Peptide receptor radionuclide therapy with ¹⁷⁷Lu-octreotate in patients with foregut carcinoid tumours of bronchial, gastric and thymic origin. *Eur J Nucl Med Mol Imaging*, 2007. **34**(8): p. 1219-27.
22. Waldherr, C., et al., The clinical value of (90Y-DOTA)-D-Phe1-Tyr3-octreotide (90Y-DOTATOC) in the treatment of neuroendocrine tumours: a clinical phase II study. *Ann Oncol*, 2001. **12**(7): p. 941-5.
23. Parisi, S., et al., Temozolomide and Radiotherapy versus Radiotherapy Alone in High Grade Gliomas: A Very Long Term Comparative Study and Literature Review. *Biomed Res Int*, 2015. **2015**: p. 620643.
24. Fine, R.L., et al., Capecitabine and temozolomide (CAPTEM) for metastatic, well-differentiated neuroendocrine cancers: The Pancreas Center at Columbia University experience. *Cancer Chemother Pharmacol*, 2013. **71**(3): p. 663-70.
25. Ekeblad, S., et al., Temozolomide as monotherapy is effective in treatment of advanced malignant neuroendocrine tumors. *Clin Cancer Res*, 2007. **13**(10): p. 2986-91.
26. Simon, G.R. and H. Wagner, Small cell lung cancer. *Chest*, 2003. **123**(1 Suppl): p. 259S-271S.
27. Pietanza, M.C., et al., Phase II trial of temozolomide in patients with relapsed sensitive or refractory small cell lung cancer, with assessment of methylguanine-DNA methyltransferase as a potential biomarker. *Clin Cancer Res*, 2012. **18**(4): p. 1138-45.
28. Schmitt, A., et al., Biodistribution and dosimetry of ¹⁷⁷Lu-labeled (DOTA₀Tyr₃) octreotate in male nude mice with human small cell lung cancer. *Cancer Biother Radiopharm*, 2003. **18**(4): p. 593-9.
29. Schmitt, A., et al., Biodistribution and dosimetry of ¹⁷⁷Lu-labeled (DOTA₀Tyr₃) octreotate in male nude mice with human small cell lung cancer. *Cancer biotherapy & radiopharmaceuticals*, 2003. **18**(4): p. 593-9.
30. Schmitt, A., et al., Radiation therapy of small cell lung cancer with ¹⁷⁷Lu-DOTA-Tyr₃-octreotate in an animal model. *J Nucl Med*, 2004. **45**(9): p. 1542-8.

31. Barber, T.W., et al., The potential for induction peptide receptor chemoradionuclide therapy to render inoperable pancreatic and duodenal neuroendocrine tumours resectable. *Eur J Surg Oncol*, 2012. **38**(1): p. 64-71.
32. Nayak, T.K., et al., Enhancement of somatostatin-receptor-targeted (177)Lu-(DOTA(0)-Tyr(3))-octreotide therapy by gemcitabine pretreatment-mediated receptor uptake, up-regulation and cell cycle modulation. *Nucl Med Biol*, 2008. **35**(6): p. 673-8.
33. Lam, T., et al., Metronomic chemotherapy dosing-schedules with estramustine and temozolomide act synergistically with anti-VEGFR-2 antibody to cause inhibition of human umbilical venous endothelial cell growth. *Acta Oncol*, 2007. **46**(8): p. 1169-77.
34. Kim, J.T., et al., Metronomic treatment of temozolomide inhibits tumor cell growth through reduction of angiogenesis and augmentation of apoptosis in orthotopic models of gliomas. *Oncol Rep*, 2006. **16**(1): p. 33-9.
35. Jain, R.K., Normalizing tumor microenvironment to treat cancer: bench to bedside to biomarkers. *J Clin Oncol*, 2013. **31**(17): p. 2205-18.
36. Bol, K., et al., Can DCE-MRI explain the heterogeneity in radiopeptide uptake imaged by SPECT in a pancreatic neuroendocrine tumor model? *PLoS One*. **8**(10): p. e77076.
37. Bernhardt, P., et al., Effects of treatment with (177)Lu-DOTA-Tyr(3)-octreotate on uptake of subsequent injection in carcinoid-bearing nude mice. *Cancer Biother Radiopharm*, 2007. **22**(5): p. 644-53.
38. Atallah, E. and L. Flaherty, Treatment of metastatic malignant melanoma. *Curr Treat Options Oncol*, 2005. **6**(3): p. 185-93.
39. Sonveaux, P., et al., Targeting lactate-fueled respiration selectively kills hypoxic tumor cells in mice. *J Clin Invest*, 2008. **118**(12): p. 3930-42.
40. J, B., Radiation Protection (Green Book). Chapter 4 - Biological Effects of Radiation. New Brunswick Power Corporation, 2001: p. 87-108.

CHAPTER 6

Treatment planning options for ^{177}Lu -DOTA,
Tyr³-octreotate; therapeutic responses
in an animal model.

Bison SM, Santini C, Koelewijn SJ, de Blois E, Melis M, de Jong M,
Konijnenberg MW

Manuscript has been submitted to EJNM

ABSTRACT

Radionuclide therapy with ^{177}Lu -labelled DOTA, Tyr³-octreotate (TATE) forms an excellent treatment for metastasized somatostatin receptor-overexpressing neuroendocrine tumours (NET). Patient-specific treatment planning might optimize the effectiveness of this therapy when aimed at delivering high-absorbed doses to the tumour lesions relative to non-toxic absorbed doses to normal organs. The radiobiology of dose-responses at various dose rates is described by the linear quadratic model, with most knowledge originating from external beam radiotherapy. Influence of fractionation and variation in dose rate on tumour volume dose-response effects as well as tumour volume response over time are the main subjects of this study.

Experiments were performed in H69 tumour-bearing nude mice. The therapeutic impact of three specific activities of TATE were studied after a single dose and after fractionation of the same dose in multiple administrations. Tumour volume responses over time were compared with response models based on the linear quadratic model (LQM) to verify the usefulness of this model for prospective treatment planning.

Both tumour growth and clearance of dead cells over time in response to radiation exposure were introduced into a treatment-planning model based on the LQM. This model appeared to be useful in predicting anti-tumour responses after therapy with different dose rates, specific activities and fractionation schemes and can be applied to calculate optimal therapy conditions for future patient studies.

Key words: specific activity, multiple dosing, radiobiology, PRRT, neuroendocrine tumor, dosimetry

INTRODUCTION

Peptide receptor radionuclide therapy (PRRT) using radiolabelled peptides specifically targeting receptors overexpressed in neuro-endocrine tumours (NETs) has been shown to be an effective cancer treatment option (1). During PRRT a high radiation dose can be delivered to tumours, with a tolerable toxicity in normal non-targeted tissues such as kidneys and bone marrow (2).

In more than 50% of the patients, NETs are diagnosed at a relatively late stage, often with metastatic spread, which leaves little chance for curative surgery (3). PRRT given at a fixed activity dosing scheme of 4x7.4 GBq ¹⁷⁷Lu/192 µg TATE has been proven to be effective in prolonging survival and delaying progression (2), even at late stage (4). Complete remissions after PRRT are however still rare (2), indicating that further optimization of PRRT is urgently needed.

Individualized treatment planning for each patient has been hypothesized as a tool for improvement, allowing escalation of PRRT by patient-specific dosimetry taking into account the tolerance dose on dose-limiting organs as kidneys and bone marrow (5). The absorbed dose to the tumour is thereby maximized. Treatment planning on reaching the tolerance dose by varying the radioactivity per therapy cycle also seems promising, but this approach implicates the use of high-specific activity (6).

Besides the amount of radioactivity, also the specific activity (MBq/mg peptide) is of importance when treating patients with PRRT. The amount of peptide influenced the biodistribution of the radiopharmaceutical in preclinical studies (7) as well as in patients. Physiologically based pharmacokinetic models have been developed to determine the optimal amount of ligand in PRRT leading to further individualized treatment by taking tumour perfusion and receptor affinity into account (8).

Prospective treatment planning with the aim to reach an efficacious dose in the tumour optimally combined with a tolerable dose to normal organs has not been established yet. Multi-cycle treatment in PRRT is considered an attractive retargeting option, like in chemotherapy, but cumulative absorbed doses in the tumour are used without considering potential influence of different dose rates. The absorbed dose and dose rate effects are described by the linear quadratic model (LQM). The basic equation in the LQM links the cell survival to the absorbed dose and the survival of irradiated cells in an exponential function with a linear and a quadratic relation with D. The linear component describes directly lethal events and the quadratic component expresses the probability for lethal combinations of repairable cell damage. In radionuclide therapy the survival S is described by:

$$S = \exp\left(-\alpha D - \beta \frac{\lambda_{\text{eff}}}{\lambda_{\text{rep}} + \lambda_{\text{eff}}} D^2\right) \quad (1)$$

Repair of sub-lethal damage occurs during the dose delivery with time constant $1/\lambda_{\text{rep}}$ during the exponential build-up of the absorbed dose with effective decay constant

I_{eff} . This repair process is more prominent in normal tissue than in tumours (9, 10). Normal organ toxicity can therefore be reduced by dose fractionation, as routinely applied for external beam radiation therapy without influencing therapeutic effects to the tumour too much (9). The LQM also played a role in explaining the dose limit for radiation-induced nephritis after ^{90}Y -DOTATOC therapy (11).

In the current study, we performed multiple experiments in SSTR-expressing H69 tumour-bearing nude mice to examine the influence of specific activity of TATE and of fractionation of the treatment on anti-tumour responses to determine absorbed doses in normal organs and in tumours. Moreover, dose-effect relations have been derived based on the LQM to produce a dose-response model for tumour volume changes over time, which will be of value for treatment planning of clinical PRRT.

MATERIALS AND METHODS

Tumour Cell Line and in vivo tumour model

Human small cell lung cancer cell line H69, overexpressing the somatostatin receptor type 2 (SSTR2) was obtained from ECACC (Salisbury, UK) and grown in RPMI medium (Gibco, Invitrogen Corp., Breda, NL) supplemented with 10% heat-inactivated fetal bovine serum. Male NMRI Nu/nu mice (Harlan, Heerlen, NL) were inoculated subcutaneously with 10^7 H69 cells in a suspension of 1:2 v/v Seligmann's buffered salt solution and Matrigel (BD Biosciences, Missisauga, CA). Number of mice per group was based on a power of 0.8. Since tumour growth in the control group of the split dose experiment appeared to be more uniform compared with the treatment groups, 5 control group mice were considered sufficient in the other experiments.

Prior to and during treatment mice and tumour growth were monitored three times per week, till all tumours exceeded 1800mm^3 or showed a complete response. All animal experiments have been conducted with prior approval of the animal ethics committee of our institution. Further information of animal handling and tumour model can be found in the Supplementary Information (SI). Volume of injections used for each treatment consisted of 0.2ml, no injection-related death occurred.

Radionuclides and peptides

DOTA-Tyr³-octreotate was obtained from BioSynthema, (St Louis, MO, USA, now owned by AAA, Saint-Genis-Pouilly, France) and $^{177}\text{LuCl}_3$ was obtained from AAA (Saint-Genis-Pouilly, France). ^{177}Lu -TATE was prepared as described previously (12). Activities of 26-60 MBq ^{177}Lu -TATE, have been used, as these activities resulted in earlier experiments in appropriate anti-tumour responses (13). Specific activities being used consisted of: 26 MBq $^{177}\text{Lu}/0.7 \mu\text{g}$ TATE, 30 MBq $^{177}\text{Lu}/0.5 \mu\text{g}$ TATE, 30 MBq $^{177}\text{Lu}/1.0 \mu\text{g}$ TATE and 30 MBq $^{177}\text{Lu}/2.0 \mu\text{g}$ TATE.

SPECT/CT imaging

A small-animal SPECT/CT camera (NanoSPECT, BioScan, Washington DC, USA) was used to image and quantify the distribution of TATE in vivo. The total amount of radioactivity in the tumour was quantified on SPECT/CT images by 3D-quantification using InVivoScope software (IVS, Bioscan, Washington DC, USA). See SD for further information on SPECT/CT specifications.

Experimental set-up

The set-up of the experiment is summarized in Table 1. The specific activity of 30 MBq/mg was compared to 60 MBq/mg and 15 MBq/mg. The study on fractionation effects was performed by comparing 2x13 MBq given with 5 day interval with 1 administration of 26 MBq. The 5 day interval was chosen to allow the first administration to decay and clear from normal organs. Effects of doubling the 30 MBq dose was studied with a 14 day interval (time needed for an optimal response to the first dose (14)). Further details on experimental settings can be found in the SD.

Table 1. Experimental setup

Groups	Treatment	Number of nude mice
Effect of different specific activity		
Control	Saline	5
0.5 µg TATE biodistribution (3 timepoints)	30 MBq ¹⁷⁷ Lu-TATE	8 3x4
1.0 µg TATE biodistribution (3 timepoints)	30 MBq ¹⁷⁷ Lu-TATE	8 3x4
2.0 µg TATE Biodistribution (3 timepoints)	30 MBq ¹⁷⁷ Lu-TATE	8 3x4
Split-dose experiment: Comparison single-dose vs. split-dose		
Control	Saline	8
Single-dose	26 MBq ¹⁷⁷ Lu/0.7 µg TATE	8
Split-dose(5days interval)	2x13 MBq ¹⁷⁷ Lu/0.35 µg TATE	8
Double-dose experiment: Comparison single-dose vs. double-dose		
Control	Saline	5
One-dose	30 MBq ¹⁷⁷ Lu/0.825 µg TATE	8
Double-dose (14days interval)	2x30 MBq ¹⁷⁷ Lu/0.825 µg TATE	8

TATE: DOTA-Tyr3-octreotate; d: day(s)

Dosimetry calculations

Dosimetry in normal organs and tumours was performed according to the Medical Internal Radiation Dose (MIRD)-scheme (15):

$$D(\text{organ}) = \sum_i \int_0^{\infty} \frac{A_i}{m_i}(t) e^{-\lambda t} dt \times m_i \times S(\text{organ} \leftarrow \text{organ}_i) \quad (2)$$

with λ the decay constant for ^{177}Lu : $\lambda = 0.00434/\text{h}$. The time-activity per gram

.....

curves were obtained by fitting the biodistribution data with a single exponential curve. The time-activity curve for the tumour was based on the combined biodistribution and SPECT data. The SPECT-based activity measurement at 4 h was normalized by the biodistribution/SPECT ratio of the activities at 48 h. Absorbed doses to normal organs were calculated with the S-values for a 25 g mouse phantom (16). The absorbed dose to the tumour was calculated for a 200 mg sphere with the spherical node S-value from OLINDA/EXM (17).

Tumour growth curve fitting and dose-response model (LQM)

The tumour growth curves $V(t)$ were modelled with an unrestricted exponential growth function:

$$V(t) = V(0) \times \exp(kt) \quad \text{with } k = \ln(2)/T_d \quad (3)$$

T_d is the tumour volume doubling time. The treatment groups were modelled with exponential growth functions for both the initial growth the therapy effect and the regrowth by:

$$V(t) = V(0) \times \exp\left(-k_1 t + k_2 \max_0(t - T_1)\right) \quad (4)$$

with k_1 the rate of tumour shrinkage and $k_2 - k_1$ the tumour regrowth rate after the volume nadir time T_1 . The data were further extrapolated beyond the censoring end-times to calculate a common growth curve. The time post injection (pi) at the lowest tumour volume is expressed as "nadir" for each treatment group (median and range).

Dose-response model for tumour volume

The tumour volume during the therapy depends on the survival S of irradiated tumour cells, described by the LQ-model of equation (1).

Tumour volume consists of proliferating cells and dead or dying cells due to the irradiation. It can be assumed that proliferation of alive cells will continue with the growth constant k and that dead cells will be cleared with clearance constant m ($= \ln(2)/T_{\text{clearance}}$ where $T_{\text{clearance}}$ is median clearance time). The tumour volume as a function of irradiation time T after administration of the activity can then be expressed by (18):

$$V(T) = V(0) \times \left\{ S(T) \times \exp(kT) + \frac{\int_0^T (1-S(t)) \times \exp(-m(T-t)) dt}{\int_0^T (1-S(t)) dt} \right\} \quad (5)$$

with the LQ-model survival S as a function of irradiation time T . The factor $\frac{\lambda_{eff}}{\lambda_{rep} + \lambda_{eff}}$ in equation 1 diminishes when the decay half-life is much longer than the sublethal damage half-life (or $t_{eff} < t_{rep}$). This simplifies $V(T)$ considerably for a single exponential dose build-up ($D(T) = D(1 - \exp(-\lambda_{eff}T))$):

$$V(T) \approx V(0) \times \left\{ \frac{\exp(kT - \alpha(D(1 - \exp(-\lambda_{eff}T)))) + \frac{1 - \exp(-mT)}{m} - \frac{\exp(-\alpha D \lambda_{eff} T) - \exp(-mT)}{m - \alpha D \lambda_{eff}}}{T - \frac{1 - \exp(-\alpha D \lambda_{eff} T)}{\alpha D \lambda_{eff}}} \right\} \quad (6)$$

Both the absorbed dose and the tumour response are assumed to be uniform. Heterogeneity in the volume dose response model can be introduced by assuming that a propagation fraction q of the cells remain unresponsive to the radiation exposure and grow undisturbedly following equation 2, whereas the complementary fraction $1-q$ will show a growth response following equation 6. More detailed information on dose-response calculation is included in SD.

STATISTICS

Prism software version 5.0 (Graph Pad, La Jolla, California, USA) was used to analyse tumour growth and determine statistical significance between the treatment groups. One-way ANOVA was used for statistical analysis of tumour uptake. Results are given as mean \pm standard deviation (SD) when the SD is $<40\%$, and as median and range (min-max) when the SD is $>40\%$. Significant results were considered for $p > 0.05$. A log-rank test was performed for comparison of the survival curves. Goodness of fits by the least-squares method was judged by the Pearson R^2 method. The corrected Akaike Information Criterion was used to decide on the complexity of the fits. Growth delay was calculated as the difference in median time needed to reach a tumour volume >1800 mm in the treated groups compared with this median time for the control group. This value was given with the range of the single tumours compared with the median time of the control group.

RESULTS

Effect of specific activity

Tumour uptake exceeded normal organ uptake in all experimental groups (Figure 1A). Stomach and pancreas showed low ^{177}Lu -TATE uptake (around 0.1% IA/g), but uptake in these organs was not detectable with SPECT/CT imaging (Figure 1B). In this experiment the retention of radioactivity in the kidneys showed no difference

between the different groups, also identifiable on the SPECT/CT scans (Figure 1B). In contrast at 7 days pi, tumour uptake was twice as high in the 0.5 mg peptide group as in the other groups.

For all peptide amounts, the tumours showed the highest absorbed dose; this resulted in 592 ± 84 mGy/MBq (0.5 μg), 471 ± 130 mGy/MBq (1 μg) and 321 ± 138 mGy/MBq (2 μg), respectively (See Table S1 in SD). The kidneys had the highest absorbed dose of the normal tissues: 140 ± 39 mGy/MBq. Only the tumour, pancreas and stomach were influenced by the specific activity.

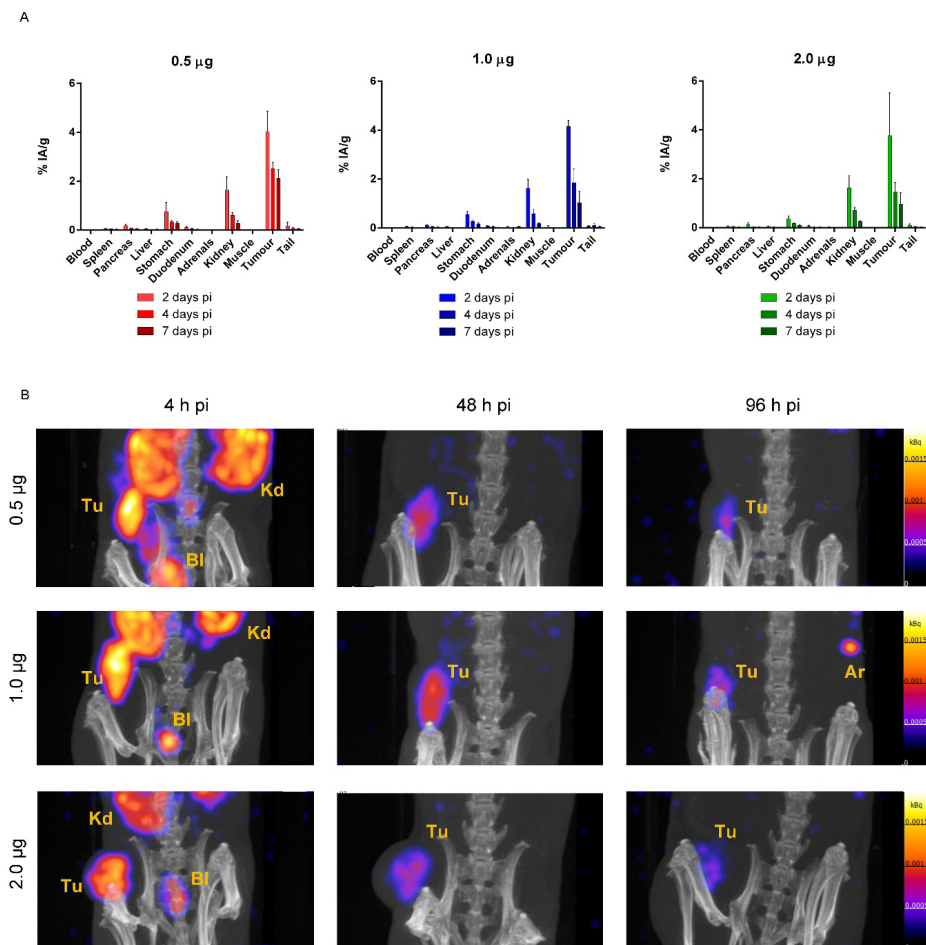
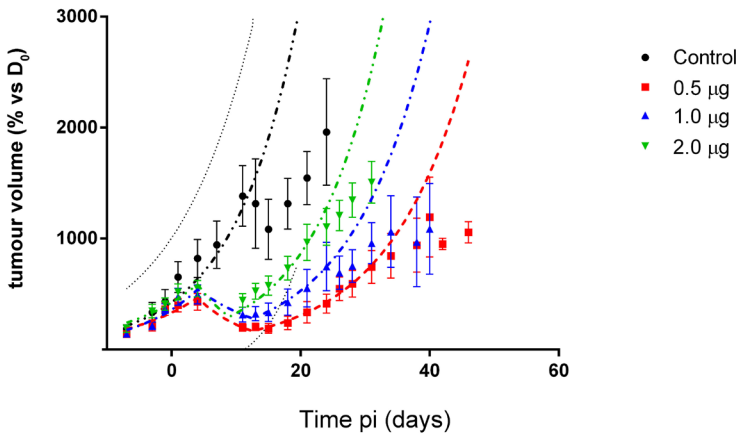


Figure 1. Uptake of ^{177}Lu -DOTA-tyr³-octreotate (^{177}Lu -TATE) applied at different specific activity. A: Percentage of injected activity per gram tissue (%IA/g) in tumour and normal organs at 2, 4 and 7 days after administration of 30 MBq ^{177}Lu -TATE: 0.5 μg peptide (red), 1.0 μg peptide (blue), 2.0 μg peptide (green); B: Uptake of radioactivity shown by the SPECT/CT scans (corrected for decay) after injection with 0.5, 1.0, 2.0 μg of ^{177}Lu -TATE.

Images are acquired at 4, 48 and 96 h pi. pi: post injection; Tu: tumour; Kd: kidney; Bl: bladder; Ar: artefact.

The tumours in the control group grew with a mean doubling time (T_d) of 9 ± 2 days (Figure 2A). After initial response to therapy with a volume nadir at 13 ± 2 days, regrowth occurred in all three experimental groups with a T_d of 9 ± 3 days. The median time to reach a volume above 1800 mm^3 and the min-max range was: 13 days (11-34) for the control group; 49 days (38-62) with $0.5 \mu\text{g}$, 42 days (24-65) with $1.0 \mu\text{g}$ and 31 days (24-42) with $2.0 \mu\text{g}$ ($p=0.002$ for $0.5 \mu\text{g}$ vs $2.0 \mu\text{g}$ group)(Figure 2B).

A



B

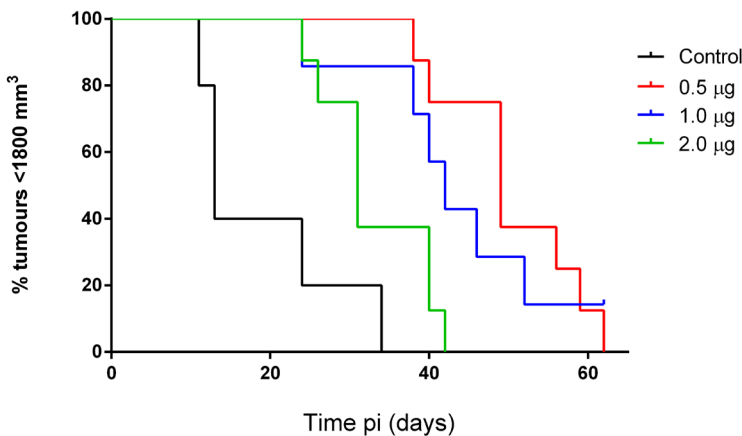


Figure 2. Tumour growth and survival curve after therapy using 30 MBq of ^{177}Lu labeled to 0.5, 1.0 or 2.0 μg TATE (^{177}Lu -TATE). A: Tumour volume (as a percentage compared to

D_0 , when treatment started) of H69 xenografts in mice after 30 MBq ^{177}Lu -TATE at 0.5 (red), 1.0 (blue) and 2.0 (green) μg . Regrowth occurred with doubling time $T_d=9\pm 3$ days ($n=8$). The volume nadir for all groups was: 13 ± 2 days. The control group growth ($n=5$) (black) with a doubling time (T_d) of 9 ± 2 days. Dots represent the measured values, dashed line represents the fitting (see text for details), dotted line represents the 95% confidence interval for the control group; B: Percentage of tumours $< 1800\text{mm}^3$, the median time to reach the maximum volume of 1800mm^3 was 49 (38-62) days with 0.5 μg (red), 42 (24-65) days with 1.0 μg (blue) and 31 (24-42) days with 2.0 μg (green). Between the 0.5 and the 2.0 μg group there was a significant difference ($p=0.002$). D_0 : day 0; pi: post injection

EFFECT OF TREATMENT SCHEME

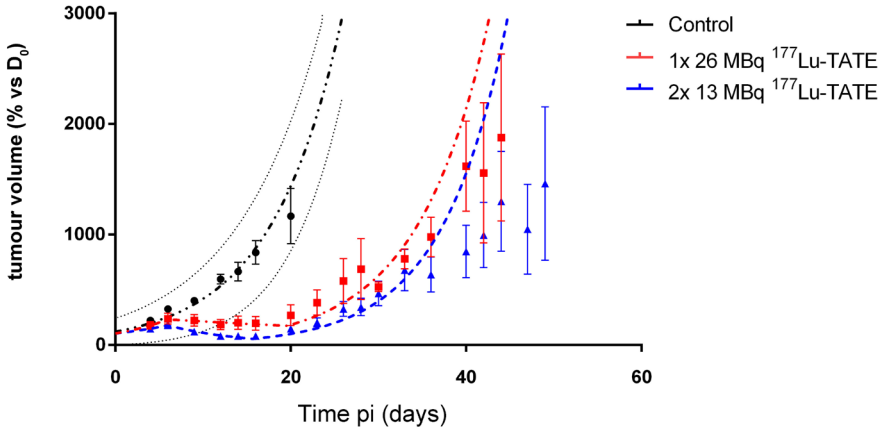
Split-dose

Tumours in the control group grew with an average T_d of 6.4 ± 2.1 d. The median survival times and the min-max range were: 17days (11-35) for the control group, 41days (25-71) for the 1x26 MBq group and 37days (27-50) for the 2x13 MBq group ($p=0.56$)(Figure 3A). Both treatment groups showed a significantly longer time to reach a tumour volume of 1800mm^3 compared to the control group ($p=0.001$ for both groups)(Figure 3B). The median tumour volume nadir was at 14 ± 2 days for 1x26 MBq/0.7 μg ^{177}Lu -TATE with regrowth at an average T_d of 6days (range:2.8-10). In the 2x13 MBq/0.35 μg ^{177}Lu -TATE group the volume nadir was at 15 ± 3 days. Regrowth occurred with a T_d of 6days (range:2.4-30). Further information on growth parameters after administration of the split-dose of ^{177}Lu -TATE are summarized in Table 2S in SD.

Double-dose

The 2x30 MBq ^{177}Lu group showed a significantly longer time to reach 1800mm^3 ($p=0.04$) compared to the 1x30 MBq group. Median survival time was 32days (range: 25-47) for the controls, 53days (range: 47-75) for 1x30 MBq, and 75days (range: 46-95) for 2x30 MBq (Figure 4A). Further information on growth parameters after administration of the double-dose of ^{177}Lu -TATE are summarized in Table 2S and 3S in SD. Dosimetry studies using SPECT/CT at 24 h pi showed no difference in radioactivity measured in the tumour after the second administration of 30 MBq compared to the first administration (Figure 5). For the mice treated with only one injection the measured radioactivity was 1.79 ± 0.21 kBq/ mm^3 . The measured values for the mice treated with the double-dose were (1.70 ± 0.26 kBq/ mm^3 after first injection and 1.68 ± 0.08 kBq/ mm^3 after second injection). This is a factor 1.14 above the 24 h value extrapolated from the biodistribution data. The absorbed dose was hence 12.3 Gy for the 1x30 MBq group and 25 Gy for 2x30 MBq.

A



B

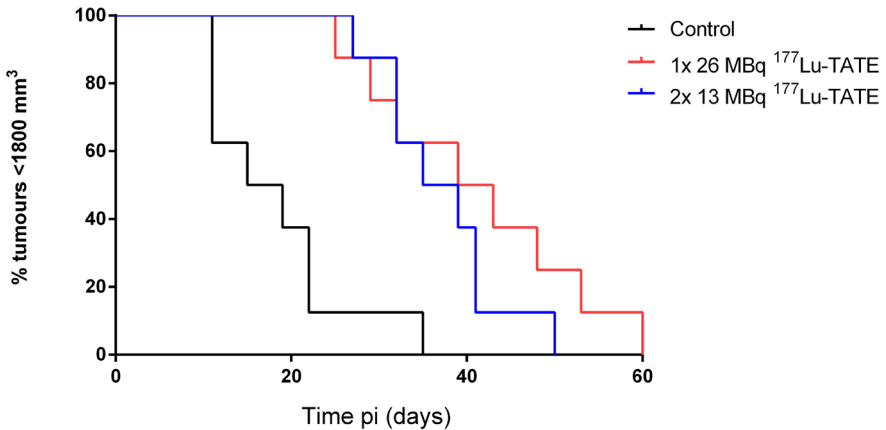
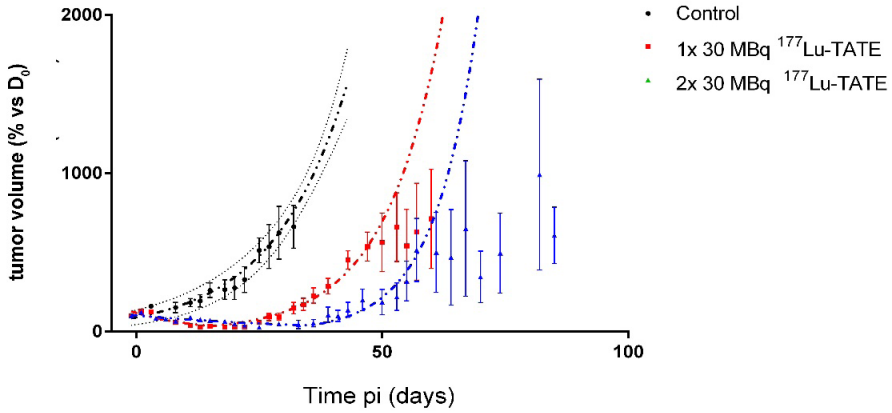


Figure 3. Tumour growth and survival curve after 26MBq (single-dose) or 2x13MBq (split-dose) of $^{177}\text{Lu-DOTA-tyr}^3\text{-octreotate}$ ($^{177}\text{Lu-TATE}$). A: Tumour volume of H69 xenografts treated with 26MBq $^{177}\text{Lu}/0.7 \mu\text{g TATE}$ (red) given and 2x13MBq (blue). After the single therapy 7 (of 8) (red) tumours showed median regrowth with a doubling time (T_d) of 6 days (range: 2.4-30), all starting regrowth after volume nadir at 14 ± 2 days. All tumours showed regrowth with $T_d = 6$ days (2.8-10 days; $n=8$) after the 2x13MBq with a nadir in the tumour volume after: 15 ± 3 days. The tumour volume in the control group ($n=8$) showed a mean doubling time of $T_d = 6.4 \pm 2.1$ days; B: Median time for the tumour to reach a volume of 1800 mm^3 in control group (black), single-dose (red) and split-dose (blue). The values of the median were 17, 37 and 41 days respectively. D_0 : day 0; pi: post injection.

A



B

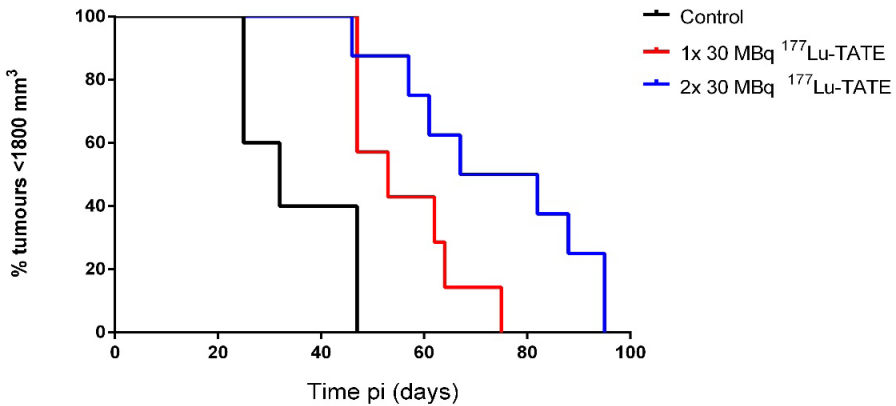


Figure 4. Tumor growth and survival curve after therapy using single- or double-dose of 30MBq ¹⁷⁷Lu-DOTA-tyr³-octreotate (**¹⁷⁷Lu-TATE**). A: Tumour volume of H69-tumours (n=8) treated with 30MBq ¹⁷⁷Lu/0.825µg TATE (100MBq/2.75µg)(red) or 2x30MBq ¹⁷⁷Lu/0.825µg TATE with 14 days interval (blue). Volume is expressed as % of the tumor volume at day 0 (D₀). All tumours after 1x30 MBq showed regrowth with T_d = 9.4±2.5 d, after the volume nadir at 15 days (11-20). After two doses, the T_d was 7.5±2 days, with a nadir of 33 days (14-59). In the control group (black) tumours growth with a doubling time of 11.6±3 days; B: Median time to achieve a tumour volume of 1800 mm³ was respectively 32, 53 and 74 d. pi: post injection.

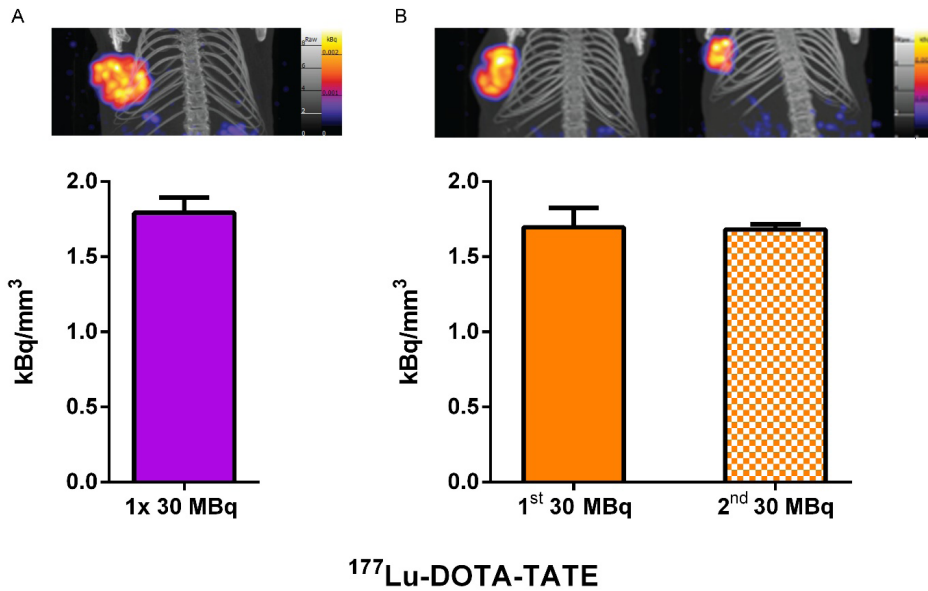


Figure 5. Tumour uptake of activity after each dose in mice 24 h after administration of 30 MBq of ^{177}Lu --DOTA-tyr³-octreo TATE (^{177}Lu -TATE). A: On top: SPECT/CT image 24 h pi of a mouse treated with a single administration of 30 MBq of ^{177}Lu -TATE; below concentration of radioactivity measured in the tumor 24 h pi (purple bar); B: On top: SPECT/CT image 24 h pi of a mouse treated with two administrations of 30 MBq of ^{177}Lu -TATE with 14days in between; Below: concentration of radioactivity measured in the tumor 24 h pi (orange bar) and 14days+24 h (spotted orange bar).

Comparison of response predicted by the tumour dose response model

The average tumour volumes responses followed the response model (equation 6) with a mean $a=0.14\pm 0.03 \text{ Gy}^{-1}$ ($b=0 \text{ Gy}^{-2}$) in all cases, under the assumption that all tumour cells responded to the radiation exposure (Figure 6). The fit parameters are indicated in Table 4S in SI. Clearance of non-dividing cells from the tumour volume proceeded with a median $T_{\text{clearance}}=3.5\text{days}$ (range: 0.9-7.1). Alternatively, the proliferation factor q was $5.5\pm 2.4\%$ (at uniform $a=0.21 \text{ Gy}^{-1}$), except for 2.0 mg (30 MBq) and 30 MBq in double-dose experiment with $q = 20\%$ (See Table S4 in SI). Clearance of non-dividing cells from the tumour volume proceeded in this case with a median $T_{\text{clearance}}=5.5\text{days}$ (range: 1.5-9.0). The double-dose group (2'30 MBq) showed immediate response in volume reduction.

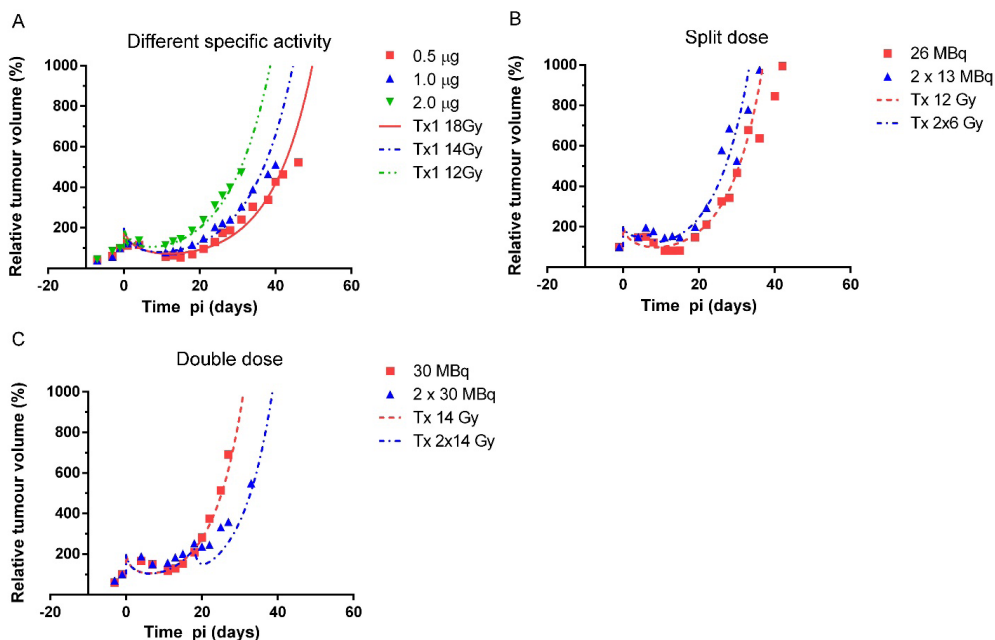


Figure 6. Comparison of anti-tumour responses predicted by the linear quadratic model (LQM) and responses measured in the different evaluations. A: The tumor growth after treatment 30 MBq of ^{177}Lu labeled to different amounts of peptide: 0.5 μg (red) the 1.0 μg (blue) and the 2.0 μg groups (green) are compared; B: The response to 1x 26 MBq (red) is compared with response to 2x 13 MBq (blue); C: Response as predicted by the LQM with the average tumour volume measured for the mice treated with 1x (red) or 2x (blue) 30 MBq ^{177}Lu -TATE. The LQM fit was performed by either using the radiation sensitivity α as a free parameter (uniform cell response) or by using the percentage of non-responding cells p as free parameter with $\alpha=0.21 \text{ Gy}^{-1}$ (uniform radiation sensitivity). Response as predicted by the LQM is given as a line whilst the response as measured during the experiments is given as dots. Tx: therapy with the dose mention after; pi: post injection.

DISCUSSION

In this study, we investigated the relation between the absorbed dose and therapy response of tumours. Tumour volumes after PRRT were shown to follow a linear-exponential response with absorbed dose. The quadratic component of the LQM could be neglected in this long half-life ($T_{1/2} = 6.647$ days for ^{177}Lu) radionuclide exposure, as shown also in the past in cell survival experiments with ^{131}I exposure (19). Multiple cycle administration of ^{177}Lu -TATE can therefore be considered a fractionation scheme like in other radiotherapies. The results we obtained in the split-dose experiment

demonstrated that fractionation had no influence on the anti-tumour response. This means that for clinical application the same therapeutic effect may be obtained, but with reduction of the risk on toxicity to healthy tissue by the principles of the LQ-model, assuming that the a/b value for tumours is larger than for normal tissue. Despite the assumed improvement of tumour perfusion after radiolabelled peptide treatment, as reported earlier (20), in the double-dose experiment the tumour uptake of ^{177}Lu -TATE after the second dose showed no increase.

The newly developed radiobiological tumour volume response model (equation 6) gives a good prediction of the tumour volume change over time during and after therapy. The model assumes uniform response to the absorbed dose following the LQ-model. The relatively fast proliferating H69 tumour model, with a Ki-67 of 70-90% (21), has some limitations as a general model for NETs.

As human NETs are slowly proliferating tumours (with a proliferation factor (Ki-67) < 3% for grade 1) (22). Another limitation of xenograft models is the genetic similarity of tumour cells, whereas human tumours are more heterogeneous. We introduced the propagation factor q in the model to take heterogeneity in response into account, which was low (5.5%) for this H69 model and will be higher for human NET tumours. Clinical application of this model is possible when the radiation sensitivity of human NET tumours is known, q should be determined empirically.

The highest absorbed dose to the tumour was reached with the highest specific activity, confirming earlier experiments (23). In a CA20948 rat model, Müller et al. (24) showed that a diagnostic dose of ^{177}Lu -TATE (3 MBq/0.5 μg peptide) resulted in a relatively high accumulation of radioactivity in SSTR2-positive tissues compared with a therapeutic peptide amount (300 or 555 MBq/15 μg). This suggests that therapeutic amounts are in the concentration range, which saturates SSTR2 in the tumour. In clinical settings this was also observed. Kratochwil et al. (25) reported receptor saturation of liver tumours when radiolabelled peptides were intra-arterially administered via the hepatic artery. And the pharmacokinetic model for radiolabelled octreotide studied by Kletting (8), showed that receptor saturation may cause reduced uptake in well-perfused tumours (8, 26).

Since the majority of PRRT patients suffer from metastases, in most cases the evaluation of the therapy is focused mainly on the larger tumour masses with relative high uptake of radionuclides. However, this information may not apply to the uptake in the smaller metastases which could be less perfused or suffer from SSTR saturation.

A dose-response relation between absorbed dose and tumour volume could be derived by accounting for the clearance kinetics of dead cells. The derived LQM parameters for H69 differ from those reported in literature for cell survival. We found $a=0.14\pm 0.03 \text{ Gy}^{-1}$ without an indication for a quadratic dose response ($b=0$); lower than the previous reported a of $0.21\pm 0.16 \text{ Gy}^{-1}$ and $b=0.06\pm 0.05 \text{ /Gy}^{-2}$ for H69 tumours (27), although the difference is not significant. The diminished quadratic

response could also be explained by a low sub-lethal damage repair half-life (T_{rep}); the quadratic part of the LQM (equation 4) diminishes when T_{rep} is below 6 h. Further experiments should consider whether the other asset of the LQM, reduction of late-occurring toxicity, also holds for ^{177}Lu -TATE.

The results from our studies and the use of the LQ-model offer possibilities for further improved individualized treatment. For pancreatic NETs, increased absorbed tumour dose has been related to an increased response (28). Breeman et al. (29) have shown that it is possible to label ^{177}Lu -TATE at a higher specific activity than the currently used 37 MBq/ μg . It is therefore feasible to increase the amount of radioactivity per therapy cycle to stay within e.g. the kidney dose limit in 4 cycles instead of adding more 7.4 GBq therapy cycles.

Treatments given at the maximal tolerated dose (for the kidneys and bone marrow), like performed in some institutes (30, 31) still remain a matter of debate. Considering PRRT as a form of radiotherapy the higher absorbed dose in the tumour at maximum tolerable dose is essential. Tumour recurrence, however, often is the result of just some (clusters of) untreated cells not clinically observable or not expressing the receptor. Treatment with β^- radiating radionuclides is not optimal to kill individual cells or small clusters below 1.2 mm diameter (32). Therefore, a more prudent approach is advisable to stay below the full tolerable maximum, and thereby keeping treatment options behind for a potential recurrence. Most importantly, personalized dosimetry should be the guidance in optimization of treatment planning approaches.

CONCLUSION

A tumour response model has been developed that enables prediction of anti-tumour response based on absorbed dose, tumor growth and radiation sensitivity. Splitting of the dose in 2 fractions does not affect anti-tumour response indicating a negligible quadratic LQM parameter. Prospective treatment planning for radionuclide therapies is feasible with this model when all relevant tumour radiobiology parameters are known.

REFERENCES

1. Bodei L, Kidd M, Paganelli G, et al. Long-term tolerability of PRRT in 807 patients with neuroendocrine tumours: the value and limitations of clinical factors. *Eur J Nucl Med Mol Imaging*. 2015;42:5-19.
2. Strosberg J, El-Haddad G, Wolin E, et al. Phase 3 Trial of 177Lu-Dotatate for Midgut Neuroendocrine Tumors. *N Engl J Med*. 2017;376:125-135.
3. Sowa-Staszczak A, Pach D, Chrzan R, et al. Peptide receptor radionuclide therapy as a potential tool for neoadjuvant therapy in patients with inoperable neuroendocrine tumours (NETs). *Eur J Nucl Med Mol Imaging*. 2011;38:1669-1674.
4. van Essen M, Krenning EP, Kam BL, de Herder WW, Feelders RA, Kwekkeboom DJ. Salvage therapy with (177)Lu-octreotate in patients with bronchial and gastroenteropancreatic neuroendocrine tumors. *J Nucl Med*. 2010;51:383-390.
5. Sandstrom M, Garske-Roman U, Granberg D, et al. Individualized dosimetry of kidney and bone marrow in patients undergoing 177Lu-DOTA-octreotate treatment. *J Nucl Med*. 2013;54:33-41.
6. Del Prete M, Buteau FA, Beauregard JM. Personalized 177Lu-octreotate peptide receptor radionuclide therapy of neuroendocrine tumours: a simulation study. *Eur J Nucl Med Mol Imaging*. 2017;44:1490-1500.
7. de Jong M, Breeman WA, Bernard BF, et al. Tumour uptake of the radiolabelled somatostatin analogue (DOTA0, TYR3)octreotide is dependent on the peptide amount. *Eur J Nucl Med*. 1999;26:693-698.
8. Kletting P, Schuchardt C, Kulkarni HR, et al. Investigating the Effect of Ligand Amount and Injected Therapeutic Activity: A Simulation Study for 177Lu-Labeled PSMA-Targeting Peptides. *PLoS One*. 2016;11:e0162303.
9. Joiner M, van der Kogel A. *Basic Clinical Radiobiology Fourth Edition*: Hodder Education; 2009.
10. Konijnenberg MW, Breeman WAP, de Blois E, et al. Therapeutic application of CCK2R-targeting PP-F11: influence of particle range, activity and peptide amount. *EJNMMI Research*. 2014;4:47.
11. Low RN, Duggan B, Barone RM, Saleh F, Song SY. Treated ovarian cancer: MR imaging, laparotomy reassessment, and serum CA-125 values compared with clinical outcome at 1 year. *Radiology*. 2005;235:918-926.
12. Breeman WA, Kwekkeboom DJ, de Blois E, de Jong M, Visser TJ, Krenning EP. Radiolabelled regulatory peptides for imaging and therapy. *Anticancer Agents Med Chem*. 2007;7:345-357.
13. Melis M, Forrer F, Capello A, et al. Up-regulation of somatostatin receptor density on rat CA20948 tumors escaped from low dose (177Lu-DOTA0,Tyr3)octreotate therapy. *Q J Nucl Med Mol Imaging*. 2007;51:324-333.
14. Bison SM, Haeck JC, Bol K, et al. Optimization of combined temozolomide and peptide receptor radionuclide therapy (PRRT) in mice after multimodality molecular imaging studies. *EJNMMI Res*. 2015;5:62.

15. Bolch WE, Eckerman KF, Sgouros G, Thomas SR. MIRD pamphlet No. 21: a generalized schema for radiopharmaceutical dosimetry--standardization of nomenclature. *J Nucl Med.* 2009;50:477-484.
16. Keenan MA, Stabin MG, Segars WP, Fernald MJ. RADAR Realistic Animal Model Series for Dose Assessment. *J Nucl Med.* 2010;51:471-476.
17. Stabin MG, Sparks RB, Crowe E. OLINDA/EXM: the Second-generation Personal Computer Software for Internal Dose Assessment in Nuclear Medicine. *J Nucl Med.* 2005;46:1023-1027.
18. Watanabe Y, Dahlman EL, Leder KZ, Hui SK. A mathematical model of tumor growth and its response to single irradiation. *Theoretical Biology and Medical Modelling.* 2016;13:6.
19. Verwijnen S, Capello A, Bernard B, et al. Low-dose-rate irradiation by ¹³¹I versus high-dose-rate external-beam irradiation in the rat pancreatic tumor cell line CA20948. *Cancer Biother Radiopharm.* 2004;19:285-292.
20. Haec J, Bol K, Bison S, et al. Optimized time-resolved imaging of contrast kinetics (TRICKS) in dynamic contrast-enhanced MRI after peptide receptor radionuclide therapy in small animal tumor models. *Contrast Media Mol Imaging.* 2015;10:413-420.
21. Erlandsson A, Forssell-Aronsson E, Seidal T, Bernhardt P. Binding of TS1, an anti-keratin 8 antibody, in small-cell lung cancer after ¹⁷⁷Lu-DOTA-Tyr3-octreotate treatment: a histological study in xenografted mice. *EJNMMI Res.* 2011;1:19.
22. Strosberg JR, Nasir A, Hodul P, Kvols L. Biology and treatment of metastatic gastrointestinal neuroendocrine tumors. *Gastrointest Cancer Res.* 2008;2:113-125.
23. Kolby L, Bernhardt P, Johanson V, et al. Successful receptor-mediated radiation therapy of xenografted human midgut carcinoid tumour. *Br J Cancer.* 2005;93:1144-1151.
24. Muller C, Forrer F, Bernard BF, et al. Diagnostic versus therapeutic doses of ((¹⁷⁷)Lu-DOTA-Tyr(3))-octreotate: uptake and dosimetry in somatostatin receptor-positive tumors and normal organs. *Cancer Biother Radiopharm.* 2007;22:151-159.
25. Kratochwil C, Giesel FL, Lopez-Benitez R, et al. Intraindividual comparison of selective arterial versus venous ⁶⁸Ga-DOTATOC PET/CT in patients with gastroenteropancreatic neuroendocrine tumors. *Clin Cancer Res.* 2010;16:2899-2905.
26. Kletting P, Muller B, Erentok B, et al. Differences in predicted and actually absorbed doses in peptide receptor radionuclide therapy. *Med Phys.* 2012;39:5708-5717.
27. Shui C, Khan WB, Leigh BR, Turner AM, Wilder RB, Knox SJ. Effects of stem cell factor on the growth and radiation survival of tumor cells. *Cancer Res.* 1995;55:3431-3437.
28. Ilan E, Sandstrom M, Wassberg C, et al. Dose response of pancreatic neuroendocrine tumors treated with peptide receptor radionuclide therapy using ¹⁷⁷Lu-DOTATATE. *J Nucl Med.* 2015;56:177-182.

29. Breeman WA, Chan HS, de Zanger RM, Konijnenberg MK, de Blois E. Overview of Development and Formulation of (1)(7)(7)Lu-DOTA-TATE for PRRT. *Curr Radiopharm*. 2016;9:8-18.
30. Sundlov A, Sjogreen-Gleisner K, Svensson J, et al. Individualised 177Lu-DOTATATE treatment of neuroendocrine tumours based on kidney dosimetry. *Eur J Nucl Med Mol Imaging*. 2017.
31. Verburg FA, Lassmann M, Mäder U, Luster M, Reiners C, Hänscheid H. The absorbed dose to the blood is a better predictor of ablation success than the administered 131I activity in thyroid cancer patients. *European Journal of Nuclear Medicine and Molecular Imaging*. 2011;38:673-680.
32. O'Donoghue JA, Bardies M, Wheldon TE. Relationships between tumor size and curability for uniformly targeted therapy with beta-emitting radionuclides. *J Nucl Med*. 1995;36:1902-1909.

CHAPTER 7

Summary, Discussion and Future Perspectives

SUMMARY

Peptide receptor radionuclide therapy is a treatment based on targeting receptors overexpressed by tumour cells. By radiolabelling of the receptor-targeting molecule with a therapeutic radionuclide, an effective treatment dose can be delivered to tumours in vivo after injection into the blood. Since the majority of neuroendocrine tumours (NETs) overexpress somatostatin (STT) receptors on their cell membrane, treatment with radiolabelled STT analogues has offered new treatment possibilities for a substantial percentage of NET patients with metastasized disease. Until now five different subtypes of the STT receptor have been found, of which subtype 2 is most commonly expressed (1, 2)

Although NETs have an incidence of only 2-5 per 100.000 a year, the relatively long survival time results in a fairly high prevalence (3). For the substantial number of patients who already have metastases at the moment of diagnoses, there is little chance of curative surgery. Standard treatment for these patients involves long acting STT analogues, reducing symptoms and possibly offering tumour growth delay (4). Compared with this standard treatment, PRRT with radiolabelled SST analogues, like e.g. ^{177}Lu -DOTA,Tyr3-octreotate (^{177}Lu -TATE), has been proven to be clearly more effective (5) regarding overall survival and quality of life (5, 6). Nevertheless, complete responses are still rare (7), further optimization and improvement of this treatment is therefore of great importance.

In this thesis several options for improvement of PRRT have been evaluated in preclinical studies. Multi-modality imaging was performed to monitor tumour response to treatment.

Chapter 1 gives a short general introduction regarding NETs plus the different treatment options currently available for NET patients.

In **Chapter 2** we highlighted some of the directions currently investigated in pilot clinical studies or in preclinical development to achieve improvement of the current treatments. Although randomized clinical trials are lacking until now, the first studies have shown that application of other therapeutic radionuclides, including α -emitters, or radionuclide combinations as well as adjustment of the administration route of radiopeptides might improve anti-tumour responses. Individualized dosimetry and better insight into tumour and normal organ radiation doses may lead to adjustment of the administered activity per cycle or the number of treatment cycles, potentially resulting in more personalized treatment schedules. Other options include the application of novel (radiolabeled) STT analogues with improved tumour uptake and radionuclide retention time, or a combination of PRRT with other systemic therapies, such as chemotherapy or treatment with radiosensitizers. We conclude that different options for PRRT improvement are encouraging and available at this moment, but additional research, including randomized clinical trials, is warranted to obtain further improvement of PRRT.

In **Chapter 3** we report on in vivo mTOR inhibition by everolimus, administered twice weekly for 4.5 weeks. This treatment resulted very unexpectedly in the occurrence of distant metastasis in a rat pancreatic neuroendocrine tumour model. Everolimus treatment was given as a single treatment or combined with ^{177}Lu -TATE, the latter targeting STT receptor subtype 2. Everolimus alone resulted in minor anti-tumour effects only, the combination treatment of ^{177}Lu -TATE plus everolimus was much more effective than everolimus alone, but this combination did not show better anti-tumor effects in comparison to ^{177}Lu -TATE alone. Unexpectedly, tumour metastasis was found in 77 % of animals treated with everolimus or everolimus plus ^{177}Lu -TATE. Metastasis was not found in control and ^{177}Lu -TATE-treated animals, not even when the primary tumour was surgically removed when tumour size was $> 4 \text{ cm}^3$ to let the animals survive for further follow up. We hypothesized the metastasizing potential of everolimus could be the result of the discontinued treatment applied; clinically this could be of importance for non-compliant patients or patients who have to stop RAD001 therapy because of adverse effects.

Chapter 4 describes further analysis of the development of metastases after treatment with everolimus (RAD001) and the decreased response to the combination of RAD001 and PRRT compared with the response to PRRT only. We questioned why this combination therapy appeared less effective and wondered if development of distant metastases could have been caused by sudden cessation of RAD001 therapy after the planned treatment period. Uptake of ^{177}Lu -TATE in tumours (pre) treated with RAD001 and non-treated tumours was compared to investigate if treatment with RAD001 affected tumour uptake of ^{177}Lu -TATE. Moreover, to study the effect of cessation of RAD001 therapy at different doses, next to groups treated with RAD001 for 4.5 weeks, also groups that were treated for 12 weeks were included. Compared with the previous study, this study was performed in Lewis rats of a different substrain (SsNsd). This substrain is often used for auto-immune studies, as these animals have a more active immune system showing an enhanced CD4+ and CD8+ T cell immune response (8, 9), this auto-immunity being linked to an increased anti-tumor immunity (10). As for the results, treatment with RAD001 did not influence tumour uptake of ^{177}Lu -TATE. Considering anti-tumour response, in the study in which the LEW/SsNsd substrain was used only 12.5% of RAD001-treated rats showed a complete anti-tumour response (CR) compared to 50% complete responses in the control group. Furthermore, occurrence of metastases after RAD001 treatment was not dose dependent in the dose range tested, nor was it related to the duration of RAD001 treatment. Moreover, less effective anti-tumour effects after combining RAD001 and PRRT could not be explained by reduced tumour uptake of ^{177}Lu -TATE. In the rats that developed metastases we studied if ^{177}Lu -TATE is an effective treatment option for metastasized disease. It turned out that for these rats, re-treatment with a high dose of ^{177}Lu -TATE resulted in a CR in only two out of seven animals. Therefore in this model, compared with primary tumours, metastases appeared to be less sensitive to treatment with ^{177}Lu -TATE.

Chapter 5 describes the use of multimodality imaging to optimize the combination of ^{177}Lu -TATE and the chemotherapeutic temozolomide (TMZ). These studies were performed in the H69 tumour bearing nude mice model. The combination of SPECT-CT and DCE-MRI was applied to study tumour perfusion as well as uptake of ^{177}Lu -TATE (30 MBq) and TMZ (50 mg/ kg for 14 days). According to these studies an optimal treatment schedule could be achieved when ^{177}Lu -TATE was administered after 14 days of TMZ treatment. This was because of an increased uptake of radioactivity at that time point, likely caused by an increased tumour perfusion induced by TMZ as measured by DCE-MRI. In the final treatment study performed in mice, again we observed a significantly higher tumour uptake of radioactivity after 14 days of TMZ treatment compared to that in tumours of control animals, not receiving TMZ “pre-treatment”. The group treated with ^{177}Lu -TATE after 14 days of TMZ showed a more pronounced anti-tumour response compared with the group treated with TMZ 14 days after administration of ^{177}Lu -TATE. Given the fact that the imaging studies predicted very well which order of treatment would render the best response, clinical translation of TMZ treatment prior to PRRT might increase tumour responses in NET patients as well.

As described before, success of PRRT depends on delivering a high absorbed radiation dose to the tumour relative to a non-toxic absorbed dose delivered to normal organs. **Chapter 6** describes experiments in which we attempted to increase the absorbed tumour dose while the dose to normal organs remained the same, to enlarge the therapeutic window of this therapy. Furthermore, we investigated if the linear quadratic model could be helpful to predict anti-tumour responses and normal organ toxicity in our model, with the aim to optimize future patient-specific treatment planning. In theory fractionation of the dose or changes in dose rate will not influence anti-tumour responses, while the risk of radiation induced adverse events will be reduced. Thereto, we have performed experiments in H69 tumour-bearing nude mice to study the effects of different molar activities on the absorbed doses in tumour versus normal organs as well as on anti-tumour effects. Furthermore different treatment schemes were studied. Finally, all experimental results obtained were compared with calculations using the linear quadratic model to verify the usefulness for prospective treatment planning. Our results indicated that decreased molar activity resulted in lower receptor-mediated uptake by tumour and normal organs, which in turn resulted in an impaired anti-tumour response. Furthermore, fractionation of the dose did not affect anti-tumour responses, indicating that the current practice of delivering the therapy in 4 cycles does not affect the therapeutic efficacy. The linear quadratic model appeared to be useful to predict anti-tumour responses and might be applied to calculate optimal therapy conditions for future patient studies.

DISCUSSION AND FUTURE PERSPECTIVES

Clinical application of pre-clinical combination therapy studies as described in this thesis:

As described in chapter 3 and 4, in our studies the combination of PRRT with everolimus did not result in an increased anti-tumour response. Instead, it resulted in a lower response rate, plus we observed metastasis in rats treated with everolimus. Translation of the results from the therapy studies in which PRRT and TMZ were combined seems to be more promising. As described in Chapter 5, treatment with TMZ increased tumour perfusion resulting in an increased uptake of ^{177}Lu -TATE as well as an increased anti-tumour response. Current FDA approval of ^{177}Lu -TATE as well as TMZ offers good possibilities to translate these results into a clinical study. Since pancreatic NETs have been shown to respond to TMZ treatment (11-13), specifically for these patients combination of PRRT with TMZ could be promising. There have been trials using a combination of ^{177}Lu -TATE with TMZ, but in these studies TMZ was administered after treatment with ^{177}Lu -TATE, the radiopeptide in that case not being able to benefit from the potential increased tumour perfusion after TMZ as found in our study.

A concern when combining different treatments is the possibility of increased toxicity as in many studies chemotherapeutics as well as PRRT are administered at a maximum tolerable dose. Besides that, administration of TMZ at a maximum tolerable dose has been shown to eventually result in development of resistance by the tumour (14). Considering these concerns, there have been several reports of TMZ administered in a much lower dose, resulting in less side effects as well as no development of treatment resistance (15, 16). When looking at the effect on tumour vasculature and thereby possibly improved tumour perfusion, a lower dose proved to be very effective (17). Therefore future experiments combining a metronomic treatment with TMZ followed by PRRT could offer good possibilities for treatment, especially for pancreatic NET patients.

Table 1. Toward an optimal strategy for the combination of PRRT with chemotherapeutics

Opportunities	Challenges
A synergized anti-tumor effect without increased toxicity	Optimal selection of agents to study in combination
To overcome treatment resistance	Optimal sequence and dose
Synthetic lethality	To take good consideration of the risk of overlapping toxicity

Clinical application of improved treatment strategies

As mentioned in Chapter 2 and Chapter 6 a more individualized treatment may offer possibilities to further increase effectiveness of PRRT. Nowadays in several treatment centres the effect of a more individualized treatment is studied (18), so the first steps are being taken to treat a patient with a absorbed tumour dose as high as possible considering the absorbed dose to the dose limiting organs of that patient. Further individualization enabling also adjustment of the molar activity and total amount of activity in the tumour as well as perfusion of the treated lesions could possibly enable even better results.

When aiming for the most durable disease control, a good prediction of the expected anti-tumour response after each administration of ^{177}Lu -TATE seems of crucial importance. Whether it depends on the use of different radionuclides, different peptides or even combination therapy, being able to make an accurate prediction of anti-tumour responses offers important advantages. The use of accurate response models, as studied in Chapter 6, can not only help to come to the optimal response after the initial treatment, it may also offer additional options if regrowth occurs. Therefore besides the earlier mentioned options for improved therapy further research on an accurate model to predict tumour response is also of major importance when aiming for optimal quality of life and overall survival.

In general, to reach an optimized patient-specific treatment

In the studies described in this thesis we focussed on combination of PRRT with chemotherapeutics and variations in treatment schemes and molar activities to obtained improved treatment effects. As described at the start of this thesis, there are several additional options to seek for improved radionuclide treatment. The use of alpha-emitters can e.g. offer a very tumour-destructive treatment (19). In a clinical report STT analogues labelled with the alpha emitting Bismuth-213 have been shown to induce remission in neuroendocrine tumours refractory to beta radiation (19).

The introduction of new receptor targeting peptides, including receptor antagonists, may as well result in improved anti-tumour responses (20). Preclinical studies have shown significant increases in (membrane-bound) tumour uptake, tumour radiation dose, and durable DNA damage after treatment with the SSTR antagonist (^{177}Lu -DOTA)JR11 compared with the SSTR agonist ^{177}Lu -TATE (21). An initial clinical pilot study performed in 4 patients resulted in an increased tumour uptake, residence time and hence a higher anti-tumour dose after the antagonist (^{177}Lu -DOTA)JR11 compared with those after the agonist ^{177}Lu -TATE (20).

Another option, not mentioned earlier, is the use of enzyme inhibitors to prolong biological availability of unstabilized STT analogues, vulnerable to enzymatic degradation (22). Preclinical studies have shown an improved uptake of radiolabelled unstable STT analogues when administered with protease inhibitors (22), resulting

in an increased tumour to kidney ratio and enabling the use of unstabilized STT analogues with a higher STT subtype 2 receptor affinity.

By combining the options for improved treatment effects as described above, further optimization of PRRT might be achieved. By investigating the specific clinical conditions of a specific patient an individual treatment plan could be created. By combining optimal choices of radionuclides and a well-validated treatment scheme, possibly combined with an uptake- or response-increasing co-treatment, optimal anti-tumour responses might be achieved. Administering a lower dose than the maximum tolerable dose during the initial treatment might leave possibilities for additional treatment cycles in a later stadium of the disease.

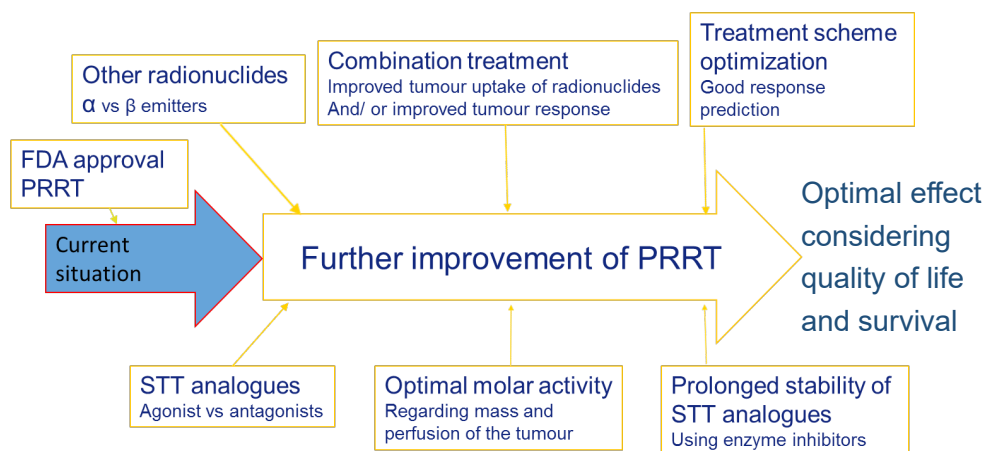


Figure 1. Graphical illustration of the current status of PRRT and options for the future for an optimal treatment schedule for NET patients

REFERENCES

1. Reubi, J.C., et al., Somatostatin receptor sst1-sst5 expression in normal and neoplastic human tissues using receptor autoradiography with subtype-selective ligands. *Eur J Nucl Med*, 2001. **28**(7): p. 836-46.
2. Hemminki, K. and X. Li, Incidence trends and risk factors of carcinoid tumors: a nationwide epidemiologic study from Sweden. *Cancer*, 2001. **92**(8): p. 2204-10.
3. Yao, J.C., et al., One hundred years after "carcinoid": epidemiology of and prognostic factors for neuroendocrine tumors in 35,825 cases in the United States. *J Clin Oncol*, 2008. **26**(18): p. 3063-72.
4. Rinke, A., et al., Placebo-controlled, double-blind, prospective, randomized study on the effect of octreotide LAR in the control of tumor growth in patients with metastatic neuroendocrine midgut tumors: a report from the PROMID Study Group. *J Clin Oncol*, 2009. **27**(28): p. 4656-63.
5. Kwekkeboom, D.J., et al., Treatment with the radiolabeled somatostatin analog (177 Lu-DOTA 0,Tyr3)octreotate: toxicity, efficacy, and survival. *J Clin Oncol*, 2008. **26**(13): p. 2124-30.
6. Teunissen, J.J., D.J. Kwekkeboom, and E.P. Krenning, Quality of life in patients with gastroenteropancreatic tumors treated with (177Lu-DOTA0,Tyr3)octreotate. *J Clin Oncol*, 2004. **22**(13): p. 2724-9.
7. Brabander, T., et al., Peptide receptor radionuclide therapy of neuroendocrine tumours. *Best Pract Res Clin Endocrinol Metab*, 2016. **30**(1): p. 103-14.
8. Cutler, L.S., D.L. Greiner, and D. Rozenski, Experimental autoallergic sialadenitis in the LEW rat. II. Target antigens are associated with cell surface and intracellular particulate fractions derived from the submandibular gland. *Cell Immunol*, 1991. **135**(2): p. 346-53.
9. Greiner, D.L., et al., Experimental autoallergic sialadenitis in the LEW rat. III. Role of CD4+ T cells in EAS induction. *Cell Immunol*, 1991. **135**(2): p. 354-9.
10. Sakaguchi, S., et al., Immunologic tolerance maintained by CD25+ CD4+ regulatory T cells: their common role in controlling autoimmunity, tumor immunity, and transplantation tolerance. *Immunol Rev*, 2001. **182**: p. 18-32.
11. Kulke, M.H., et al., Phase II study of temozolomide and thalidomide in patients with metastatic neuroendocrine tumors. *J Clin Oncol*, 2006. **24**(3): p. 401-6.
12. Kulke, M.H., et al., A phase II trial of irinotecan and cisplatin in patients with metastatic neuroendocrine tumors. *Dig Dis Sci*, 2006. **51**(6): p. 1033-8.
13. Ekeblad, S., et al., Temozolomide as monotherapy is effective in treatment of advanced malignant neuroendocrine tumors. *Clin Cancer Res*, 2007. **13**(10): p. 2986-91.
14. Koumariou, A., et al., Temozolomide in Advanced Neuroendocrine Neoplasms: Pharmacological and Clinical Aspects. *Neuroendocrinology*, 2015. **101**(4): p. 274-88.
15. Kim, J.T., et al., Metronomic treatment of temozolomide inhibits tumor cell growth through reduction of angiogenesis and augmentation of apoptosis in orthotopic models of gliomas. *Oncol Rep*, 2006. **16**(1): p. 33-9.

16. Kong, D.S., et al., A pilot study of metronomic temozolomide treatment in patients with recurrent temozolomide-refractory glioblastoma. *Oncol Rep*, 2006. **16**(5): p. 1117-21.
17. Ko, K.K., et al., Metronomic treatment of temozolomide increases anti-angiogenicity accompanied by down-regulated O(6)-methylguanine-DNA methyltransferase expression in endothelial cells. *Exp Ther Med*, 2011. **2**(2): p. 343-348.
18. Sandstrom, M., et al., Individualized dosimetry of kidney and bone marrow in patients undergoing ¹⁷⁷Lu-DOTA-octreotate treatment. *J Nucl Med*, 2013. **54**(1): p. 33-41.
19. Kratochwil, C., et al., (2)(1)(3)Bi-DOTATOC receptor-targeted alpha-radionuclide therapy induces remission in neuroendocrine tumours refractory to beta radiation: a first-in-human experience. *Eur J Nucl Med Mol Imaging*, 2014. **41**(11): p. 2106-19.
20. Wild, D., et al., Comparison of somatostatin receptor agonist and antagonist for peptide receptor radionuclide therapy: a pilot study. *J Nucl Med*, 2014. **55**(8): p. 1248-52.
21. Dalm, S.U., et al., Comparison of the Therapeutic Response to Treatment with a ¹⁷⁷Lu-Labeled Somatostatin Receptor Agonist and Antagonist in Preclinical Models. *J Nucl Med*, 2016. **57**(2): p. 260-5.
22. Nock, B.A., et al., "To serve and protect": enzyme inhibitors as radiopeptide escorts promote tumor targeting. *J Nucl Med*, 2014. **55**(1): p. 121-7.

CHAPTER 8

Nederlandse Samenvatting

Curriculum Vitae

PhD portfolio

List of publications

Dankwoord

NEDERLANDSE SAMENVATTING

Peptidenreceptor-radionuclidentherapie (PRRT) is een behandeling via bindingsplaatsen (receptoren) voor kleine eiwitten (peptiden) die door tumorcellen tot (over) expressie worden gebracht. Door een receptorbindend klein eiwit (peptide) te labelen met een therapeutisch radionuclide kan een effectieve stralingsdosis aan een tumor worden toegediend na intraveneuze injectie. Veel neuroendocriene tumoren (NETs) brengen somatostatinerceptoren tot expressie op hun cellen, dit biedt mogelijkheden voor behandeling met radioactief gelabelde somatostatine-analogen; een goede behandeloptie voor patiënten met uitgezaaide NETs. Ondanks de lage incidentie van slechts 2-5 per 100.000 per jaar zorgt de relatief lange overleving van NET-patiënten voor een betrekkelijk hoge prevalentie. Omdat bij veel van deze patiënten op het moment van diagnose reeds sprake is van uitzaaiingen, is curatieve chirurgie dan geen optie meer. De standaardbehandeling voor deze patiënten bestaat uit o.a. intraveneuze toediening van langwerkende somatostatine-analogen. Deze behandeling resulteert in verlichting van de symptomen en mogelijk ook groeivertraging van de tumoren. Van PRRT met radioactief gelabelde somatostatine-analogen, zoals ¹⁷⁷Lu-gelabeld DOTA,Tyr3-octreotate, is reeds aangetoond dat dit effectiever is dan de standaardbehandeling. Ondanks het bewezen effect van deze behandeling, met betrekking tot zowel het verhogen van de kwaliteit van leven als het verlengen van het leven, komt genezing na deze behandeling slechts zeer zelden voor. Het is daarom van groot belang om deze therapie verder te verbeteren. In deze thesis zijn verschillende opties voor het verbeteren van PRRT onderzocht in preklinische experimenten. Om de reactie van tumoren op de therapie goed in beeld te brengen, hebben we verschillende medische beeldvormingstechnieken gecombineerd. Doel was om op deze manier tot een optimale behandelstrategie te komen.

Hoofdstuk 1 geeft een korte algemene introductie over NETs. Tevens wordt een opsomming van verschillende behandelopties gegeven.

In Hoofdstuk 2 gaan we dieper in op een aantal preklinische en klinische studies die als doel hebben het bereiken van verbetering van PRRT. Er zijn op dit gebied nog geen gerandomiseerde klinische studies verricht, maar desondanks zijn er duidelijke aanwijzingen dat het gebruik van krachtiger radionucliden, zoals alfa-emitters, of de combinatie van verschillende radionucliden verbeterde anti-tumoreffecten zouden kunnen bewerkstelligen. Een meer geïndividualiseerde therapie, op basis van geïndividualiseerde dosimetrie gecombineerd met beter inzicht in de stralingsdosis die tumoren en normale organen ontvangen, zou kunnen resulteren in optimalisatie van de activiteit per cyclus, of van het aantal behandelcycli. Andere opties voor verbetering van PRRT zijn het gebruik van nieuwe (radioactief gelabelde) somatostatine-analogen met een verhoogde tumoropname en een langere bindingstijd, of een combinatie van PRRT met systemische therapieën, zoals chemotherapie of behandeling met medicatie die tumoren gevoeliger maken voor straling. Tot slot concluderen we dat verschillende opties voor verbetering van PRRT veelbelovend zijn en goed voorhanden. Wel is er nog verder onderzoek nodig, waaronder ook gerandomiseerde klinische studies.

In Hoofdstuk 3 beschrijven we hoe behandeling met de mTOR remmer everolimus, twee maal per week toegediend gedurende vierehalve week, leidde tot het ontstaan van metastasen in een rattenpancreastumormodel. De behandeling met everolimus werd gegeven als enige behandeling danwel gecombineerd met ^{177}Lu -DOTA,Tyr³-octreotate (^{177}Lu -TATE). Everolimus alleen gaf maar een beperkt anti-tumor effect. De combinatie van ^{177}Lu -TATE met everolimus was duidelijk effectiever dan behandeling met enkel everolimus, de combinatie van everolimus en ^{177}Lu -TATE gaf echter geen betere anti-tumor effecten dan behandeling met enkel ^{177}Lu -TATE. Een onverwachte bevinding was de ontwikkeling van metastasen in 77% van de dieren die behandeld werden met everolimus of de combinatie van everolimus en ^{177}Lu -TATE. In dieren uit de controlegroep en dieren die enkel met ^{177}Lu -TATE werden behandeld, ontstonden geen metastasen, ook niet als de dieren langer werden vervolgd. Deze ontwikkeling van metastasen zou mogelijk een gevolg kunnen zijn van het plotseling staken van de behandeling met everolimus, zoals gedaan is in onze studie. Deze bevindingen zouden daarom klinisch van belang kunnen zijn voor patiënten die behandeling met everolimus dienen te staken vanwege bijvoorbeeld ernstige bijwerkingen.

In hoofdstuk 4 wordt verder onderzoek naar het ontstaan van metastaten na behandeling met RAD001 beschreven, evenals de verminderde respons op de combinatie van RAD001 en PRRT vergeleken met enkel PRRT. Wat betreft het ontwikkelen van metastasen werd onderzocht of het plots stoppen van RAD001 toediening hiervan een oorzaak zou kunnen zijn. Om dit effect te onderzoeken werden er naast groepen ratten die gedurende 4,5 week behandeld werden met RAD001 tevens groepen in de studie geïncubeerd welke 12 weken met RAD001 werden behandeld. Verder werd gekeken of het toedienen van RAD001 voordat ^{177}Lu -TATE werd toegediend invloed had op de tumoropname van ^{177}Lu -TATE. In vergelijking met het eerder beschreven onderzoek werd deze keer een ander subtype Lewis ratten gebruikt. Dit subtype wordt vaak gebruikt voor auto-immuun studies, deze dieren hebben namelijk een meer actief immuun systeem, resulterend in een verbeterde CD4+ en CD8+ immuunrespons. Deze auto-immuniteit houdt verband met een toegenomen anti-tumor-immuniteit. Behandeling met RAD001 bleek geen invloed te hebben op de tumoropname van radionucliden. Wat betreft de anti-tumorrespons bleek dat van de ratten behandeld met RAD001 slechts 12,5% een complete respons toonde, vergeleken met een complete respons bij 50% van de ratten in de controlegroep. Verder bleek het ontstaan van metastasen na behandeling met RAD001 niet dosisafhankelijk te zijn, noch was er een relatie met het aantal weken dat RAD001 werd toegediend. Bij de ratten die metastasen ontwikkelden werd nogmaals ^{177}Lu -TATE toegediend om te onderzoeken of ^{177}Lu -TATE een effectieve behandelingsmethode is voor deze metastasen. Toediening van een hoge dosis ^{177}Lu -TATE resulteerde echter maar in 2 van de 7 dieren in het verdwijnen van de tumor; in ons model bleek dat metastases minder gevoelig zijn voor behandeling met ^{177}Lu -TATE dan de primaire tumoren.

In hoofdstuk 5 wordt het gebruik van multimodality imaging voor het optimaliseren van de combinatie van ^{177}Lu -TATE en het chemotherapeutikum temozolomide

beschreven. De beschreven onderzoeken werden uitgevoerd in het humane H69-tumormodel in naakte muizen. Door SPECT/CT en DCE-MRI te combineren werden tumorperfusie en opname van radionucliden gedurende de behandeling met 30MBq ^{177}Lu -TATE en/of 50 mg/kg TMZ gedurende 14 dagen gemonitord. De gevonden resultaten gaven aan dat het beste effect verwacht zou kunnen worden als de ^{177}Lu -TATE toegediend zou worden na 14 dagen behandeling met TMZ. Dit als een gevolg van toegenomen tumor perfusie na 14 dagen behandeling met TMZ, zoals werd gemeten met DCE-MRI. In het therapie-experiment dat we hierna uitvoerden bleek opnieuw dat er sprake was van een significant hogere opname van radionucliden na 14 dagen behandeling met TMZ. De groep die de ^{177}Lu -TATE kreeg toegediend na eerst 14 dagen behandeld te zijn geweest met TMZ toonde bovendien een anti-tumorrespons die significant beter was dan die van de groep die eerst ^{177}Lu -TATE kreeg toegediend, 14 dagen later gevolgd door een TMZ-behandeling gedurende 2 weken. Gezien de goede overeenkomst tussen de beeldvormingsstudies en de therapiestudie wat betreft het voorspellen van de groep met de beste anti-tumorrespons zou een behandeling met TMZ voorafgaande aan toediening van ^{177}Lu -TATE ook in de klinische situatie een verbeterde respons kunnen geven.

In hoofdstuk 6 worden tenslotte experimenten beschreven die als doel hadden de door de tumor geabsorbeerde stralingsdosis te verhogen, zonder dat dit gepaard zou gaan met toegenomen belasting van gezonde organen. In theorie zou het toedienen van een bepaalde dosis in meerdere fracties hiertoe een mogelijkheid kunnen zijn. De cellen in de organen kunnen in de periode tussen de verschillende doses herstellen van de minder gecompliceerde stralingsschade aan het DNA, terwijl het effect op de tumor vergelijkbaar is met die na het toedienen van een grotere dosis in een keer. Verder zou het verhogen van de hoeveelheid radioactiviteit per eenheid peptidemassa kunnen resulteren in een hogere tumoropname en geabsorbeerde dosis. Om de beschreven effecten te onderzoeken, hebben we meerdere experimenten uitgevoerd in het H69-tumormodel in naakte muizen. In deze experimenten werd gevarieerd met de hoeveelheid peptide waaraan de radioactiviteit was gelabeld (de zogenaamde molaire activiteit) en met de toedieningsschema's (het toedienen van een enkele dosering werd vergeleken met het toedienen van meerdere doses). Tot slot werd voor alle resultaten van de experimenten het behaalde effect vergeleken met de geabsorbeerde dosis, waarbij werd bekeken of dit overeen kwam met de door het lineair kwadratisch model voorspelde resultaten. Het lineair kwadratisch model beschrijft de radiobiologie van respons op ioniserende straling door weefsel en wordt in de radiotherapie gebruikt om patiënten bestralingen zo effectief en veilig mogelijk te plannen. De resultaten van onze experimenten lieten zien dat een lage molaire activiteit resulteerde in een lagere tumoropname en een verminderde therapeutische respons. Verder bleek fractioneren van de geabsorbeerde dosis geen effect te hebben op de therapeutische respons. Tot slot bleek het lineair kwadratisch model een goed model te zijn om de therapeutische respons, met in de tumor een verwaarloosbare kwadratische bijdrage, te voorspellen. Hetgeen heel nuttig kan zijn om bij patiënten de optimale behandelstrategie te bepalen.

CURRICULUM VITAE

Sander Bison was born in Amsterdam, the Netherlands, on February 16 1980. In 1988 he moved to Heerenveen where he attended secondary school at the "Bornego College". In 2000 he started veterinary studies in Belgium. In 2004 he received his bachelor in veterinary medicine at the University of Antwerp and in 2007 he received his master degree in veterinary medicine at Gent University.

After working as a veterinarian for 2 years, in 2010 he started his PhD project at the department of Nuclear Medicine at the Erasmus MC, Rotterdam, under supervision of prof. dr. M. de Jong, dr. M. Bernsen, and dr. M. Konijnenberg.

In 2012 he was accepted for the lateral entry program for medical studies at Rijksuniversiteit Groningen where he obtained the degree of medical doctor in 2016.

PHD PORTFOLIO

<u>Title</u>	<u>Institute</u>	<u>year</u>	<u>ECTS</u>
NKRV	Radboud MC	2010	0,3
AMI course	Erasmus MC	2010	1,4
Art. 9 proefdierkunde	LUMC	2010	3,0
Radiation safety 5b	Erasmus MC	2010	0,9
Molmed day	Erasmus MC	2010	0,3
NKRV	Delft University	2010	0,3
EANM congress Vienna	EANM	2010	0,3
Oncology	Eramus MC	2010	1,8
Molmed day	Erasmus MC	2011	0,3
Research techniques	Erasmus MC	2011	1,6
NKRV	Eindhoven	2011	0,3
Presentation Birmingham	EANM	2011	1,0
NKRV	UMCG	2011	0,3
Outplacement Melbourne	Peter mcCallum Cancer Center	2011	15,0
Oncology day	Rene Vogelsstichting	2012	0,3
Trainee HLO student	Erasmus MC	2012	7,5
Presentation skills	Erasmus MC	2012	1,0
Course on Mol Med	Erasmus MC	2012	0,7
Pear review	CBTandRF	2012	0,3
Research lunch presentation	Erasmuc MC	2012	0,5
EANM Lyon presentation	EANM	2013	0,5
Journal club	Erasmuc MC	2010-2012	1,0
Molmed day	Erasmus MC	2014	0,3
Research presentations for medical students	UMCG, MCL	2012-2016	2,0
		<u>Total ECTS:</u>	<u>40,5</u>

LIST OF PUBLICATIONS

- Optimization of combined temozolomide and peptide receptor radionuclide therapy (PRRT) in mice after multimodality molecular imaging studies.
Bison SM, Haeck JC, Bol K, Koelewijn SJ, Groen HC, Melis M, Veenland JF, Bernsen MR, de Jong M. EJNMMI Res. 2015 Dec;5.
- Peptide receptor radionuclide therapy (PRRT) with [(177)Lu-DOTA(0),Tyr(3)] octreotate in combination with RAD001 treatment: further investigations on tumor metastasis and response in the rat pancreatic CA20948 tumor model.
Bison SM, Pool SE, Koelewijn SJ, van der Graaf LM, Groen HC, Melis M, de Jong M. EJNMMI Res. 2014 May 30.
- Peptide receptor radionuclide therapy using radiolabeled somatostatin analogs: focus on future developments.
Bison SM, Konijnenberg MW, Melis M, Pool SE, Bernsen MR, Teunissen JJ, Kwekkeboom DJ, de Jong M. Clin Transl Imaging. 2014;2:55-66. Epub 2014 Mar 5. Review.
- mTOR inhibitor RAD001 promotes metastasis in a rat model of pancreatic neuroendocrine cancer.
Pool SE, Bison SM, Koelewijn SJ, van der Graaf LM, Melis M, Krenning EP, de Jong M. Cancer Res. 2013 Jan 1;73(1):12-8.
- Optimized time-resolved imaging of contrast kinetics (TRICKS) in dynamic contrast-enhanced MRI after peptide receptor radionuclide therapy in small animal tumor models.
Haeck J, Bol K, Bison S, van Tiel S, Koelewijn S, de Jong M, Veenland J, Bernsen M. Contrast Media Mol Imaging. 2015 Nov;10(6):413-20.

DANKWOORD

In dit hoofdstuk wil ik graag enkele mensen bedanken die in belangrijke mate hebben bijgedragen aan de totstandkoming van dit proefschrift.

Om te beginnen wil ik mijn promotor Prof. Dr. Ir. Marion de Jong bedanken voor alle begeleiding, adviezen en steun. Nadat ik op het sollicitatiegesprek vertelde dat ik als dierenarts graag in bultjes prikte om vervolgens onder de microscoop te kijken wat erin zat, concludeerde jij dat ik iemand ben die het leuk zou vinden om onderzoek te doen. Tijdens mijn PhD onderzoek gaf jij me de kans om vervolgens de overstap te maken naar de studie geneeskunde. Ondanks dat het door deze bijkomende studie een veel langduriger traject is geworden dan in eerste instantie het plan was, heb jij mij toch steeds van harte gesteund en geholpen bij het maken van dit proefschrift.

Mijn copromotor Dr. Monique Bernsen, bedankt voor begeleiding bij het schrijven van verschillende artikelen. Jouw adviezen over de opbouw van een manuscript en het meenemen van de lezer zijn zeker behulpzaam geweest.

Mijn copromotor Dr. Mark Konijnenberg, jouw inbreng en begeleiding bij met name het schrijven van het review en het artikel van hoofdstuk 6 zijn van grote waarde geweest. De beschrijving en berekeningen van de dosimetrie en het linear quadratisch model zorgen voor een vergrote wetenschappelijke waarde van de betreffende stukken.

Prof. emeritus Dr. E.P. Krenning en Prof. Dr. J.F. Verzijlbergen, de afdelingshoofden van de nucleaire geneeskunde tijdens mijn promotietraject en Prof. Dr. G. Krestin het afdelingshoofd van de radiologie. Bedankt voor het op fijne manier leiden van de afdeling en jullie nauwe betrokkenheid bij het onderzoek.

De analisten op het lab, Stuart, Saskia en Linda, bedankt voor jullie hulp bij het uitvoeren van experimenten en voor de sturing bij het wegwijs worden in het lab. Stuart, ook hartelijk bedankt voor het ontwerp van de cover van dit proefschrift.

Jan de Swart, bedankt voor je hulp en adviezen bij SPECT quantificaties en bij computervragen in het algemeen.

Gaby en Sandra, bedankt voor alle adviezen en gezelligheid in de uitwerkkamer, de pauzes en de leuke activiteiten buiten het werk om.

Joost, Karin en Jifke, jullie waren onmisbaar in het samenwerkingsverband tussen de Nucleaire Geneeskunde, Radiologie en de Medische Informatica en in het project waarop ik in 2010 startte. Bedankt voor het meedenken bij de experimenten en voor de grote inbreng bij de multimodality imaging.

CHAPTER 8

Harald en Marleen, twee toenmalige postdoc's in het team en Stefan, inmiddels nucleair geneeskundige, bedankt voor jullie fijne bijdrage aan de artikelen, jullie adviezen om mij verder wegwijs te maken in de wereld van de wetenschap.

Wout, Erik en Ho Sze, bedankt voor heel veel labelling en jullie expertise met betrekking tot het gebruik van de radionucliden.

Ingrid, bedankt voor je hulp bij computerproblemen en voor het meedenken over het verdere verloop van mijn carrière. Bedankt natuurlijk ook voor de gezellige koffietjes. Al het personeel van de afdeling Nucleaire Geneeskunde, bedankt voor jullie collegialiteit, meedenken bij presentaties, de leuke afdelingsdagen en jullie hulp bij ^{177}Lu -TATE en ^{18}F FDG studies.

Furthermore I would like to thank Prof. R. Hicks and all the lab workers in the Peter McCallum Cancer Center in Melbourne for their expertise and the great experience I had during my research visit to Australia.

Uit mijn persoonlijke omgeving wil ik graag mijn moeder bedanken voor haar grote steun: mede hierdoor heb ik uiteindelijk dit proefschrift af kunnen maken. Verder Corine en Tjipke, voor alle gezelligheid, maar ook voor de hulp bij de verschillende verhuizingen.

Uiteraard wil ik ook graag de paranimfen Anne en Hugo graag benoemen voor hun hulp bij de organisatie van de promotiedag.

Verder zijn er vele andere mensen, hier niet specifiek bij naam genoemd, die meer achter de schermen een rol hebben gespeeld bij het onderzoek en mijn werkzaamheden in het Erasmus MC, ook hen wil ik uiteraard heel graag bedanken.

